INTERNAL AND ACOUSTIC DAMPING OF VIBRATING BEAMS AND RODS

THESIS PRESENTED FOR THE DEGREE OF

DOCTOR OF PHILOSOPHY

OF THE

UNIVERSITY OF EDINBURGH

BY

ROBERT A. JOHNSTON, B.Sc.

JULY 1966

CONTENTS

SYNOPSIS

The internal and acoustic damping of rods vibrating longitudinally and beams vibrating transversely at frequencies up to 20 Kc.p.s. has been investigated. The work has been restricted to the study of circular and rectangular cross sections and to small amplitude vibration under sinusoidal forcing.

A detailed account of the experiments performed is given together with a description of a number of preliminary investigations aimed at ascertaining the sources and levels of any extraneous damping.

The experiments have shown that the internal damping of mild steel bodies vibrating such that the stresses are either uniform tension or compression or a combination of both, is unaffected by frequency at frequencies up to 20 Kc.p.s., provided the stresses are not high enough to introduce non-linear effects, and that the internal damping factor of cold rolled mild steel may be assumed to have the approximate value 0.6×10^{-4}. A comparison of the experimental results from cold rolled mild steel specimens and a more homogeneous mild steel specimen showed no great difference in the damping properties of the two types of steel and it has been concluded that the effects of cold rolling may only be significant in very small bodies.

It has been demonstrated that acoustic radiation is the primary source of damping due to the presence of air and theoretical expressions have been developed for the acoustic damping factors of cylindrical and rectangular beams in transverse vibration. Experiment showed that acoustic damping of longitudinal vibrations was negligeable.

The theory for both the cylindrical and rectangular beams has proceeded from the fundamental three dimensional wave equation. For cylindrical beams the wave equation in cylindrical coordinates was solved leading to a closed form expression for the acoustic damping factor in terms of Bessel Functions. The method used for the rectangular beams necessitated transformation of the wave equation to elliptic cylinder coordinates the solution leading to a series expression for the acoustic damping factor in terms of Mathieu Functions.

The theoretical and experimental results for both cross sections are in good agreement.

It has been shown that the acoustic damping factor depends largely on the wave length of the radiated sound, λ_0, the beam wave length, λ, and the beam circumference. For both cross sections the acoustic damping factor is zero when $\lambda_0 = \lambda$. When $\lambda_0 > \lambda$ the acoustic radiation results in a mass reactance on the beams. For cylindrical beams the acoustic damping factor is a maximum when $\lambda_0 \simeq$ circumference of the beams the value of the maximum being the same for all diameters. For rectangular beams the acoustic damping factor is a maximum when $\lambda_0 \simeq$ three quarters of the circumference of the beams the values of the maxima being nearly linearly related to the breadth/depth ratios of the beams.

- - - o O o - - -

INTRODUCTION

With few exceptions vibrations of engineering components are unwanted occurences which are the result of the components being subjected to dynamic loading. The response of the components is largely determined by their mass/stiffness distributions and the amount of damping present. The effects of the vibrations may manifest themselves simply as personal discomfort, which is nevertheless a real problem, or they may lead to premature failure of components which can have very serious consequences. Clearly the mechanisms which reduce vibration response are of vital importance; damping may be placed under such a heading.

There are many methods of damping the vibrations of components among these being the addition of dashpot elements or damping layers. There are however damping mechanisms which are inherent properties of the components under given physical and environmental conditions. Internal damping and air damping are typical of such mechanisms. It is with these that the work of this thesis is concerned.

Internal damping has for the most part defied analytic treatment due to the many parameters on which such damping depends; there is however a vast amount of literature on the subject, see Kimball[12]* and Plunkett[32] for fairly extensive bibliographies.

A survey of the literature has revealed that the great complexity of the phenomenon has led to a considerable amount of obscurity in some of the early research. An example of this is

---

* Numbers in parenthesis refer to the bibliography at the end of the thesis.

the summary given by Kimbal[12] of the most important research up to 1941, which includes a table summarising the findings: it is almost impossible to make any comparisons of the results given and, from an engineers standpoint, the table seems to be of little value.

The problem has mostly been studied by physicists, noteable among these being Zener[38, 39] and Kolsky[15]. Zener has pointed out that although stresses may be small, stress and strain may not be single valued functions of each other e.g. strain may lag behind stress in periodic vibration, no permanent set remaining after removal of all stresses: he denotes this property of the material anelasticity and discusses this in terms of relaxation phenomena. He has also considered the damping effects of microscopic and macroscopic thermal currents and states that when the period of flexural vibration of a reed is comparable with the time it takes for heat to flow across the reed there will be an irreversible conversion of mechanical energy into heat which will appear as internal damping. Kolsky in his monograph describes the use of stress pulses in internal damping investigations and he also gives a good historical note of the various possible sources of internal damping as postulated by other workers. Physicists in general in their experimental work concern themselves with either single crystals of material or extremely small specimens and although they have had a good deal of success in predicting observed phenomena, it is no simple matter for the engineer to use their methods when considering the damping in engineering components.

Some work has of course been done which is of more direct use to engineers, that of Lazan[17] being among the most important. He has analysed the resonance response of members in terms of three

basic factors i) a material factor ii) a cross sectional shape factor and iii) a longitudinal stress distribution factor. He has derived expressions for each of these and has shown how they may be used in practice. His work covers the region where stresses are significant and on the basis of his experiments he states that the damping capacity for many materials is proportional to the n'th power of stress, n depending on temperature, stress history and stress mangitude. He does not consider the effect of frequency. Other workers such as Kimball and Lovell[13], Leaderman[18], Ockleston[31], Hopkinson and Williams[17] and Rowett[35] have in fact found no frequency effect when stresses are significant although the frequencies they worked at were generally very low.

In the present investigation it is proposed to study the frequency dependence of internal damping at low stresses over a wide frequency range in mild steel specimens whose dimensions and shapes are of engineering relevance. Surprisingly, such an approach has not previously been made but it is considered that there is a need for such information as it provides what may be regarded as a background level of internal damping which would provide a good footing for further work at higher stresses.

At the outset of this investigation it was known that both internal and air damping would be present but it was not known what the relative importance of these would be. In addition, it was not known what would be the main cause of energy absorption in the air. It will be shown that acoustic radiation accounts for the major part of the energy absorption.

This is a form of damping which, from the engineers viewpoint, has received very little attention in the past but has

recently grown in importance. Foxwell and Franklin[5] give a good theoretical demonstration of acoustic effects on a stiffened thin cylinder. They consider incident and scattered acoustic waves and also the internal transmissions. They show that the external effects primarily damp the vibratory motion of the cylinder while the internal reactive effect may cause great differences in the "in vacuo" and "in air" response characteristics of the cylinder. Junger[10] has also considered the acattering effects of thin cylinders. The acoustic radiation from vibrating cylinders of infinite length has been treated analytically by Junger[11] and he has shown that radially symmetric modes are suppressed at certain frequencies due to the reactive impedance becoming infinite.

Little study has been made of the acoustic radiation from rectangular bodies, other than flat bodies with essentially zero thickness (see Mazelsky[24]) and a common feature of all the work is the distinct lack of experimental verification of the theoretical predictions - the present work seeks to shed light on both these aspects.

- - - o 0 o - - -

1.0 STATEMENT OF THE OBJECT AND LIMITATIONS OF THE INVESTIGATION.

It is probably a consequence of the rapid growth of the aircraft industry that precise quantitative knowledge of the effect of damping on the vibration of engineering components has become important. Previously a qualitative appreciation that resonance involved large stresses was sufficient for most purposes. This need for greater knowledge has stimulated the work of this thesis.

The damping of vibrating structures is clearly extremely complex, there being many parameters on which such damping may depend. Because of the great complexity of the subject any investigations may only proceed under well defined terms of reference.

The terms of reference for this investigation are stated below but it is hoped the work will inspire further research in the fields suggested at the conclusion of the thesis.

The object of the research is to improve the understanding of the way in which damping influences the vibration response of engineering components and the work is based on the need to relate research to the engineers needs.

In order that complexities be restricted to manageable proportions certain specific limitations were made, namely,

(a) only the effect of damping on the response of components to harmonically varying forces was studied.

(b) the work was restricted to the study of the response of beams and rods; it was felt that these were probably of more engineering importance than single (spring/mass) elements.

(c) in order to consider the effect of component dimensions simple shapes were used.

(d) all work was carried out at low stress levels i.e. in the non-amplitude dependent region of internal damping.

Previous researchers have shown that internal damping can be assumed to occur under three main headings viz., non-amplitude dependent, amplitude dependent and stress history dependent. The first of these occurs when the stresses are small. It was desired to conduct this investigation over a fairly wide frequency range and to ascertain the variation of overall damping with frequency in this range; it was not intended at this stage to study the amplitude dependence of internal damping. For this reason (d) above was a necessary limitation.

The main effort was concentrated on specimens of cold rolled mild steel, this being considered to be of greater engineering interest, but some work was also carried out on a more homogeneous mild steel to ascertain whether there were any great differences in the damping properties of the two types of steel.

- - - o O o - - -

2.0 THE DAMPING FACTOR

In discussing the damping in a system a quantity called the Q-factor is often used. The term Q-factor was first used in electric circuit theory to define the damping properties of circuits but it has a useful mechanical analogy which is defined in this section. The quantity used in this work is the inverse of the Q-factor and this inverse will be referred to as the "damping factor".

The damping factor may be conveniently defined in terms of energy dissipation and an expression will now be derived from which its physical meaning will be apparent.

Consider a single degree of freedom system whose equation of motion is

$$M\ddot{x} + C\dot{x} + Kx = F(t) \qquad (2.0.1)$$

For this system the energy dissipated by damping during motion with period $\frac{2\pi}{\omega}$ is given by

$$\Delta E = \int_0^{2\pi/\omega} C(\dot{x})^2 dt \qquad \text{per cycle}$$

When harmonic motion occurs at the undamped resonant frequency such that $x = \hat{x} \sin\omega_0 t$ where $\omega_0 = \sqrt{K/M}$ then

$$\Delta E = C\,\hat{x}^2 \pi\omega_0 \qquad (2.0.2)$$

The maximum kinetic energy of the system at resonance is given by

$$E = \tfrac{1}{2}M(\hat{\dot{x}})^2$$

$$= \tfrac{1}{2}M\hat{x}^2\omega_0^2 \qquad (2.0.3)$$

Thon $$\frac{\Delta E}{E} = 2\pi \frac{C}{M\omega_0} \qquad (2.0.4)$$

The damping factor will now be defined as

$$Q^{-1} = \frac{1}{2\pi}\frac{\Delta E}{E}$$

$$= \frac{C}{M\omega_0} \qquad (2.0.5)$$

The above argument has been applied to a single degree of freedom system but its use may readily be extended to continuous systems.

In continuous systems if analysis is performed in terms of normal co-ordinates the equations of motion will in general be of the form

$$a_r \ddot{\xi}_r + b_{rs}\dot{\xi}_s + c_r \xi_r = Z_r \qquad (2.0.6)$$

$(r,s = 1, 2, 3, \ldots)$

where a_r, b_{rs}, c_r are the generalised mass, damping and stiffness respectively.

$\xi_{r,s}$ are normal co-ordinates

and Z_r are generalised forces corresponding to the normal co-ordinates.

It will be seen that in general cross coupling between the modes arises due to the damping but if the damping is small the coupling effect may be negligeably small and we may assume

$$b_{rs}\dot{\xi}_s = 0 \qquad s \neq r$$

Equations (2.0.6) then become

$$a_r \ddot{\xi}_r + b_r \dot{\xi}_r + c_r \xi_r = Z_r \qquad (2.0.7)$$

$(r = 1, 2, 3, \ldots)$

Thence each equation is that of a single degree of freedom system and the damping factor will therefore be given by

$$Q^{-1} = \frac{b_r}{a_r \omega_r} \qquad (2.0.8)$$

where ω_r is the frequency of the rth mode of vibration.

In all subsequent analysis it is assumed that cross coupling effects are negligeable and that equations (2.0.7) are representative equations of motion.

- - - o 0 o - - -

3.0 MEASUREMENT OF THE DAMPING FACTOR

The damping factor may be measured in a variety of ways: Mead[27] has given a good summary of some of the methods. The particular method chosen will be determined to a large extent by the nature of the experiments being performed and will also depend on the amount of damping in the system.

In this work two methods were used these being

(a) the bandwidth method

(b) the logarithmic decrement method

For (a) it is necessary that the system be undergoing forced vibration whereas for (b) it is necessary that the system be in free vibration. The underlying theory of each of these methods is derived below.

3.1 THE BANDWIDTH METHOD

Considering again the single degree of freedom system whose equation of motion is

$$M\ddot{x} + C\dot{x} + Kx = F(t) \qquad (3.1.1)$$

We have by definition $Q^{-1} = \frac{C}{M\omega_0}$ therefore substituting for C in (3.1.1) we obtain

$$\ddot{x} + Q^{-1}\omega_0\dot{x} + \omega_0^2 x = \omega_0^2 \frac{F(t)}{K} \qquad (3.1.2)$$

Assuming sinusoidal motion under force $F = F_0 e^{i\omega t}$ equation (3.1.2) has the steady state solution

$$x = \frac{F_0/K \; e^{i(\omega t - \eta)}}{\sqrt{\left(1 - \frac{\omega^2}{\omega_0^2}\right)^2 + \frac{\omega^2}{\omega_0^2}\left(Q^{-1}\right)^2}} \qquad (3.1.3)$$

This amplitude has its maximum value when

$$\omega/\omega_0 = \sqrt{(1 - \tfrac{1}{2}(Q^{-1})^2)}$$

Now if the damping is small $(Q^{-1})^2 \ll 1$ then

$$\omega/\omega_0 \simeq 1 \qquad (3.1.4)$$

For this case the amplitude/frequency response will be of the form shown in fig. (1).

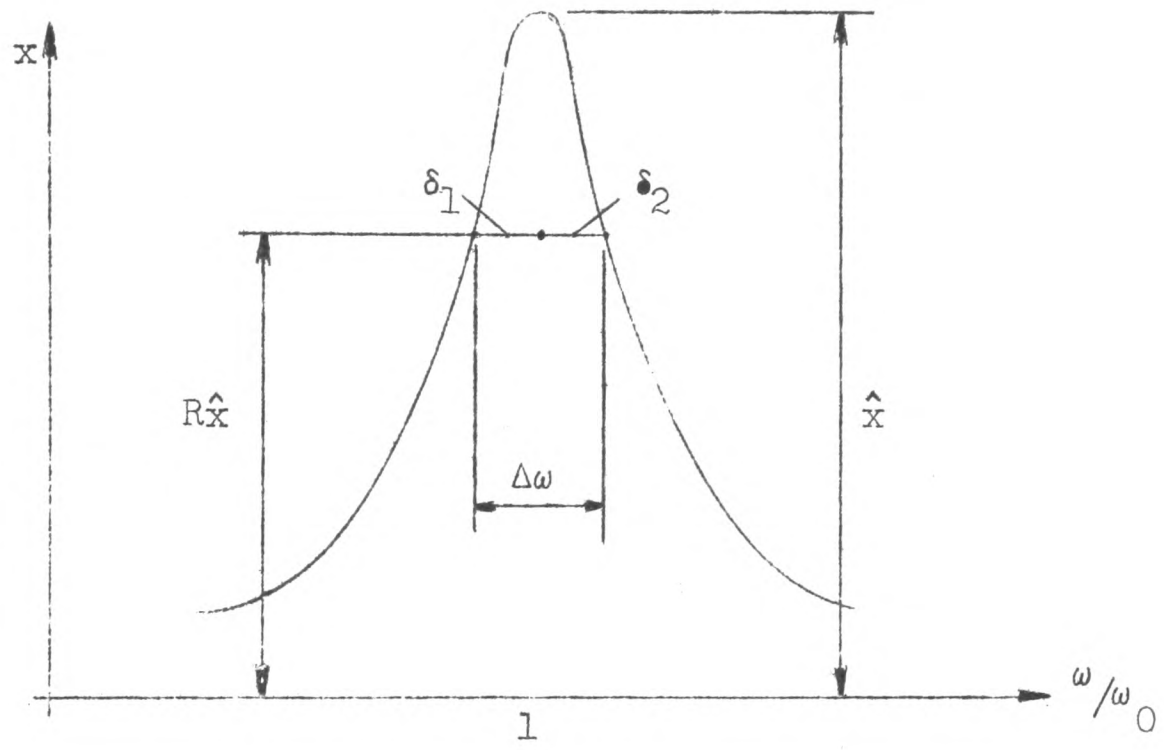

Fig. (1)

Substituting (3.1.4) in (3.1.3) we obtain

$$\hat{x} = \frac{1}{Q^{-1}} \frac{F_0}{K} e^{i(\omega t - \eta)} \qquad (3.1.5)$$

Letting $x = R\hat{x}$ and substituting in (3.1.3) gives

$$(1 - \frac{\omega^2}{\omega_0^2})^2 + \frac{\omega^2}{\omega_0^2}(Q^{-1})^2 - \frac{1}{R^2}(Q^{-1})^2 = 0$$

Neglecting terms of higher order than $(Q^{-1})^2$ this gives

$$\frac{\omega^2}{\omega_0^2} = -\tfrac{1}{2}\left((Q^{-1})^2 - 2\right) \pm Q^{-1}\sqrt{\frac{1}{R^2} - 1} \qquad (3.1.6)$$

Letting the solutions of this equation be $\omega_0 - \delta_1$ and $\omega_0 + \delta_2$ where δ_1 and δ_2 are small we obtain

(i) $$\frac{(\omega_0 + \delta_2)^2}{\omega_0^2} = -\tfrac{1}{2}\left((Q^{-1})^2 - 2\right) + Q^{-1}\sqrt{\frac{1}{R^2} - 1}$$

(ii) $$\frac{(\omega_0 - \delta_1)^2}{\omega_0^2} = -\tfrac{1}{2}\left((Q^{-1})^2 - 2\right) - Q^{-1}\sqrt{\frac{1}{R^2} - 1}$$

Neglecting the terms δ_1^2 and δ_2^2 and subtracting (ii) from (i) gives

$$\frac{(\delta_1 + \delta_2)}{\omega_0} = \sqrt{\frac{1}{R^2} - 1}\; Q^{-1}$$

Therefore $$\frac{\Delta\omega}{\omega_0} = \sqrt{\frac{1}{R^2} - 1}\; Q^{-1} \qquad (3.1.7)$$

The physical implication of (3.1.7) is that if a system is known to have small damping then a knowledge of the resonant frequency and the frequencies above and below resonance at which the amplitude is a known fraction of the resonant amplitude will enable the damping factor to be calculated.

Throughout this work the value of R used was $\frac{1}{2}$, thus

$$Q^{-1} = \frac{1}{\sqrt{3}}\,\frac{\Delta\omega}{\omega_0} \qquad (3.1.8)$$

3.2 THE LOGARITHMIC DECREMENT METHOD

If a damped single degree of freedom system is undergoing forced vibration at its natural frequency, or a continuous system is forced into one of its normal modes of vibration, and the forcing is suddenly removed then, neglecting transient effects and assuming the damping mechanism is linear, the amplitude of the vibration will decay exponentially. The logarithmic decrement is defined as the natural logarithm of the ratio of successive peaks. Thus

$$\text{Log. dec.} = \text{Log.}\ (x_1/x_2) \qquad (3.2.1)$$

where if x_1 occurs at time t, x_2 occurs at time $(t + 2\pi/\omega)$

In practice measurements over one cycle are generally not convenient; it is more desirable to let a time τ elapse before x_2 is observed. In this case

$$\text{Log. dec.} = \frac{\text{Log.}\ x_1/x_2}{f\tau} \qquad (3.2.2)$$

where f is the frequency of vibration.

This quantity can be simply related to the damping factor as follows.

Consider the single cycle of the decaying oscillation shown in fig. (2) and assume $\Delta x \ll x_1$.

The kinetic energy at 1 is given by $E_1 = \frac{1}{2} M x_1^2 \omega^2$ and that at 2 is given by $E_2 = \frac{1}{2} M(x_1 - \Delta x)^2 \omega^2$.

The energy dissipation due to damping is therefore given by

$$\Delta E = E_1 - E_2 \simeq M x_1 \Delta x \omega^2$$

therefore

$$\frac{\Delta E}{E_1} = 2\frac{\Delta x}{x_1} \qquad (3.2.3)$$

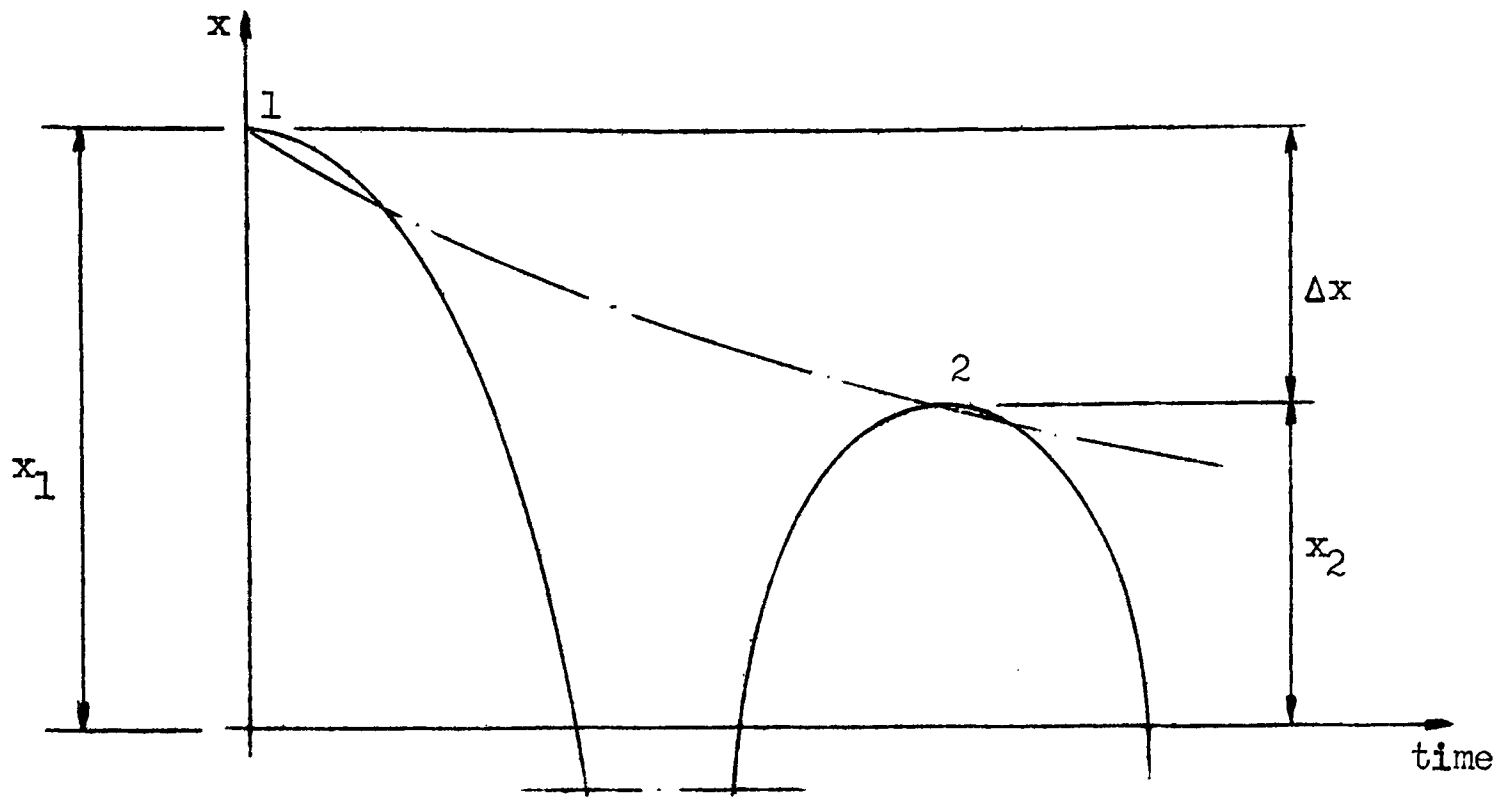

Fig. (2)

But from (2.0.5) $\frac{\Delta E}{E} = 2\pi Q^{-1}$, thus

$$Q^{-1} = \frac{1}{\pi}\frac{\Delta x}{x_1} \qquad (3.2.4)$$

Now the logarithmic decrement is by definition $\text{Log.}(x_1/x_2)$, then

$$\text{Log. dec.} = \text{Log.}\left(\frac{x_1}{x_1 - \Delta x}\right)$$

$$= -\text{Log.}\left(1 - \frac{\Delta x}{x_1}\right)$$

$$\simeq \frac{\Delta x}{x} \quad \text{for} \quad \frac{\Delta x}{x_1} \ll 1$$

Substituting this in (3.2.4) gives

$$Q^{-1} = \frac{1}{\pi} \cdot \text{Log. dec.} \qquad (3.2.5)$$

- - - o 0 o - - -

4.0 EXPERIMENTAL SET UP

Before discussing the experimental work it is expedient to describe the equipment used and to elaborate on the methods of exciting, detecting and recording the vibrations of the specimens. For convenience the methods of suspension are also treated in this section.

A block diagram of all the equipment used is shown in fig.(3): equipment specifications were as follows.

Decade oscillator: Muirhead-Wigan model D-890-A

Power amplifier: Goodman's: model P.A.50V.A.

Frequency counter: Venner: type TSA 3336

Frequency analyser: Bruel and Kjaer: Type 2107

Pre-amplifier: Bruel and Kjaer: Type 1606

Double beam oscilloscope: Cossor: model 1049 Mk. III.

F.M. Pre-amplifier: Southern Instruments: MR513

Oscillator: Southern Instruments: M785

Proximity Pickup: Southern Instruments: Inductive type

Vacuum pump: Speedivac: model 2S.20.

Vacuum guage: Genevac: type T.D.2.

Oscilloscope camera and motor unit: J. Langham-Thompson: series 205 type F.

Views of the equipment can be seen in Plates I and II.

4.1 METHOD OF EXCITATION

Excitation was carried out by means of a small electro-magnet; this was driven by a decade oscillator through a 50 V.A. amplifier. Also included in the circuit were an ammeter and a variable resistance. The primary function of these was to enable the current to the electro-magnet to be maintained at a constant value during any one resonance test.

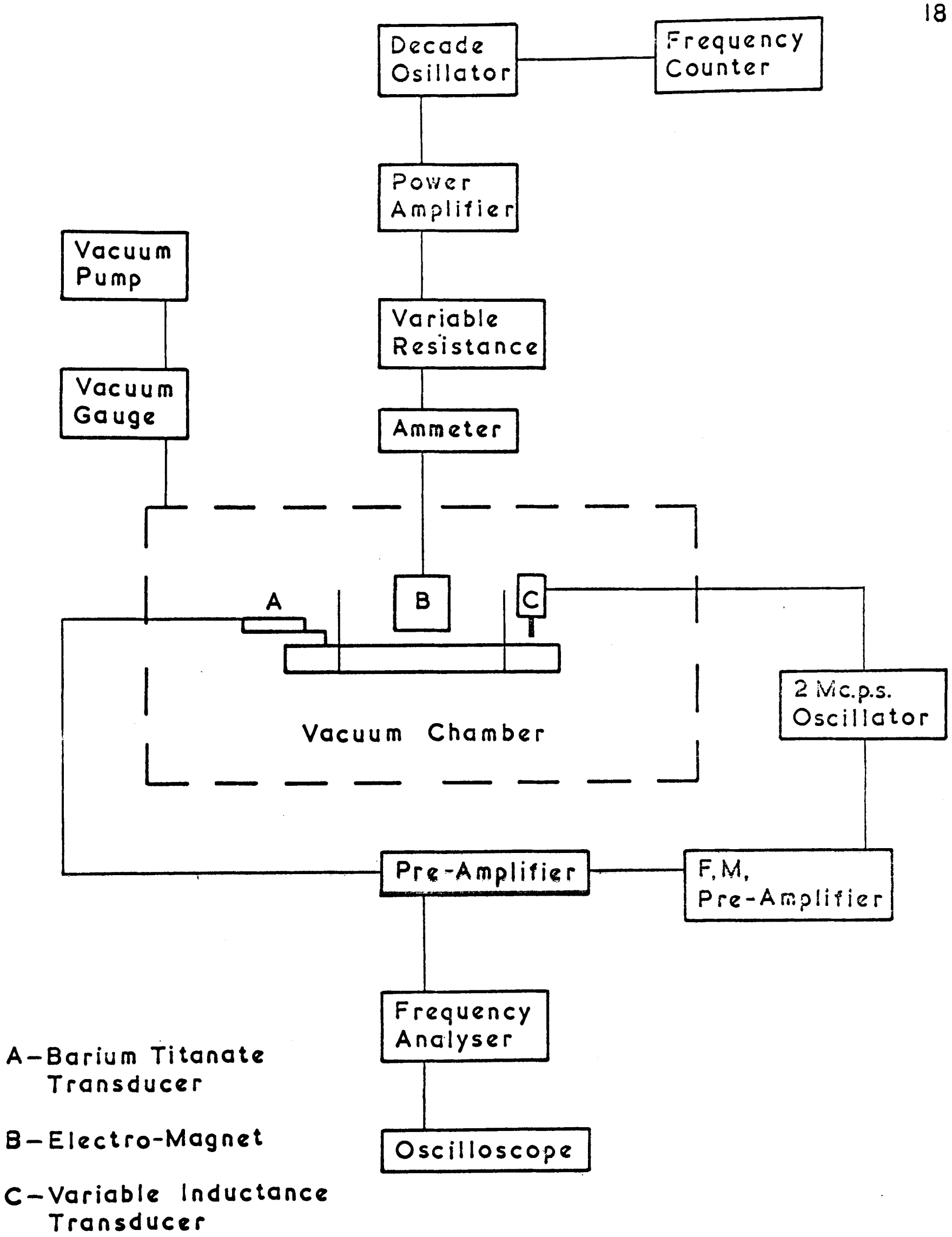

Block Diagram of Equipment

FIG (3)

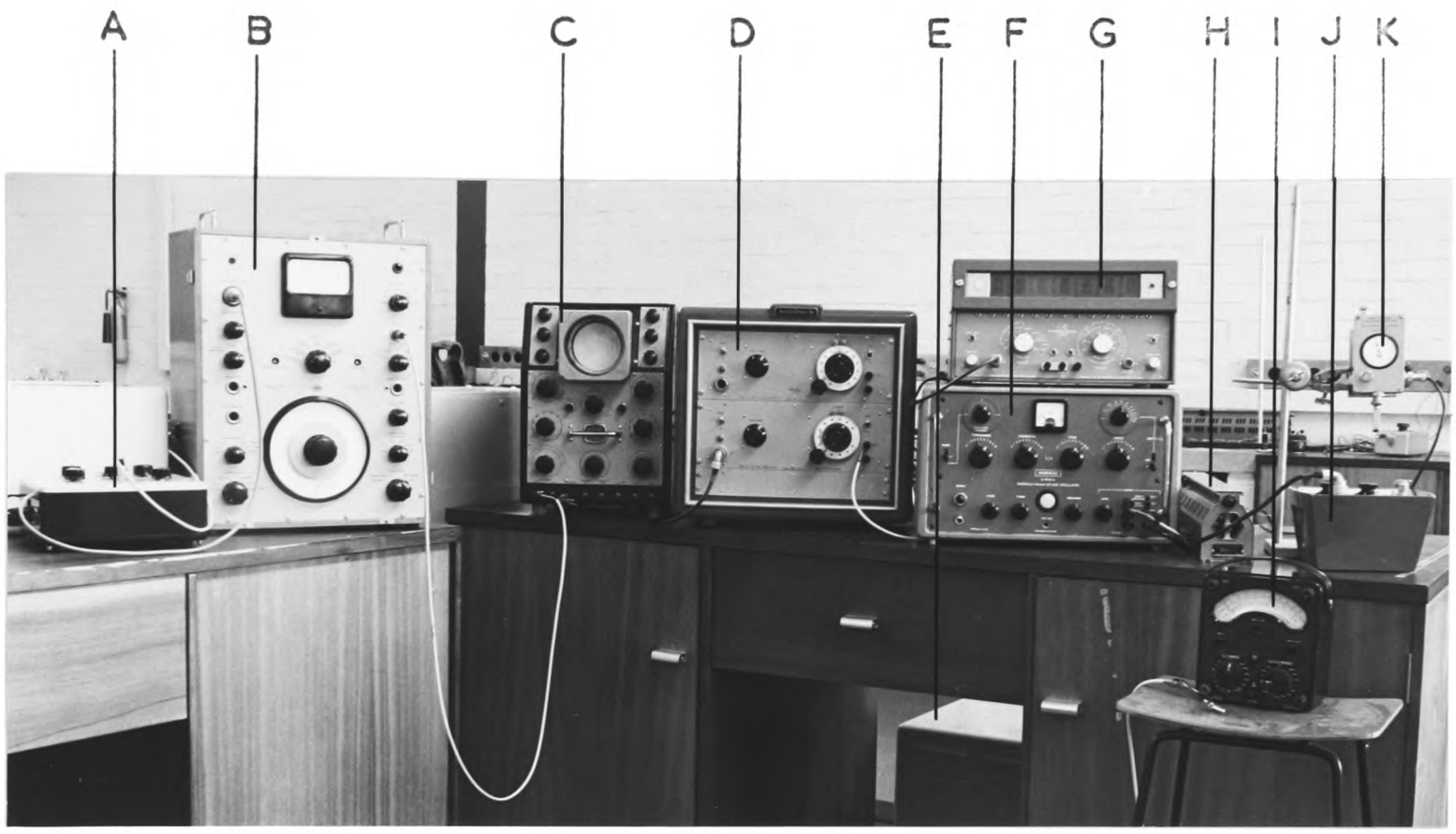

General View of Equipment

A — Pre-Amplifier

B — Frequency Analyser

C — Oscilloscope

D — F.M. Pre-Amplifier

E — Power Amplifier

F — Decade Oscillator

G — Frequency Counter

H — Variable Resistance

I — Ammeter

J — 2 Mc.p.s. Oscillator

K — Inductance Transducer

PLATE I

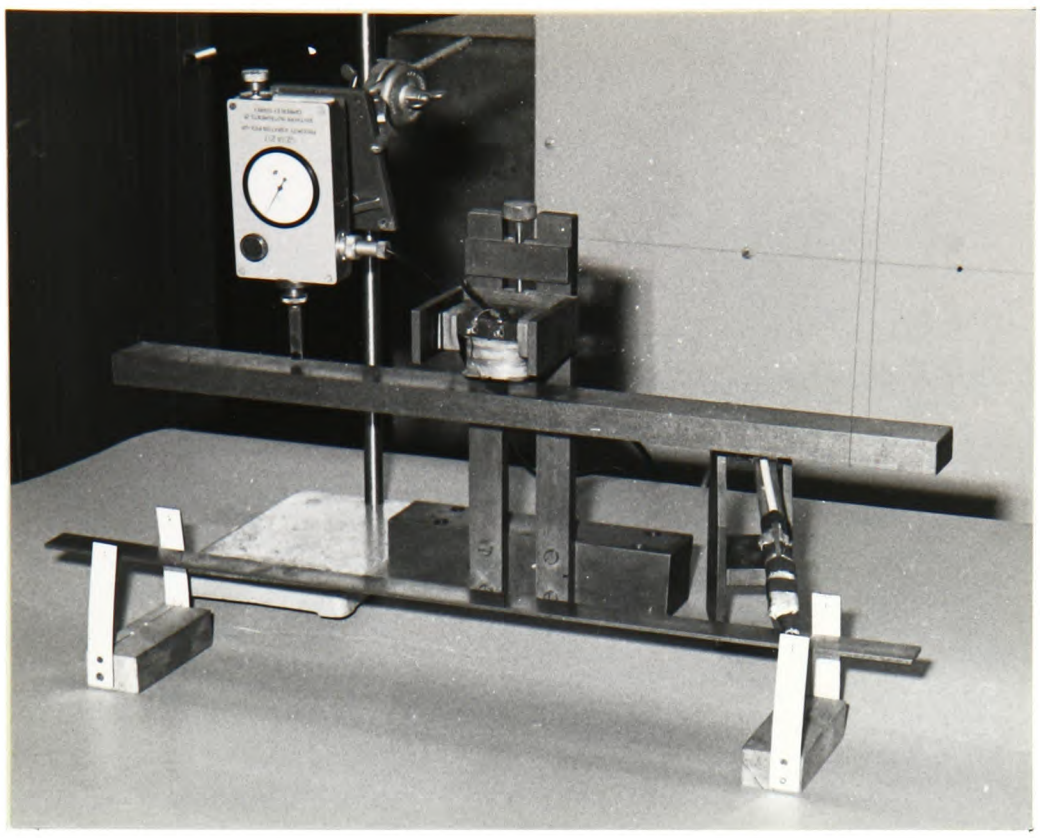

Transducers, Forcing Device and Suspension Systems

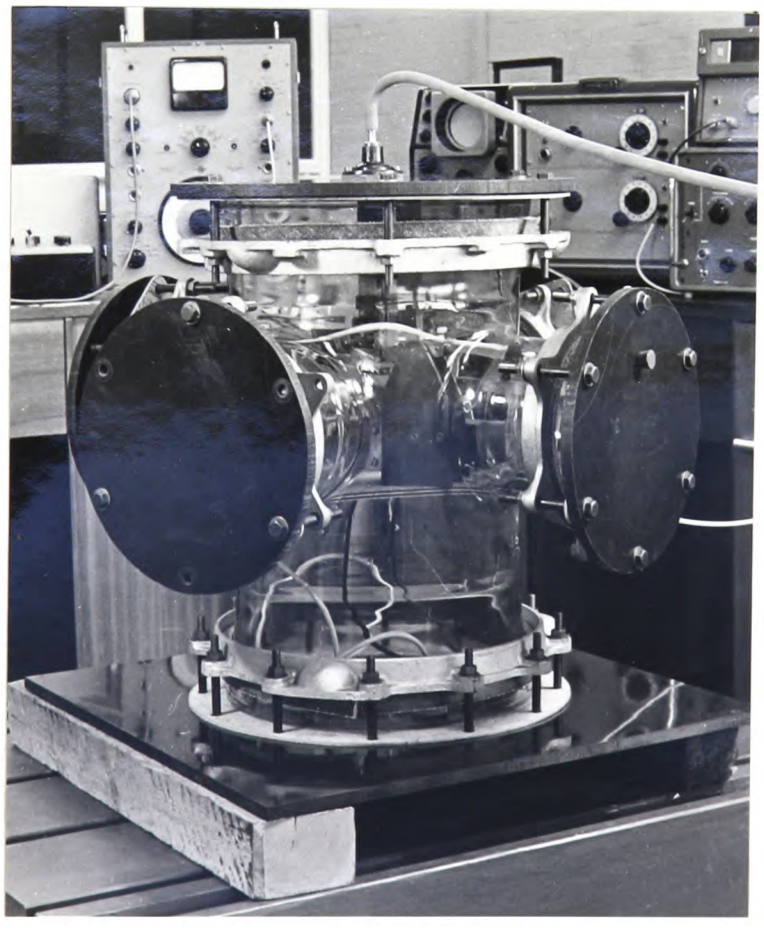

Vacuum Chamber

PLATE II

As the damping was small the difference between the resonant frequency and the frequencies at which the amplitude of vibration was half that at resonance, was very small; it was therefore considered that by maintaining constant current to the electro-magnet during a test, the driving force could also be considered constant.

The electro-magnet was mounted on a stand which permitted the air gap between magnet and specimen to be set at any desired value and the stand could be situated at any point along the length of the specimen.

4.2 METHODS OF DETECTION

Two methods of detecting the vibrations were used, namely;

(a) a method utilising a moveable barium titanate transducer.

(b) a method utilising a variable inductance transducer used in conjunction with a frequency modulated system.

These methods are described below.

4.2(a) BARIUM TITANATE TRANSDUCER

Briefly, the working principle of the transducer is that contact between the transducer and a vibrating surface causes a flexible arm to bend. The bending produces straining of the barium titanate crystal which, by virtue of its piezoelectric properties, converts the mechanical strains into voltage signals which may be amplified and displayed as required.

A diagramatic arrangement of the active section of the transducer is shown below.

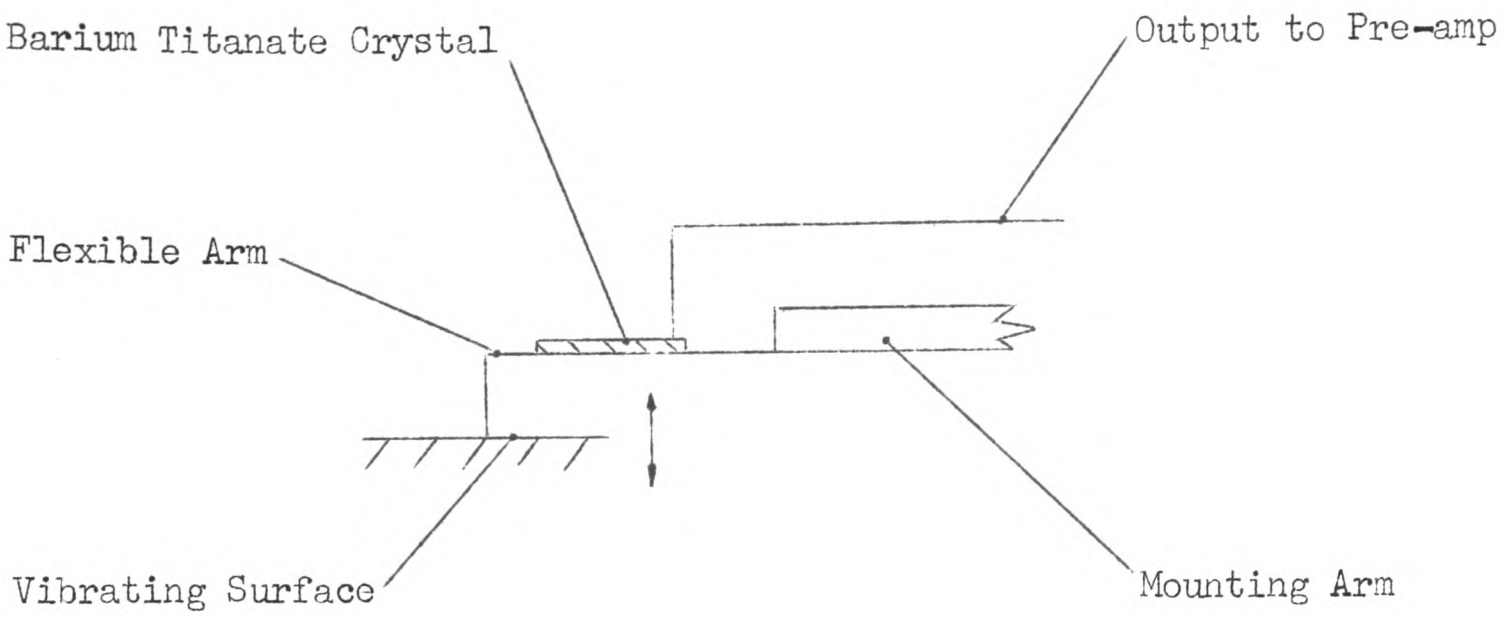

The active section comprises a flexible arm, in the form of a cantilever, to which the barium titanate crystal was secured by means of a suitable cement. This assembly was attached to a mounting arm which was in turn connected to a pivot block. The whole could be moved to any station along the length of the specimen and the flexible arm could be positioned at any point on the specimen. The output from the transducer was taken through a pre-amplifier to a frequency analyser; the output from the analyser was taken to an oscilloscope. A salient feature of the pre-amplifier was that the amplification was continuously variable thus enabling the meter reading on the analyser to be set at any convenient value during a resonance test.

An essential point in the construction of the transducer is that it shall be adequately shielded. It was found that without shielding a considerable amount of stray signals were picked up, particularly from the electro-magnet. Shielding was effected by placing earthing mesh or thin foil between two layers of insulating material and shrouding the active section of the transducer in this; the shield and the earth side of the transducer were taken to the same earthing point.

In all the experimental work it was by using this transducer that the modes were identified and the suspension nodes located.

4.2(b) VARIABLE INDUCTANCE TRANSDUCER

The system used is commercially available from Southern Instruments Ltd.

The details of the electronics of the system will not be considered here but a brief statement of the principle of operation is in order. The transducer forms part of the tuned circuit of an oscillator running at about 2 Mc.p.s. If the pick-up is situated close to a vibrating surface then the inductance between the pick-up and the surface will vary at the same frequency as that of the vibrating surface; such variations cause frequency modulation of the oscillator. The modulated signal from the oscillator is passed through an amplifying and limiting stage and is then fed on to a demodulating stage. The output from this stage may be displayed as required.

In this work the output from the demodulating stage was treated in the same manner as the output from the barium titanate transducer of 4.2(a).

The transducer could be situated at any point on the specimen but was generally sited as near to an antinode as possible in order that maximum output could be obtained.

The main difference between this method of detection and that of 4.2(a) is that the latter requires physical contact with the vibrating body whereas the former does not: when low damping is involved this could be an overriding consideration. It will however be shown that, by careful use of the barium titanate transducer, contact effects were reduced to a negligeable order over the greater part of the frequency range covered.

4.3 METHODS OF RECORDING

As stated in 3.0 two methods of measurement were used - the bandwidth method and the logarithmic decrement method.

The bandwidth method necessitates the performing of resonance tests from which the amplitude/frequency response may be plotted. Amplitude measurements were made on the voltmeter integral with the frequency analysing unit. (as only the relative values of amplitudes were required absolute calibration was unnecessary) Frequency measurements were made using a frequency counter fed by a decade oscillator. In general direct measurement of frequency gave inaccurate results due to the small changes of frequency involved but the counter used had a period measuring facility use of which allowed very small changes of period to be recorded very accurately.

In terms of periods the damping factor is given by

$$Q^{-1} = \frac{1}{\sqrt{3}} \frac{T_R(T_1 - T_2)}{T_1 T_2} \qquad (4.3.1)$$

where T_R is the resonant period

T_1 and T_2 are the periods below and above resonance respectively at which the amplitude of vibration is half that at resonance.

For the logarithmic decrement method the oscilloscope and cine-camera were used to record the decaying oscillations.

4.4 METHODS OF SUSPENSION

The experiments carried out involved the vibration of beams and rods in their bending and longitudinal modes of vibration over a given frequency range. The frequencies at which the modes of vibration occur may be fairly accurately calculated using classical

theories, such theories indicating the existence of a number of nodes depending on the mode of vibration; the nodes are points of zero motion. However classical theories generally ignore the effect of damping. As is evidenced by equations (2.0.6), in general, if damping is present the motions are affected by damping terms involving all the normal coordinates; therefore true nodes do not exist. If however the damping is small then, within the assumptions of small damping, equations (2.0.7) are indeed representative of the motion but the above is not designed to detract from theory it is merely an attempt to indicate that experimental determination of damping must proceed on the complete understanding that "nodal" motion does exist and should therefore be taken into account. (Other reasons for nodal motion are discussed in 5.4) In what follows the word "node" will be used freely but it will be defined as "a point of minimum motion".

Another point worthy of mention here is that in performing resonance tests vibration does not always occur at the resonant frequency. In consequence of this the longitudinal positions of the nodes will not remain fixed. If the damping is large such positional variation of the nodes could be considerable. If the original suspension points had been at the nodes at resonance it is clear that the off resonance motion of these points may introduce prohibitive damping effects. However if small damping is again assumed, it may be effectively considered that the positions of the nodes are fixed during any one resonance test.

The form of the suspension chosen will obviously depend on the nature of the experiment and the shape and dimensions of the specimens but the best form will be that which produces the lowest

measured damping factor.

In this investigation the greater part of the work was performed in the frequency range 500 c.p.s. to 20 Kc.p.s. For this reason it was desireable that the system comprising the specimen and suspension should have a very low natural frequency i.e. the stiffness of the suspension should be low. This requirement was adequately fulfilled by the forms of suspension described below.

For the experiments conducted in air the best form of suspension proved to be that illustrated in fig. (4 a-b). The suspension consisted of two long loops of 0.010 in. dia. piano wire, the suspension points being approximately 2 ft. 6 in. apart. The length of the loops was such that it was possible to support specimens at points

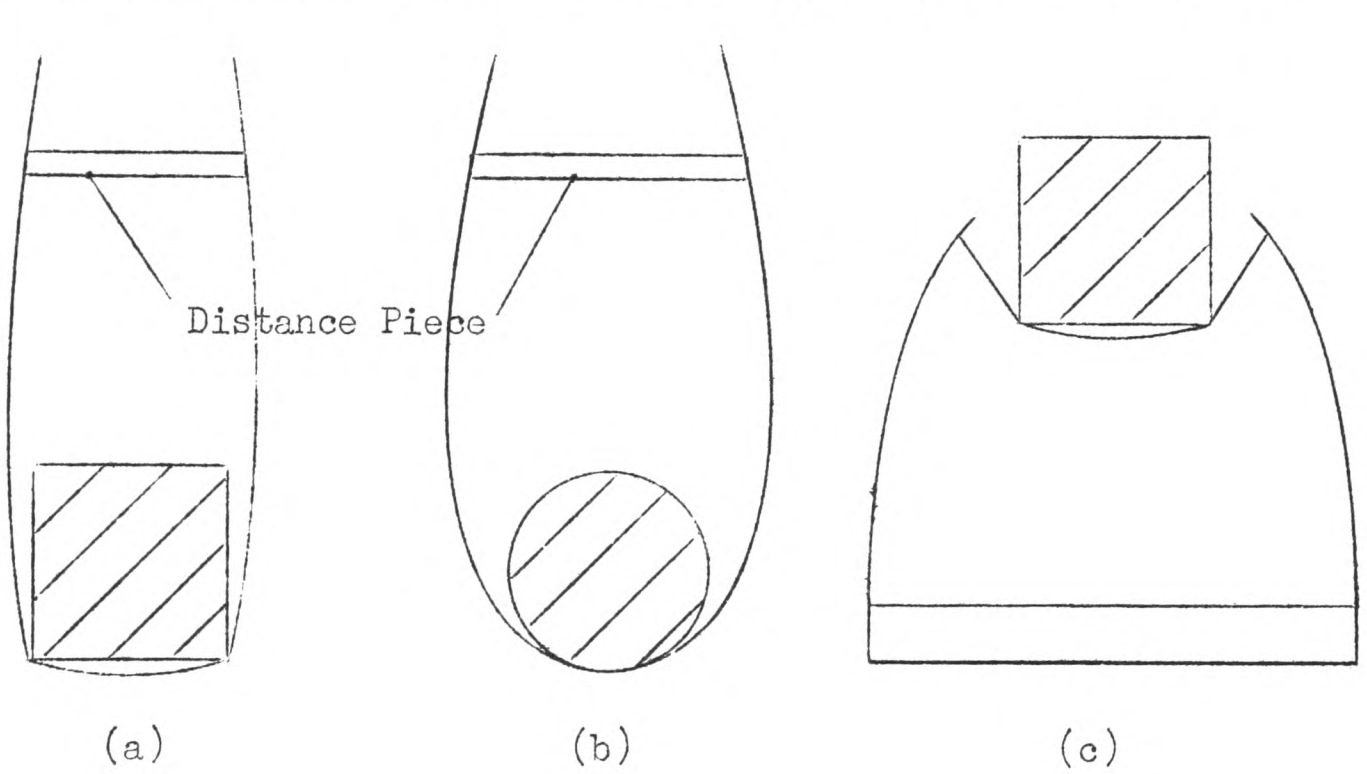

Fig. (4)

about 4 ft. apart if necessary. Piano wire was chosen in preference to cotton thread because, with all but the heaviest specimens, use of the distance piece ensured that only two point contact was made at each support node on the rectangular specimens and in the same way minimal contact was ensured on the circular specimens.

The above suspension system was not suitable for the experiments conducted in the vacuum chamber; it was necessary to design a new system and this is shown in fig (4 c). Again the suspension cord was of 0.010 in. piano wire this being connected to two arms which had a low stiffness: the arms were fixed to a base plate. This system had similar contact properties to the previous system.

Note: It was found that the form of suspension used for the longitudinal vibration experiments was not critical. This is probably accounted for by the fact that the nodes in longitudinal vibration were much less well defined than those in transverse vibration there being comparitively broad regions of essentially zero amplitude.

4.5 THE VACUUM EQUIPMENT

The vacuum chamber is shown in Plate II. This chamber was the most readily available piece of equipment large enough to contain the specimen, exciter and detector. It was possible, with the vacuum pump used, to obtain a chamber pressure of 50 m.m. Hg. fairly rapidly.

- - - o0 o - - -

5.0 PRELIMINARY EXPERIMENTAL WORK

In entering into an experimental programme it must first be decided what information is required and thence decided how such information may be obtained. For this particular investigation the information required, together with the scope of the work, has been set out in 1.0 leaving the problem of obtaining the information.

It was desired to study the damping of the vibrations of beams and rods of various cross sections over frequencies ranging up to 20 Kc.p.s. The intention was to study both internal and air damping and in designing the experiments it must be established that only these effects are present or that they may be isolated from all other effects.

It must first be decided what the boundary conditions on the specimens shall be. Obviously imposing any form of constraint on any boundary, e.g. the built in end of a cantilever, introduces parameters which may or may not be known, the effects of which may in either case be difficult to separate from the effects it is desired to observe. For this work it was therefore decided to maintain all boundaries free. To obtain the desired information the most convenient method would seem to be that of exciting the various normal modes of vibration of the specimens within the given frequency range and measuring the damping factor corresponding to each mode; this method was adopted. The next problem was that of suspension. For this work the method chosen was two node suspension: with this type of suspension, if it is assumed that energy transmission to the suspension is negligeable, the only damping present is that caused by the air and that inherent in the material of the specimens. The final considerations are those of exciting the

vibrations, detecting the vibrations and recording the necessary data; the methods adopted for each of these are described in 4.1 - 3.

In 4.4 it was stated that because of the cross coupling effects of damping no true nodes exist. This being the case there will always be losses to the suspension the magnitude of which may or may not be acceptable; it is required to ascertain the level of such losses. In positioning the suspension it is not always possible to be sure that it is situated exactly at a point of minimum motion hence a degree of arbitrariness is introduced into the suspension loss characteristic. It was deemed necessary that these and other considerations be looked into before the actual investigation should proceed.

The remainder of this section is therefore devoted to a series of experiments to ascertain the effect of various factors on the measured damping factor.

5.1 LINEARITY OF OVERALL DAMPING MECHANISM

If a continuous body is being forced to vibrate in one of its normal modes of vibration and the forcing is suddenly removed then, neglecting any transients which may be set up due to the removal of the force the vibration will decay in a manner and at a rate which depend on the nature of the damping forces; the whole process of decay will take place at the natural frequency of the mode. From a plot of amplitude of vibration against time of decay it may be established whether or not the damping mechanism is linear. If the mechanism is linear the ratio of any two consecutive peak amplitudes will be constant; any departure from constancy indicates the presence of some non-linear effect. (For small amplitude

vibrations it may confidently be expected that the internal damping will be linear but it cannot readily be assumed that the air damping will be linear also.)

For this experiment a rectangular cold rolled mild steel specimen was used: dimensions $1\frac{3}{8}$ in. wide, $\frac{3}{8}$ in. deep and 36 in. long.

The specimen was set on the suspension cords with its major axis horizontal. Using the electro-magnet a normal mode of bending was excited, detection being made by the barium titanate transducer. Using this transducer two nodes were located. The suspension was then moved to these node positions and the mode was again excited. This process generally resulted in a movement of the node positions; it was therefore necessary to relocate the nodes and to reposition the suspension. The procedure was repeated until no significant nodal movement was observed. This procedure was assumed to converge to the "true" nodes.

With the specimen vibrating in the mode, the amplitude of vibration being kept small, the transducer was positioned as near to a node as possible, consistent with being sufficiently far away to ensure a readable output. The output from the transducer was fed to a frequency analyser which was tuned to the frequency of vibration of the mode and the output from the analyser was fed into a C.R.O.. With the time base shut off the trace on the oscilloscope appeared as a vertical line. The oscilloscope camera was positioned, the film set in motion and the power to the electro magnet cut off. In this way the decay of the oscillation was recorded: the decay could also be visually observed on the meter integral with the frequency analyser.

Timing Signal 15·4 c.p.s.

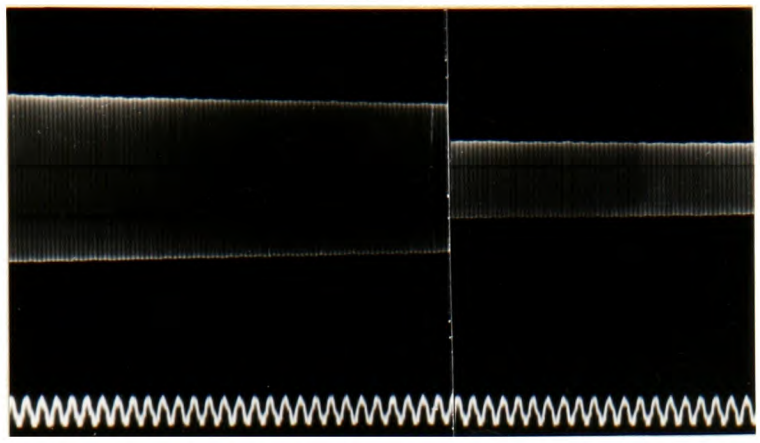

Frequency 309 c.p.s. $Q^{-1} = 0{\cdot}6 \times 10^{-4}$

Timing Signal 15·5 c.p.s.

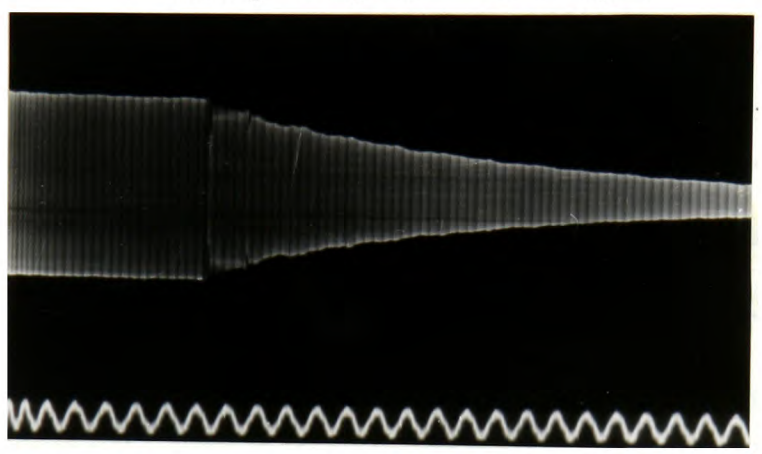

Frequency 2282 c.p.s. $Q^{-1} = 2{\cdot}0 \times 10^{-4}$

Timing Signal 30·9 c.p.s.

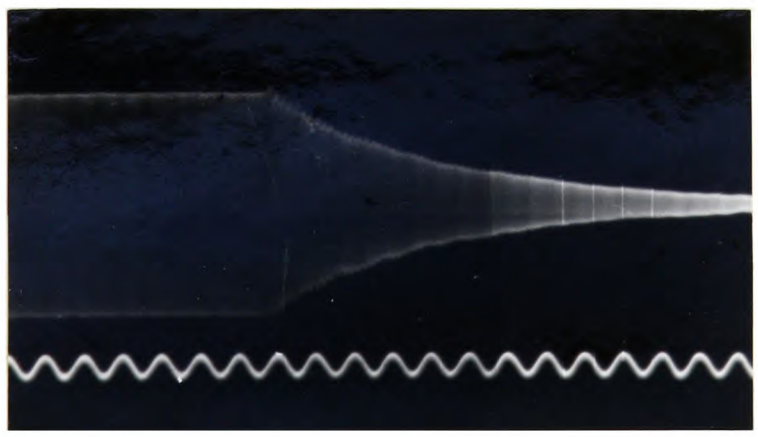

Frequency 8366 c.p.s. $Q^{-1} = 2{\cdot}7 \times 10^{-4}$

Typical Decrements Obtained From Free Vibration of Transverse Modes of $1\frac{3}{8}$ in. wide $\frac{3}{8}$ in. deep Cold Rolled Mild Steel Specimen.

PLATE III

In the above manner records were taken of the decays of a selection of bending modes at frequencies up to 10 Kc.p.s. Three typical decays are shown in Plate III.

Each trace was projected onto a screen and by comparing (for a given trace) the ratios of amplitudes at equal time intervals it was established that in all cases the oscillations decayed exponentially, i.e. the ratios of amplitudes at equal time intervals was constant.

It can thus be assumed that the overall damping mechanism is effectively linear.

5.2 COMPARISON OF RESULTS GIVEN BY THE METHODS OF DETECTION

As the use of different methods of detection was envisaged it was important to know to what extent the results given by the methods were comparable. There were two methods, one in which physical contact with the specimen was required - barium titanate transducer - and one in which no physical contact was required - variable inductance transducer: experiment was aimed at comparing the results given by the barium titanate transducer with the presumably more accurate results given by the variable inductance transducer.

It might be asked at this point 'why use two methods at all'? The answer will be apparent at the conclusion of this sub-section but it may be said here that over the greater part of the frequency range covered the amplitudes of vibration of the specimens were extremely small; and the output from the variable inductance transducer was correspondingly very small. To obtain a useable output reading very large amplification was required resulting in a large noise to signal ratio which, indeed, proved prohibitive. On the other hand use of the barium titanate transducer always ensured

a useable output with a low noise to signal ratio. However, as will be shown in what follows, the results from the barium titanate transducer, although reliable over the greater part of the frequency range covered, were not reliable over the <u>whole</u> of the range.

Cold rolled mild steel specimens were used. The dimensions of the specimens were,

Specimen N°1. : 1 in. wide, $\frac{1}{4}$ in. deep, 24 in. long

Specimen N°2. : $\frac{1}{4}$ in. wide, $\frac{1}{4}$ in. deep, 24 in. long

These specimens were chosen because they were representative of the lower and middle ranges of the mass/unit length (hereafter referred to as the 'specific mass') scale of specimens to be used in the final investigation: also their mode shape/frequency characteristics would be almost identical.

The logarithmic decrement method of measurement was used throughout.

The procedure for setting the specimens vibrating in their normal bending modes was identical to that of 5.1. The decrements were either recorded as in 5.1 or, using a stop watch, the time taken for the amplitude to decay to a set fraction of some initial value was noted (this practice was permissable since linearity of the overall damping mechanism was proved in 5.1). The damping factor was calculated using equation (3.2.5).

Two decrements were taken for each mode of vibration - one using the variable inductance transducer and one using the barium titanate transducer.

The results obtained are shown in Tables (1) and (2).

It can be seen from these tables that at the lower frequencies the values of Q^{-1} given by the barium titanate transducer are somewhat higher than those given by the variable inductance

SPECIMEN N°1 - 1 in. wide, $\frac{1}{4}$ in. deep

MODE	FREQUENCY c.p.s.	DAMPING FACTOR - Q^{-1} VAR. IND. TRANS.	BAR. TIT. TRANS.
1	90	0.9×10^{-4}	1.2×10^{-4}
2	250	0.9 "	1.1 "
3	492	0.9 "	0.9 "
4	815	0.8 "	0.8 "
5	1230	0.8 "	0.9 "

TABLE (1)

SPECIMEN N°2 - $\frac{1}{4}$ in. wide, $\frac{1}{4}$ in. deep

MODE	FREQUENCY c.p.s.	DAMPING FACTOR - Q^{-1} VAR. IND. TRANS.	BAR. TIT. TRANS.
1	90	1.3×10^{-4}	1.7×10^{-4}
2	249	1.2 "	1.5 "
3	491	1.1 "	1.3 "
4	810	0.9 "	1.2 "
5	1209	0.9 "	1.1 "
6	1680	1.0 "	1.1 "
7	2230	1.0 "	1.1 "
8	2860	0.9 "	1.0 "

TABLE (2)

transducer but as the frequency is increased the results givenby both methods converge on each other. Beyond the modes given in the tables the results from each of the methods corresponded. It can

also be seen that the results from specimen N°1 converge much more quickly than do those of speciment N°2. This would seem to indicate that contact effects become more serious the smaller the specific mass of the specimen.

The identification of modes and location of nodes always required use of the barium titanate transducer. It would therefore seem clear that sole use of this transducer for as much of the experimental work as possible would be desireable. However, as can be seen from the foregoing, this transducer does not give dependable results over the whole of the frequency range to be investigated. It thence seems reasonable to suggest that the following procedure be adopted during the experimental work.

(1) Up to the frequencies at which the results given by the two methods of detection correspond, for a given specimen, only the variable inductance transducer should be used.

(2) Beyond the frequencies at which the results correspond only the barium titanate transducer need be used.

5.3 COMPARISON OF RESULTS GIVEN BY THE METHODS OF MEASUREMENT

To date only one method of measurement has been used that being the logarithmic decrement method. This method is for the most part very time consuming it being necessary beyond about 1000 c.p.s. to photograph the decrements, develop the films and then to analyse the film. In general below about 1000 c.p.s. the time taken for a given initial amplitude to halve itself was sufficiently long for fairly accurate decrement times to be measured, using a stop watch,

from visual observations of the decrements on the voltmeter. As the frequency increased the decrement times became extremely small and the whole process of recording decrements gradually became quite prohibitive (around 10,000 c.p.s. was the limit to which the logarithmic decrement method could satisfactorily be extended).

To obviate the necessity of recording decrements resort was made to resonance tests but before doing so it was considered adviseable to conduct an experiment to ascertain how the two methods of measurement compared; such is the nature of this experiment.

Here specimens representative of the upper and lower ranges of the specimen specific mass scale were used. These were,

Specimen N°1: $1\frac{3}{8}$ in. wide, $\frac{3}{8}$ in. deep, 36 in. long

Specimen N°2: $\frac{1}{4}$ in. wide, $\frac{1}{4}$ in. deep, 24 in. long

The specimens were vibrated in their normal modes of bending in accordance with the procedure of 5.1. For each mode of vibration a resonance test and a logarithmic decrement test were performed the methods of detection being used in accordance with the findings of 5.2. In performing the resonance tests it was necessary, at the lowest frequencies, to plot amplitude/frequency curves and to extract from the curves the resonant frequency and the bandwidth at half the resonant amplitude. As the frequency increased it was only necessary to follow the following procedure,
(a) set a specimen vibrating in a normal mode and note the frequency
(b) with the frequency analyser tuned to the frequency of the mode set the transducer output reading on the voltmeter to some convenient value (this then corresponds to the resonant amplitude)

(c) increase/decrease the driving frequency until the amplitude reading is half the set initial value and note the frequencies - the difference of these frequencies gives the bandwidth. Tho damping factor can now be calculated using equations (3.1.8) or (4.3.1). The logarithmic decrements were recorded as in the previous sub-sections.

The results obtained are shown in Tables (3) and (4).

From the tables it can be seen that the bandwidth method tends to give higher values than the logarithmic decrement method at the lower frequencies but that the results given by both methods converge on each other as the frequency is increased. Beyond the modes given in the tables the results from both methods corresponded.

SPECIMEN N^{o}1 - $1\frac{3}{8}$ in. wide, $\frac{3}{8}$ in. deep

MODE	FREQUENCY c.p.s.	DAMPING FACTOR - Q^{-1} BANDWIDTH	LOG. DEC.
1	57	1.1×10^{-4}	0.8×10^{-4}
2	159	0.9 "	0.7 "
3	309	0.8 "	0.6 "
4	514	0.7 "	0.6 "
5	780	0.7 "	0.6 "
6	1074	0.6 "	0.5 "
7	1442	0.7 "	0.7 "
8	1829	1.0 "	0.9 "
9	2282	1.9 "	2.0 "

TABLE (3)

SPECIMEN N°2 - $\frac{1}{4}$ in. wide, $\frac{1}{4}$ in. deep

MODE	FREQUENCY c.p.s.	DAMPING FACTOR - Q^{-1} BANDWIDTH	LOG. DEC.
1	90	2.0×10^{-4}	1.3×10^{-4}
2	249	1.7 "	1.2 "
3	491	1.6 "	1.1 "
4	810	1.3 "	0.9 "
5	1209	1.1 "	0.9 "
6	1680	1.1 "	1.0 "
7	2230	1.1 "	1.0 "
8	2860	1.1 "	0.9 "
9	3570	1.1 "	1.1 "
10	4350	1.3 "	1.2 "

TABLE (4)

It can also be seen that the rate of convergence of the results depends on the dimensions of the specimens i.e. the smaller the specific mass of the specimen the longer do the results take to converge.

The above results are similar in character to those obtained in 5.2 and therefore in the same way as in 5.2, the following experimental procedure was adopted.

(1) Up to the frequencies at which the results given by the two methods of measurement corresponded, for a given specimen, only the logarithmic decrement method was used.

(2) Beyond the frequencies at which the results corresponded only the bandwidth method was used.

5.4 SUSPENSION LOSSES

The definition of a node given in 4.4 was "a point of minimum motion". To appreciate better the significance of this statement, consider what happens at a node when a beam is vibrating.

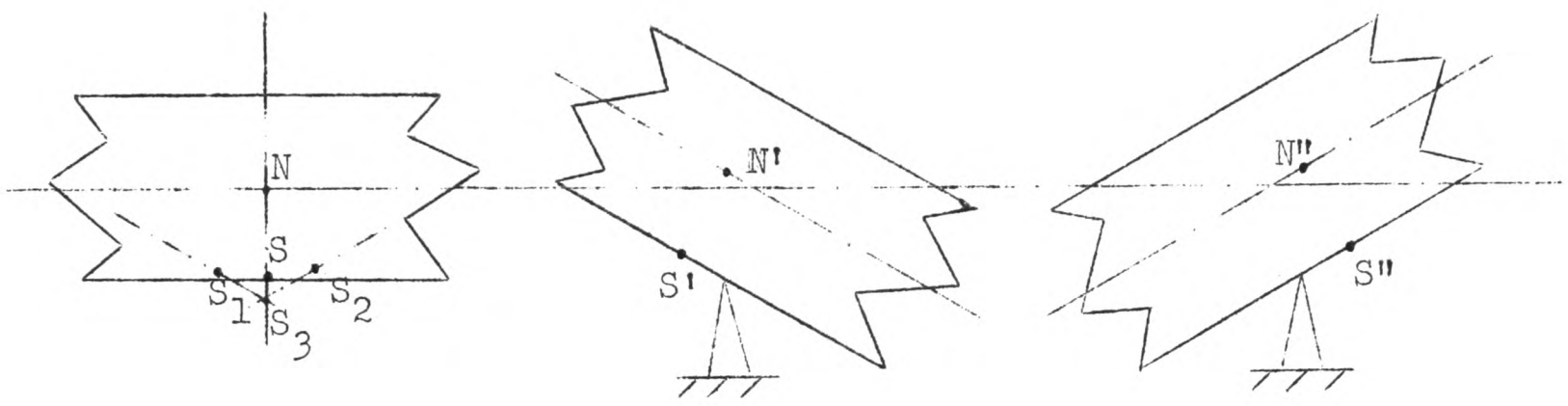

(a) (b) (c)

Fig. (5)

Refering to fig.(5a) let s be a point on the outer fibre of the beam and let N be a point on the neutral axis in the same plane as s. If this is considered to be a nodal plane then, if there is no damping and the specimen is vibrating in free space with no suspension, tho point N will, to a first order approximatinn, remain stationary; the point s will move in the path s_1 s s_2. It is seen from this that even with no damping there is motion at the "node" when the depth of the beam is taken into account: the amplitude of the motion is given by s s_3. If a rigid suspension system is now introduced it can be seen from (b) and (c) that the contact point between the suspension and the beam slides between s'

and s". It can also be seen that the whole beam is given vertical translation. Both of these effects require energy to sustain them thence their ultimate effect is to damp the vibration. Adding internal and air damping produces further nodal motion which in turn causes further losses to the suspension. It is thus clear that the introducation of any form of suspension results in losses; such losses can only be minimised they cannot be removed altogether. Obviously a rigid suspension system is a poor choice - what should in fact be sought is a system with a low vertical stiffness to minimise translatory effects and the system should also have some degree of freedom in the direction of the axis of the beam in order that it maintain single point contact or that it reduce the degree of sliding.

Note: The foregoing has been included simply to illustrate the points regarding nodal motion and its possible consequences but it should be remembered that when the amplitudes of vibration are small the losses may also be small.

Having established the above and designed the suspension, the problem of positioning the suspension remains.

As stated in 5.0 the positioning of the suspension is to some degree arbitrary it being impossible to ensure that the suspension is always positioned on the point of minimum motion. It was therefore decided to conduct an experiment to ascertain how critical the suspension position was.

A specimen was vibrated in a normal bending mode and the suspension positioned, as accurately as possible on the nodes, as in 5.1: the damping factor was measured. The suspension was then moved in stages to $\frac{1}{8}$ in. on either side of the nodes and the damping

factor at each stage measured. (It should be said here that such movements of the suspension caused negligeable changes in the natural frequency of the mode and also that when the barium titanate transducer was being used its position on the specimen was the same for each stage). The damping factor at each stage was compared with the initial damping factor and the difference recorded as a percentage error. This procedure was carried out in a selection of the bending modes of various specimens with different cross sections.

The experiment showed that the smaller the specific mass of the specimen and the lower the order of the mode the more critical did the suspension position become. The greatest error obtained occured in the first mode of the $\frac{1}{4}$ in. wide $\frac{1}{4}$ in. deep specimen: the magnitude of the error was approximately 20% when the suspension was $\frac{1}{8}$ in. from the nodes. By the fourth mode this error had reduced to about 5%.

Overall, the results obtained allowed the following generalisation to be made. If the suspension is always placed within 1/16 in. of the nodes then the measured damping factors will, over the greater part of the frequency range, be within approximately 5% of the "true" values.

5.5 EFFECT OF POSITION OF BARIUM TITANATE TRANSDUCER

In the same way as in 5.4, where the effect of the position of the suspension with respect to the nodes was considered, it was also necessary to consider the effect of the position of the barium titanate transducer.

The experiment was conducted as in 5.4 but in this case the suspension position was fixed while the transducer was moved in

stages to $\frac{1}{8}$ in. on either side of a node.

Again the position became more critical the smaller the specific mass of the specimen and the lower the order of the mode. In the very low frequency range the transducer had a distinct tendency to bounce on the specimens but the findings of 5.2 suggest that this transducer will not be used in this range.

The results obtained again allowed the generalisation that, in the frequency range where this transducer is likely to be used, results within about 5% of the "true" values may be expected if the transducer is always placed within 1/16 in. of a node.

5.6 MODE INTERACTION

If the electro-magnet is considered to be driven by a sinusoidal voltage then the flux density in the magnet must also vary sinusoidally. Owing to the shape of the B-H curve of the magnet core material the magnetising current waveform will not be sinusoidal and, since the magnetic force depends on this current, it also will not be sinusoidal. This means that the excitation system, although subject to a purely sinusoidal input, will not give a purely sinusoidal force output in consequence of which the output may contain significant or insignificant amounts of the harmonics of the input fundamental depending on the degree of distortion. The danger in this situation is that although a specimen may be vibrating predominantly in a given mode there could conceivably be significant amounts of other modes present (driven by the harmonics of the output) which may lead to erroneous experimental results. This experiment was designed to give a clearer picture of the importance of these effects in the experimental work.

Since the longitudinal modes of vibration of a rod are, theoretically, harmonically related it was thought that mode interaction would be most likely to occur with this type of vibration. A rod was selected and its 2nd and 6th mode frequencies were found experimentally to be 2420 c.p.s. and 7260 c.p.s. respectively: these frequencies will be referred to as ω_2 and ω_6. Consider the second mode (the rod was suspended at the second mode nodes). If the force is non-sinusoidal it may, neglecting the D.C. component, be represented by a Fourier series of the form

$$P_0 = P_1 \sin \omega t + P_2 \sin 2\omega t + P_3 \sin 3\omega t + \ldots\ldots\ldots$$

where ω represents the frequency at which the electro-magnet is driven.

With $\omega = \omega_2$ and the frequency analyser tuned to ω_2 the second mode of the rod was easily excited; the measured damping factor was,

$$Q^{-1} = 0.33 \times 10^{-4}$$

With the rod vibrating steadily in the mode the frequency analyser was tuned to $2\omega_2$, $3\omega_2$, etc. but no significant amplitudes were measured.

The analyser was re-tuned to ω_2 and with $\omega = \frac{1}{2}\omega_2$ it was again possible to excite the second mode: this means that the second mode of the rod has been excited using the second harmonic of the driving force. The measured damping factor was,

$$Q^{-1} = 0.31 \times 10^{-4}$$

With the rod vibrating steadily in the mode the frequency analyser was tuned to $\frac{1}{2}\omega_2$, $\frac{3}{2}\omega_2$, etc. but no significant amplitudes were measured.

Procedure akin to the above was carried out in the 6th longitudinal mode of the rod: in this case the driving forces could be represented by,

(a) $P_0 = P_1 \sin\omega_6 t + P_2 \sin 2\omega_6 t + P_3 \sin 3\omega_6 t + \ldots\ldots\ldots$

(b) $P_0 = P_1' \sin\tfrac{1}{2}\omega_6 t + P_2' \sin\omega_6 t + P_3' \sin\tfrac{3}{2}\omega_6 t + \ldots\ldots\ldots$

(c) $P_0 = P_0'' \sin\tfrac{1}{3}\omega_6 t + P_2'' \sin\tfrac{2}{3}\omega_6 t + P_3'' \sin\omega_6 t + \ldots\ldots\ldots$

In (a) the fundamental of the driving force is being used to excite the mode, in (b) the second harmonic is being used and in (c) the third harmonic is being used.

The results obtained were:

corresponding to (a) $Q^{-1} = 0.42 \times 10^{-4}$

" to (b) $Q^{-1} = 0.44 \times 10^{-4}$

" to (c) mode not excitable

No significant amplitudes were measured at any frequencies other than the mode frequency.

The experiment shows that whether the fundamental or a harmonic of the driving force is used to excite a mode the damping factors will be essentially the same. The fact that no significant amplitudes were recorded at other than the mode frequencies shows that the modes are almost pure and would consequently suggest that the force can be considered to be sinusoidal.

The first conclusion to be drawn from the results is that mode interaction from the above source is not as likely to occur as may have originally been feared. It seems that the problem may only become serious when, for example, the frequency of the mode being excited is ω and the fundamental frequency of the driving force is ω then, if any other mode frequencies are <u>exactly</u> equal to $n\omega$

(n = 2, 3, ...), two or more modes will be excited their relative amplitudes depending on the magnitudes of their respective coefficients in the expression for the driving force. Also, if the frequency of a mode which has high damping is almost an integer multiple of ω then a significant amount of this mode may be excited. Although the experiment did not illustrate any of these effects it cannot be assumed that they will at no time occur. In the experimental work it was therefore deemed adviseable that spot checks be carried out by sweeping the analyser through a wide frequency range to establish whether the only significant amplitudes occur at the frequency of the mode being excited.

5.7 LENGTH EFFECT

For any given specimen cross section what effect will length have on the results? This question must be answered in order that the importance of the length of the specimens used in the experimental work be established i.e. it is wished to ascertain whether the length of the specimens is a parameter.

To do this two rods with equal diameters but different lengths and two rectangular beams with equal cross sectional dimensions but different lengths, were used. The former were vibrated in their longitudinal modes and the latter in their bending modes at frequencies up to 20 Kc.p.s. All the specimens were of cold rolled mild steel.

Taking into account all that has gone before, the damping factors corresponding to each mode were measured. The results obtained are shown in fig. (6). These show that changing the length of a specimen has no significant effect on the damping factor/

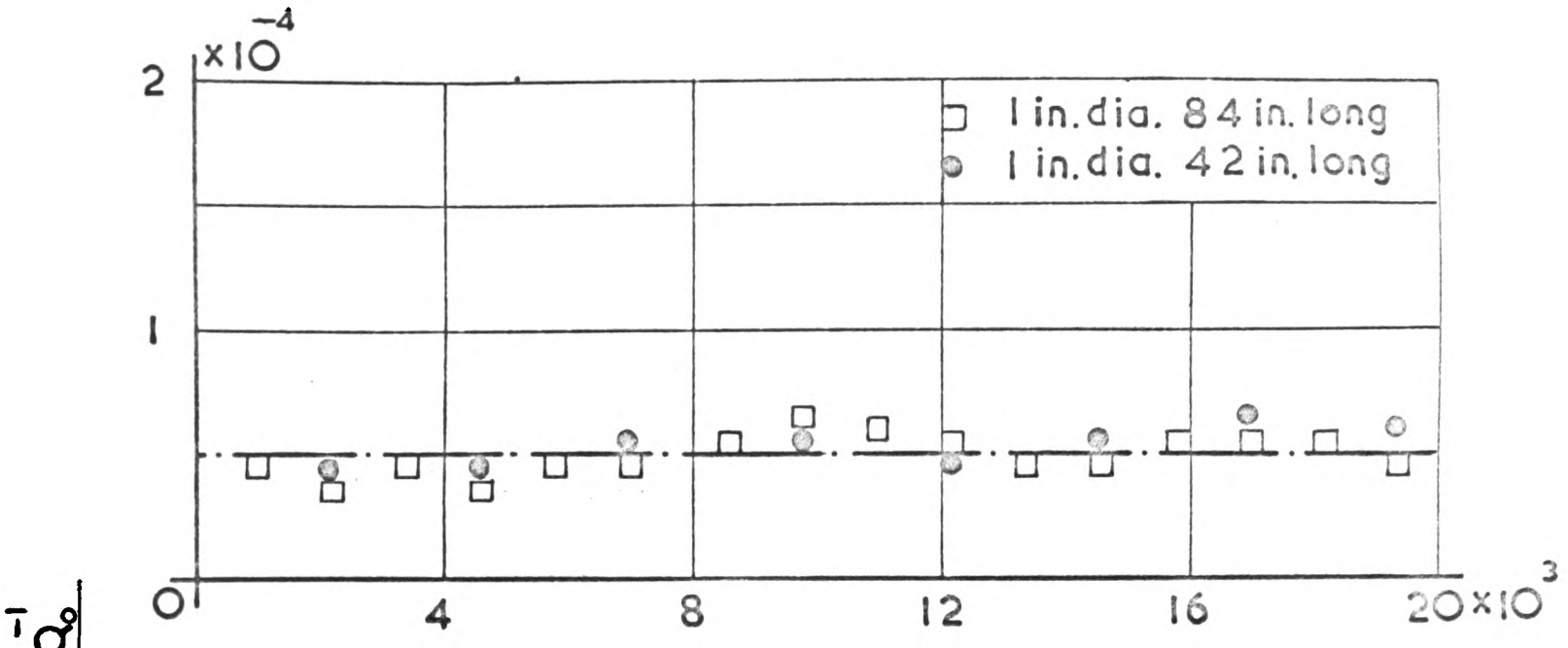

(a) Longitudinal Vibration

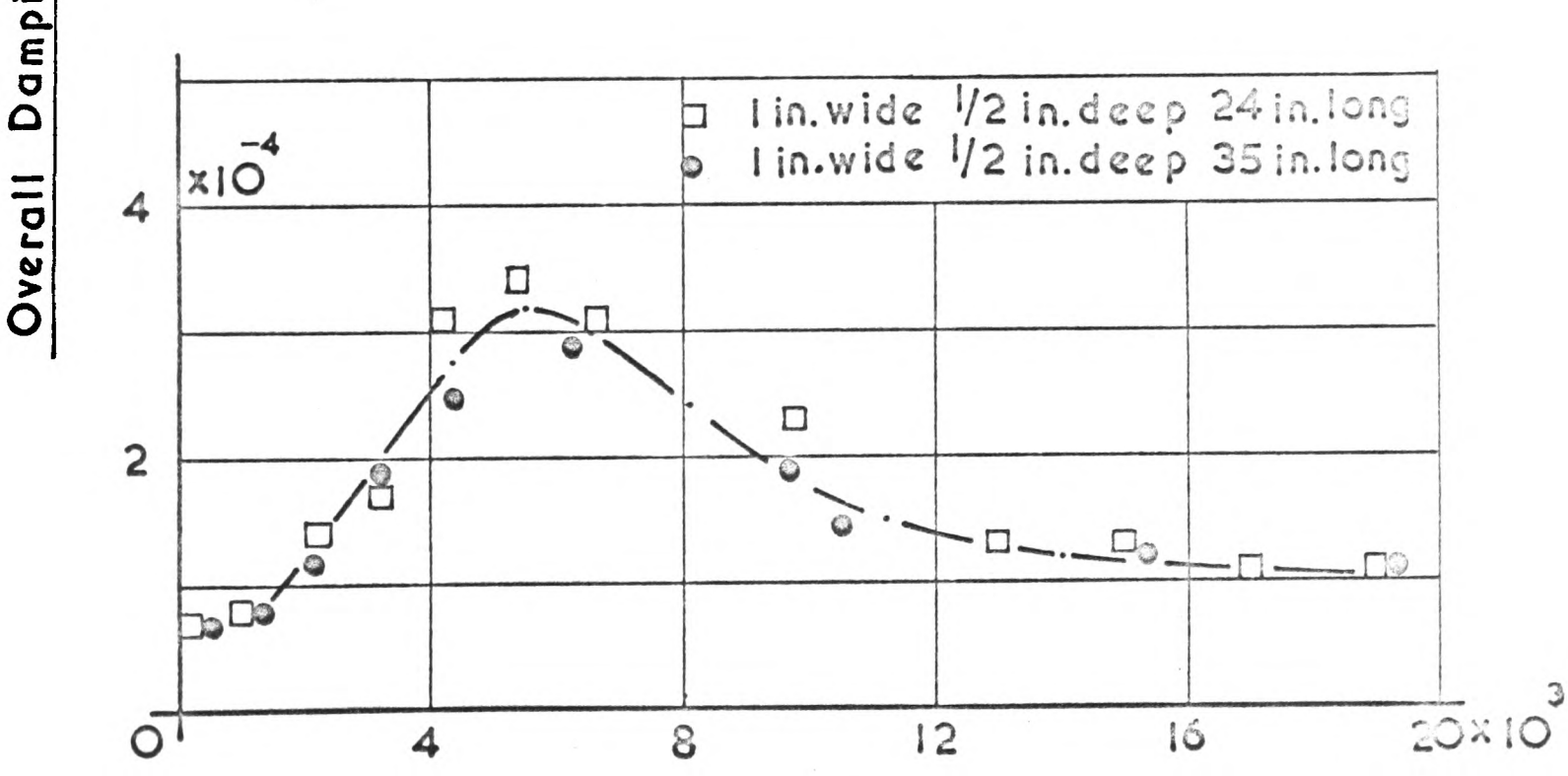

(b) Transverse Vibration

FIG (6)

frequency characteristic and therefore that the length is not a parameter. Hence in the experimental work any convenient length of specimens may be used.

5.8 MISCELLANEOUS ASPECTS

Finally, a consideration will be made of some of the aspects not as yet treated in detail.

(i) In the foregoing reference has been made to "true" values of the damping factors. The word true is intended to imply that such values of the damping factors are the minimum values it is possible to measure using the existing experimental set up.

Because there are always losses at the suspension points (the losses can only be minimised, not removed) the measured damping factors must exceed the actual damping factors; to establish the absolute amount of this excess would require extremely refined experimentation. However, the main source of losses is friction between the suspension and the specimen and if this existed in any significant quantity it would manifest itself as a nonlinearity in the damping mechanism. In 5.1 it was shown that when the amplitudes of vibration are small the damping mechanism is in fact linear. It would therefore seem reasonable to assume that suspension losses are for the most part very small and thence that the measured damping factors are essentially the same as the actual damping factors.

(ii) In all the experimental work the outputs from the transducers were fed through a frequency analyser. For ease of operation during resonance tests a pre-requisite of the analyser is that its Q factor should be much less than the Q factor being measured.

The reason for this will be best seen by considering a very narrow bandwidth analyser to be in use when a highly damped mode of a specimen is being excited. Any slight deviation from the resonant frequency will little affect the amplitude of vibration of the specimen but the analyser output may drop considerably; to find what the true output corresponding to the new frequency is it would be necessary to re-tune the analyser. This procedure would obviously be very laborious during normal resonance tests.

(iii) One cause of mode interaction has already been discussed in 5.6: mode interaction may also occur as a result of the frequency of excitation being such that two modes very close to each other are excited. When exciting the transverse modes of the cylindrical beams it was often found that the response curve had two distinct peaks. The reason for this was attributed to the fact that the general inhomoginuity of the specimens could be considered to give rise to two orthogonal principal inertia planes. The natural frequencies in each of these planes would be very close and if excitation took place in a plane between the principal planes the response curves would frequently display two peaks. Obviously damping factors measured from such response curves would be erroneous. To eliminate one of the peaks the specimens were simply rotated until vibration took place in one of the principal planes only (it was established that, for any given mode of vibration, the damping factors in each of the principal planes had the same value).

In the case of the rectangular beams mode interaction, when it occured, was generally the result of a bending mode and a torsional mode being excited simmultaneously. Due to the nature of the electro-magnet, which could not be considered to be applying a point force,

it was not normally possible to separate the modes in consequence of which the damping factors, corresponding to the particular frequencies at which such mode interaction occured, could not be measured.

(iv) In 5.1 it was established that, for small amplitudes of vibration, the overall damping mechanism was linear. This being the case and not at this stage wishing to introduce amplitude dependant effects it was essential that work was always carried out in the linear region. It was therefore desireable that a reasonably quick method of carrying out spot checks be available. The method used was as follows. With a specimen vibrating in a given mode at a given amplitude a damping factor was measured. The amplitude was then respectively doubled and halved and damping factors corresponding to these amplitudes measured. If work is being performed in the linear region the damping factors so measured will have equal values.

- - - o O o - - -

5.9 SUMMARY OF PRELIMINARY EXPERIMENTAL WORK

The preliminary work has

(a) compared the two methods of detection and indicated when each may be used.

(b) compared the two methods of measurement and indicated when each may be used.

(c) discussed suspension losses and shown how they will affect the results.

(d) shown to what extent transducer contact will affect the results.

(e) discussed the principal causes and effects of mode interaction.

(f) discussed some miscellaneous aspects.

(g) established that;

(i) for small amplitudes of vibration the overall damping mechanism is linear.

(ii) for a given specimen cross section the damping factor corresponding to any particular frequency is independant of the length of the specimen.

The main investigation can now be approached with a much improved understanding of the problem as a whole and the nature of the experimental difficulties likely to be encountered.

- - - o O o - - -

6.0 EXPERIMENTAL DETERMINATION OF OVERALL DAMPING FACTOR

The work of this section will be considered under three headings: the first concerns only the longitudinal vibration of rods and the remaining two concern the transverse vibration of cylindrical beams and rectangular beams respectively.

The procedure throughout was essentially that described in 5.1 but the methods of detection and measurement were used in accordance with the findings of 5.2 and 5.3 respectively. Due regard was also taken of the findings and the proposals made in the remainder of the preliminary work.

The specimens used were all of cold rolled mild steel.

All the experimental results obtained from the transverse vibration work are shown in the sections comparing theory with experiment, therefore, to avoid undue repetition only results characteristic of those obtained in the transverse work will be given here.

No attempt is made at this stage to explain the results but the relevent features of the overall damping factor/frequency characteristics obtained are noted. Fuller discussion is deferred until section 9.0

6.1 LONGITUDINAL VIBRATION OF RODS

In this work it was not possible to use the barium titanate transducer to measure directly the axial motions of the rods; such use of the transducer resulted in large errors in the measured damping factors. It was however possible to measure the radial motions, i.e. the Poison effects, with the transducer situated close to a node. (Since the axial and radial motions are

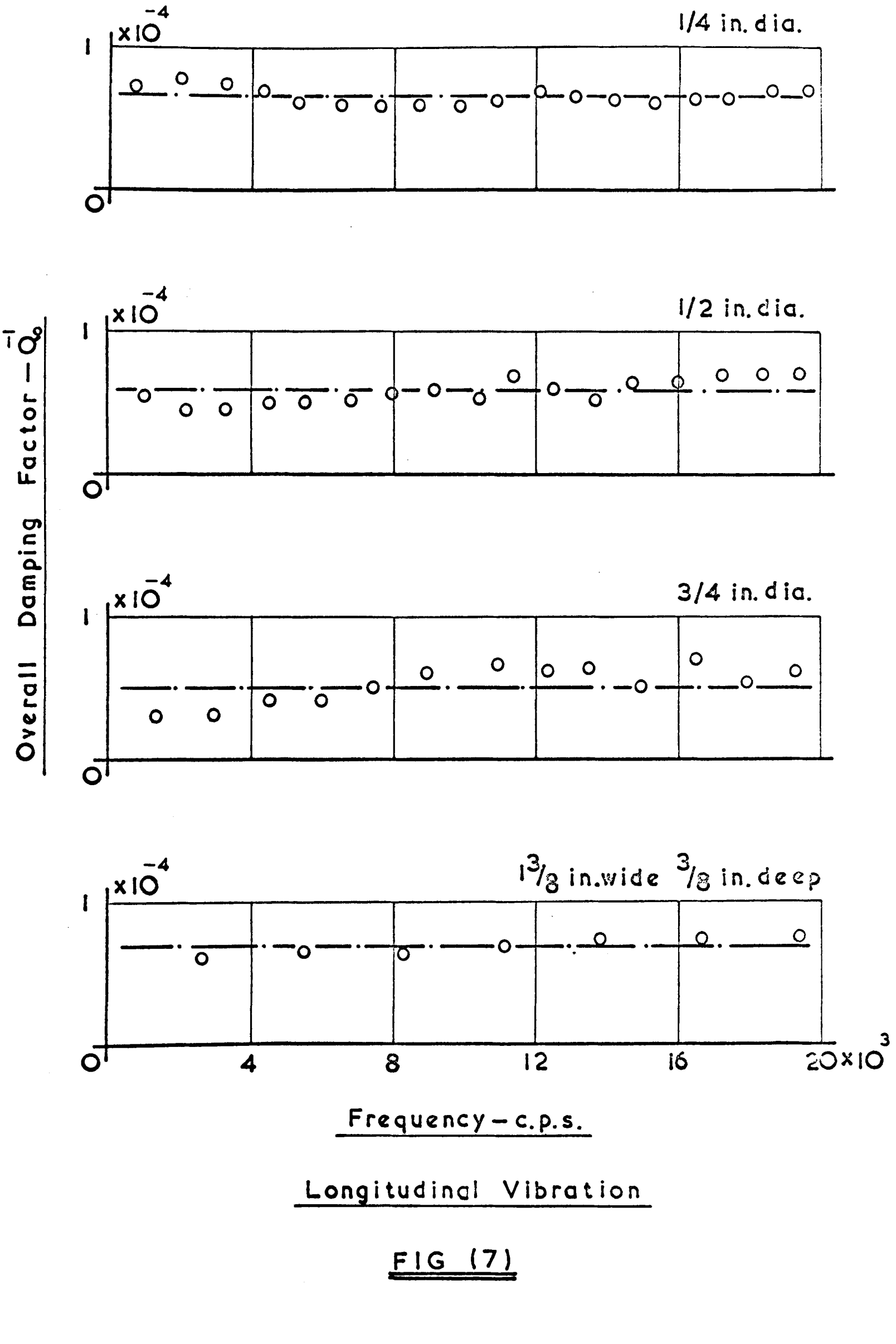

Longitudinal Vibration

FIG (7)

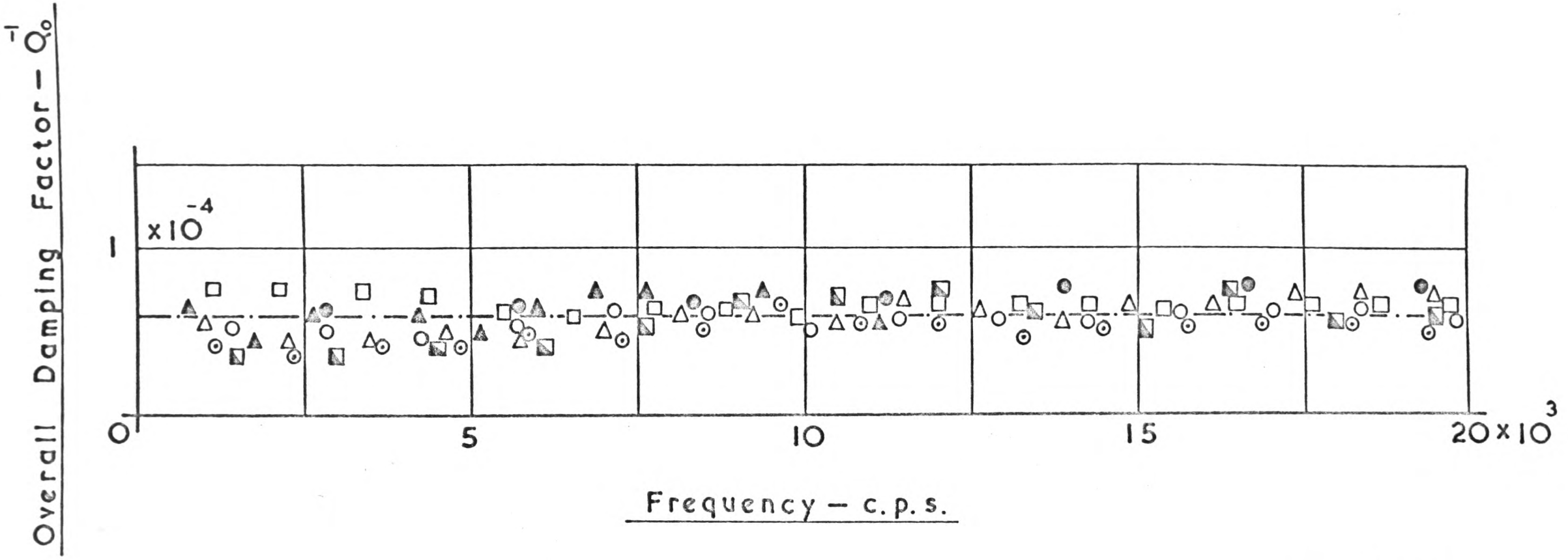

Longitudinal Vibration

□ 1/4 dia.
○ 3/8 dia.
△ 1/2 dia.
▨ 3/4 dia.
⊙ 1 dia.
▲ 2 dia.
● $1\frac{3}{8} \times \frac{3}{8}$

FIG (8)

approximately related to each other by Poison's ratio either motion may be used to measure the damping factor).

The specimens used were $\frac{1}{4}$, $\frac{3}{8}$, $\frac{1}{2}$, $\frac{3}{4}$, 1 and 2 inches diameter, the lengths varying from 3 to 10 feet. One rectangular specimen $1\frac{3}{8}$ in. wide $\frac{3}{8}$ in. deep 3 feet long was also included.

In fig. (7) are shown a series of overall damping factor/ frequency characteristics typical of those obtained from the experiment. It is immediately seen from these that the damping of the longitudinal vibrations of rods displays no obvious dependence on frequency, mode shape, cross sectional shape or cross sectional dimensions.

All the results obtained from the complete series of experiments are shown in fig. (8). Allowing for some degree of scatter it would seem reasonable to assume that the damping factor in longitudinal vibration remains constant at about 0.6×10^{-4} over the frequency range covered.

6.2 TRANSVERSE VIBRATION OF CYLINDRICAL BEAMS

The cylindrical specimens used in 6.1 were also used here in addition to $1\frac{1}{4}$ and $1\frac{3}{4}$ inches diameter specimens. Experimental difficulties however made it impossible to obtain dependable results from the $\frac{1}{4}$ in. diameter specimen. The main difficulty arose from the fact that, due to the smallness of the diameter of the specimen, the barium titanate transducer persistently slipped making the process of resonance testing almost impossible.

Results typical of those obtained are shown in fig. (9). From the curves it can be seen that the damping factors remain fairly constant up to frequencies which appear to be determined by

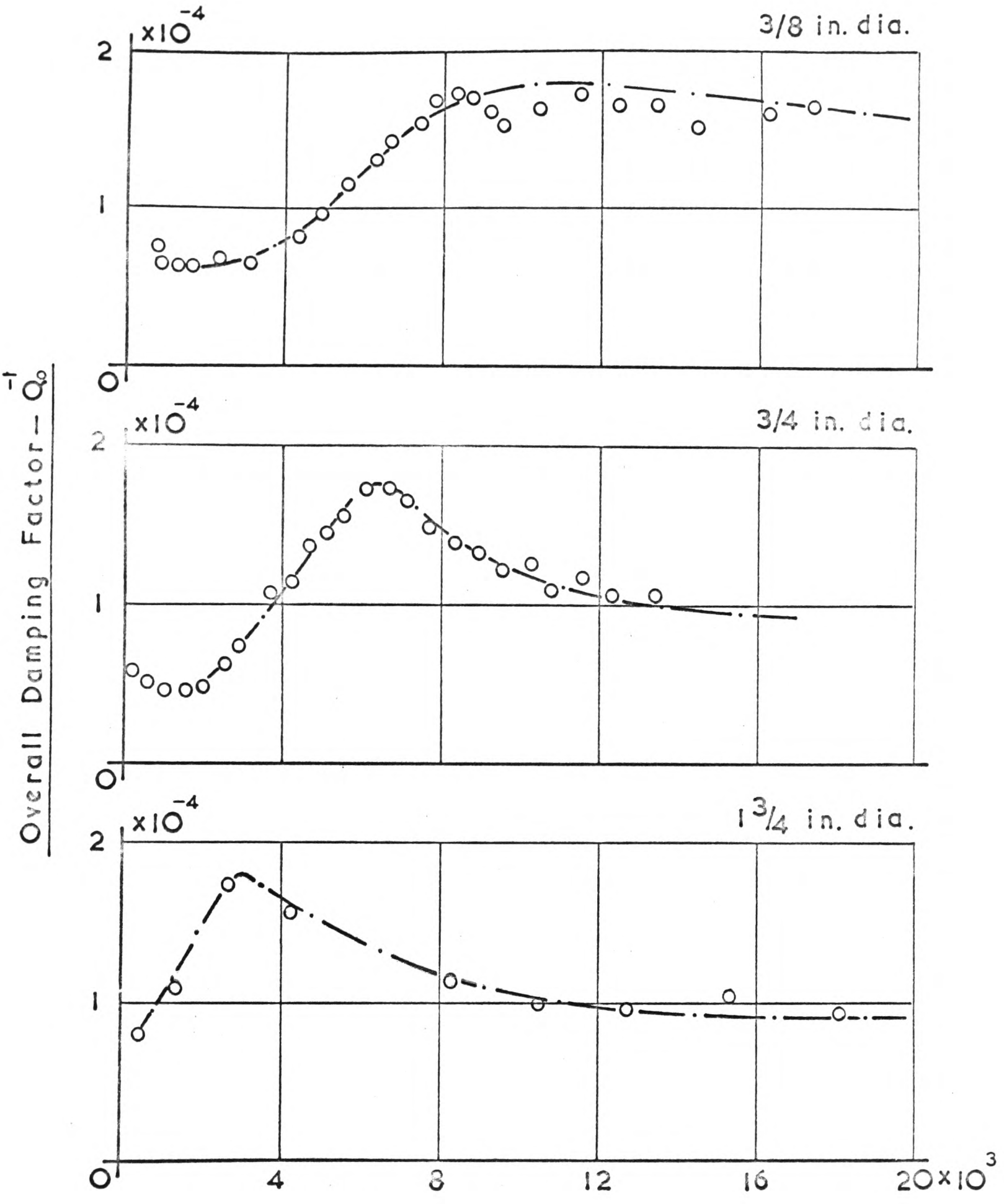

Transverse Vibration

FIG (9)

the diameters of the specimens. From these frequencies the damping factors rise to peaks of approximately the same magnitude but which occur at frequencies which would again seem to depend on diameter. These comments apply to the whole series of experimental curves.

6.3 TRANSVERSE VIBRATION OF RECTANGULAR BEAMS

The dimensions of the specimens used were as follows;

Width - inches	Depth - inches
2	$\frac{1}{2}$
2	$\frac{1}{4}$
1	$\frac{1}{8}$
1	$\frac{1}{4}$
1	$\frac{1}{2}$
1	1
$\frac{1}{2}$	$\frac{1}{2}$
$\frac{1}{2}$	$\frac{1}{4}$
$\frac{1}{2}$	$\frac{1}{8}$
$\frac{1}{4}$	$\frac{1}{4}$

All the specimens were 2 feet long and, where applicable, each was vibrated first with its major axis horizontal then with its major axis vertical.

Typical overall damping factor/frequency characteristics obtained from the experiment are shown in figs. (10) and (11). Again it is seen that the damping factors tend to remain constant initially and then to rise to peak values at various frequencies. Here however the peak values do not all have the same magnitude; the magnitudes would appear to depend on the cross sectional

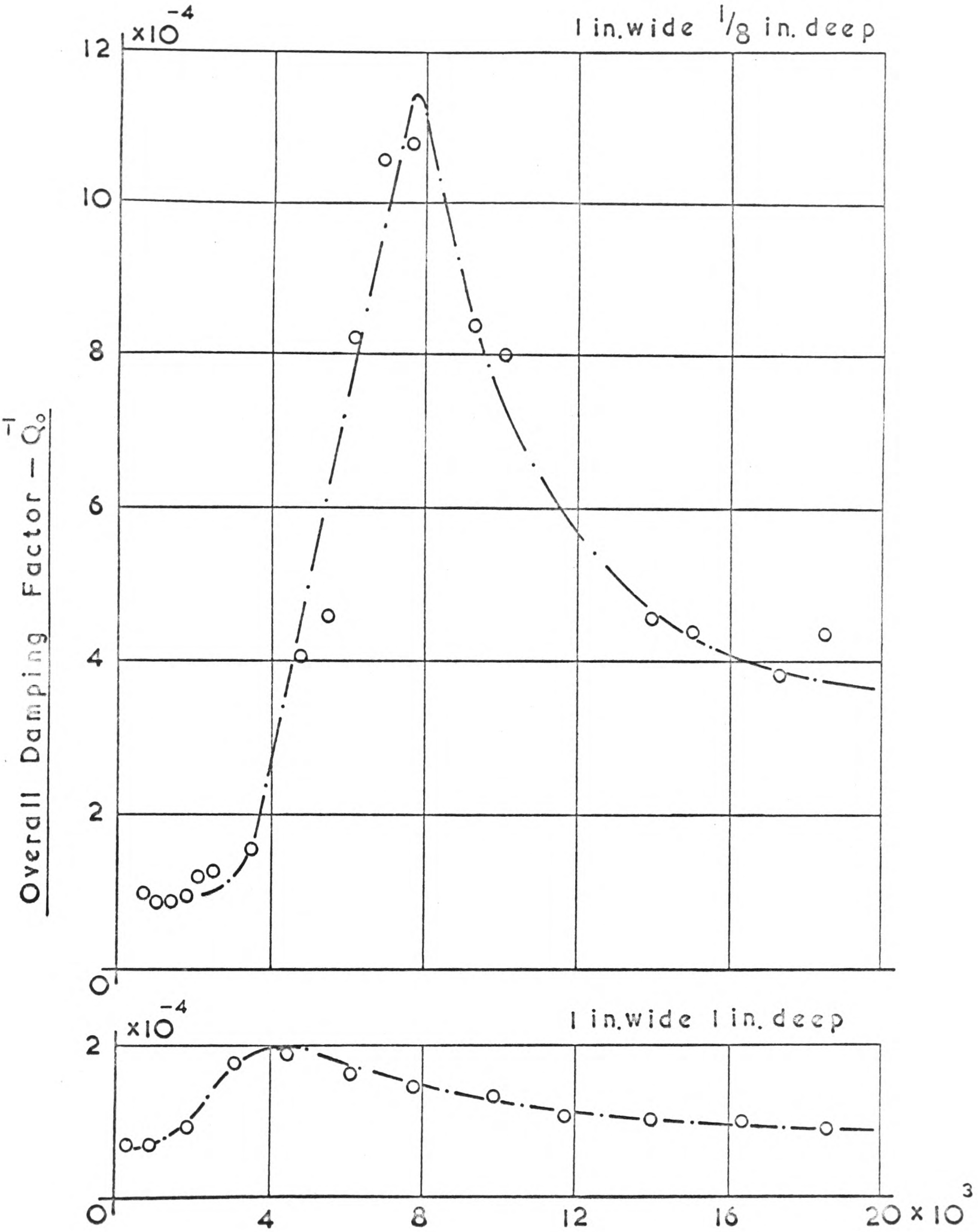

Transverse Vibration

FIG (10)

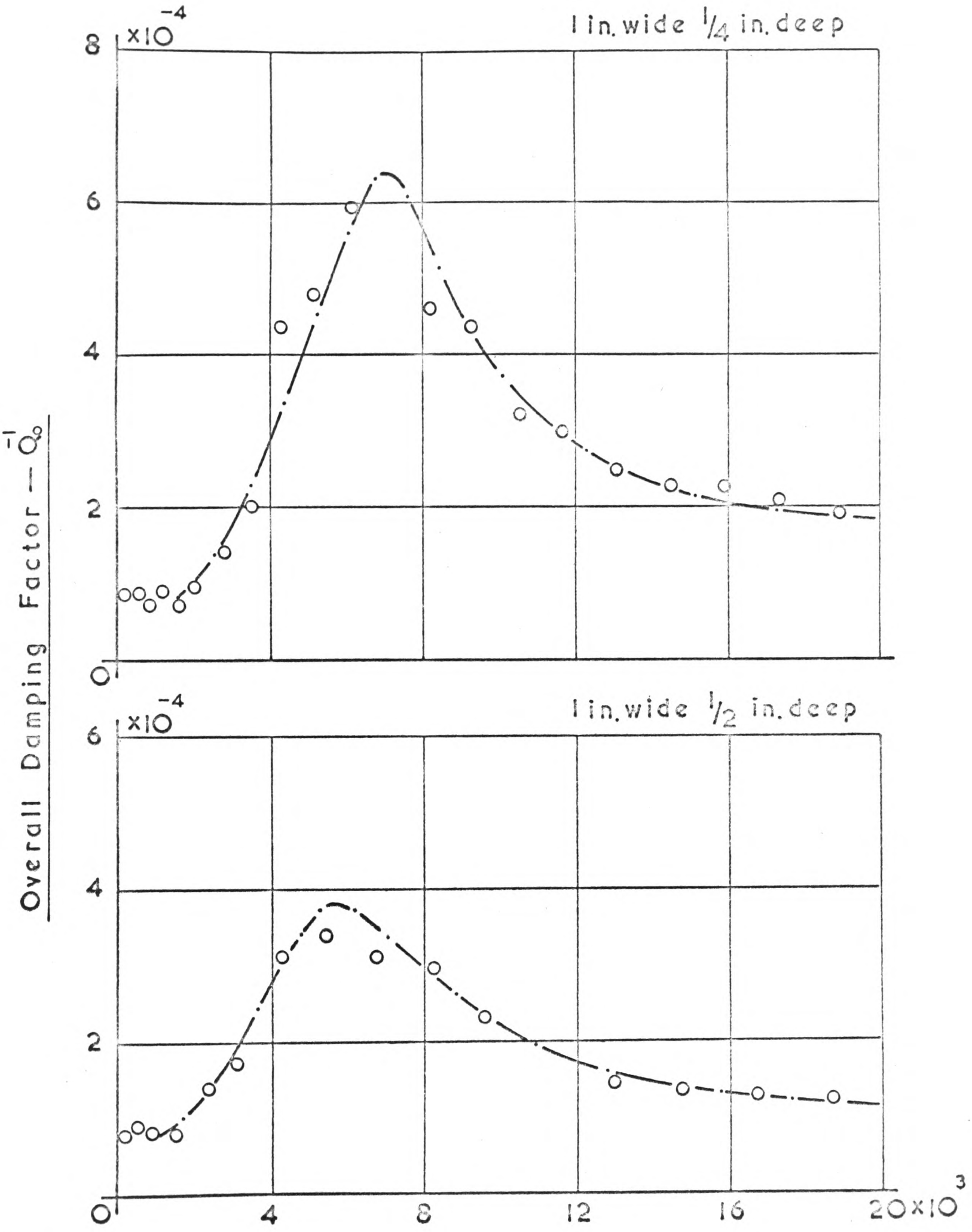

Transverse Vibration

FIG (11)

dimensions and configurations of the specimens.

At first sight the case of rectangular beams would seem to be somewhat more complicated than that of the cylindrical beams

- - - o O o - - -

7.0 ELIMINATION OF AIR DAMPING

Before any reasoned assessment of the experimental results can be made it is necessary that the effect of the surrounding air be known. To this end some experiments were carried out in a vacuum chamber.

Some necessary preliminary work is first described and thereafter the results obtained from the vacuum work are given.

7.1 PRELIMINARY TO VACUUM WORK

The system of suspension used for the experiments in air was not suitable for inclusion in the vacuum chamber; it was therefore necessary to design a new system. To avoid introducing further unknowns the new system must have essentially the same properties as the one used in air.

Remembering that the object was to separate the air effects from the overall effects already observed it is obvious that the new suspension system should give the same results in air as the previous system. An experiment was therefore carried out in which, using the new suspension system (described in 4.4) the overall damping factor/frequency characteristics for the 1 in. wide $\frac{1}{8}$ in. deep and 1 in. wide 1 in. deep specimens in transverse vibration were obtained. These are shown, together with the results obtained on the previous suspension, in fig. (12). It is considered that the agreement between the results is adequate and, therefore, that the new suspension system fulfills the necessary requirements for the vacuum work.

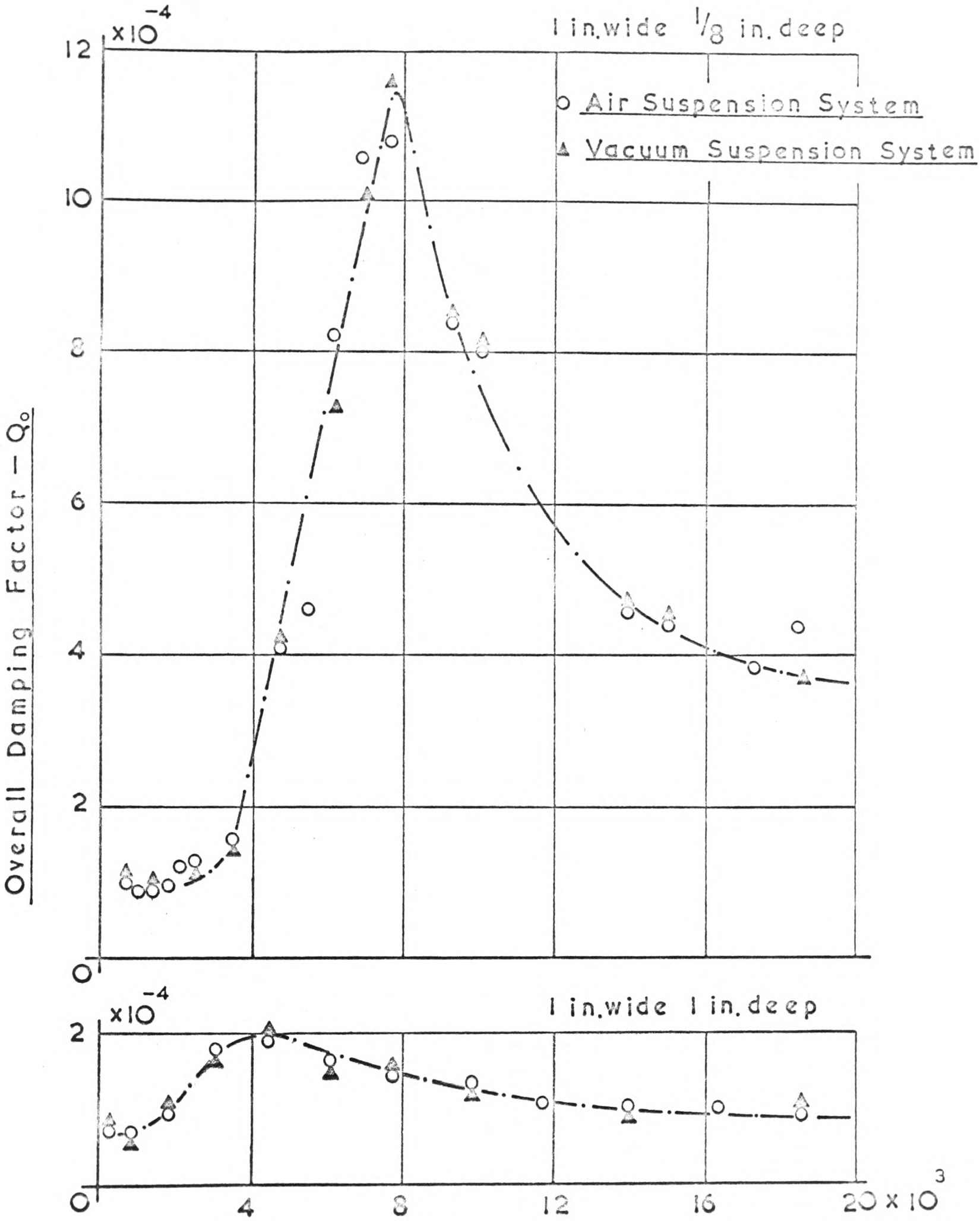

Transverse Vibration

FIG (12)

7.2 EXPERIMENTS IN VACUUM

The results of the transverse vibration experiments in air on the 1 in. wide $\frac{1}{8}$ in. deep and the 1 in. wide 1 in. deep specimens were respectively representative of the highest and lowest general levels of damping obtained from the rectangular specimens. It was for this reason that these specimens were selected for the vacuum work it being considered that the results in vacuum would indicate the overall pattern to be expected from the full range of rectangular specimens.

An experiment in vacuum was also carried out on the $1\frac{1}{4}$ in. diameter specimen in transverse vibration.

The chamber pressure used throughout was 50 m.m. Hg. In setting the suspension on the nodes corresponding to each mode of vibration of each specimen it was always necessary to enter the vacuum chamber and therefore to re-evacuate the chamber before each test. The time taken to attain a pressure of 50 m.m. Hg. was about 10 minutes; to go much below this pressure took a substantially longer time. It was felt that experiments carried out at 50 m.m. Hg. would clearly show how the surrounding air had affected the previous results and that the additional time involved in attaining lower pressures would not be justified. (For convenience the chamber pressure is referred to as "vacuum")

The results obtained from the experiments are shown in figs (13) and (14). The immediate impression to be gained from these results is that the presence of air has been the main cause of the phenomemon observed in 6.2 and 6.3.

In the case of longitudinal vibration it was not possible to

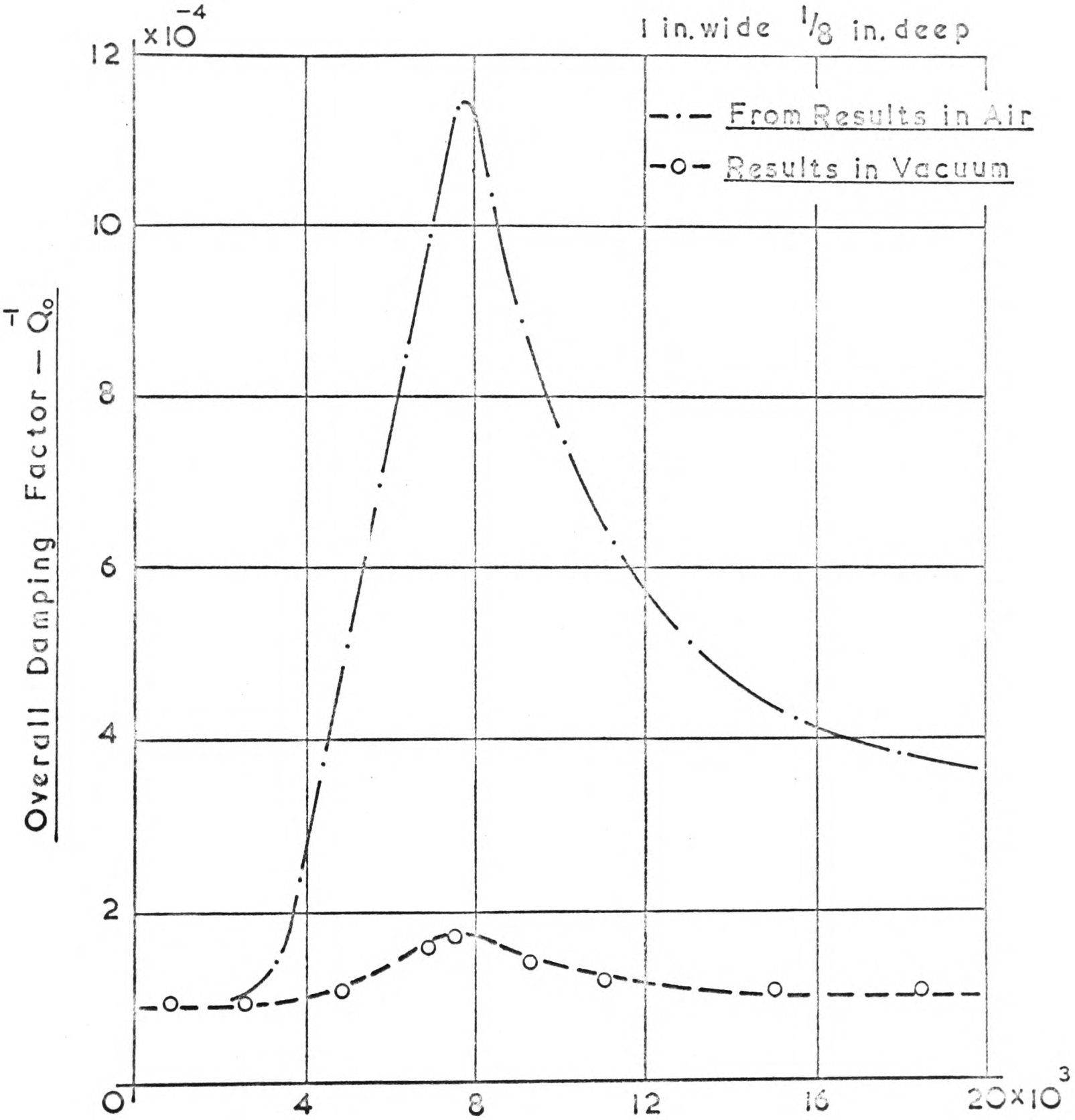

Transverse Vibration

FIG (13)

— · — From Results in Air

— o — Results in Vacuum

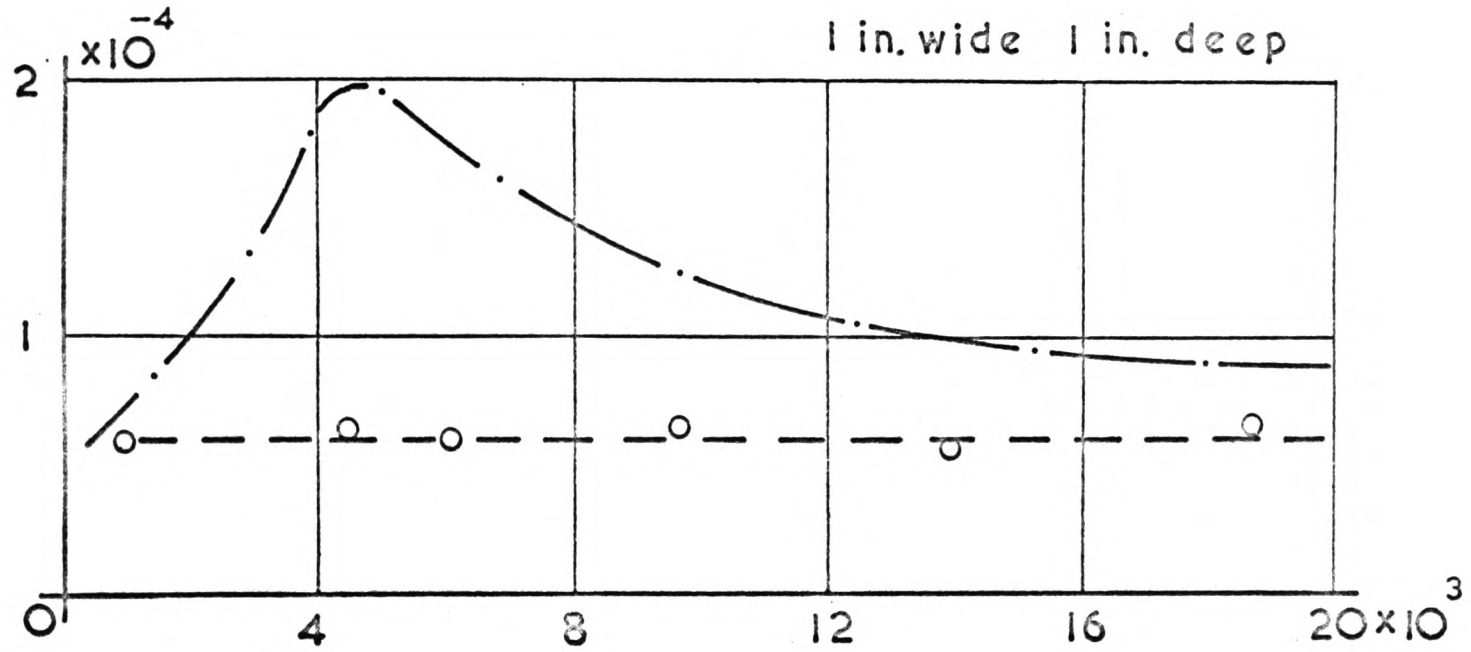

Frequency — c.p.s.

Overall Damping Factor — Q_o^{-1}

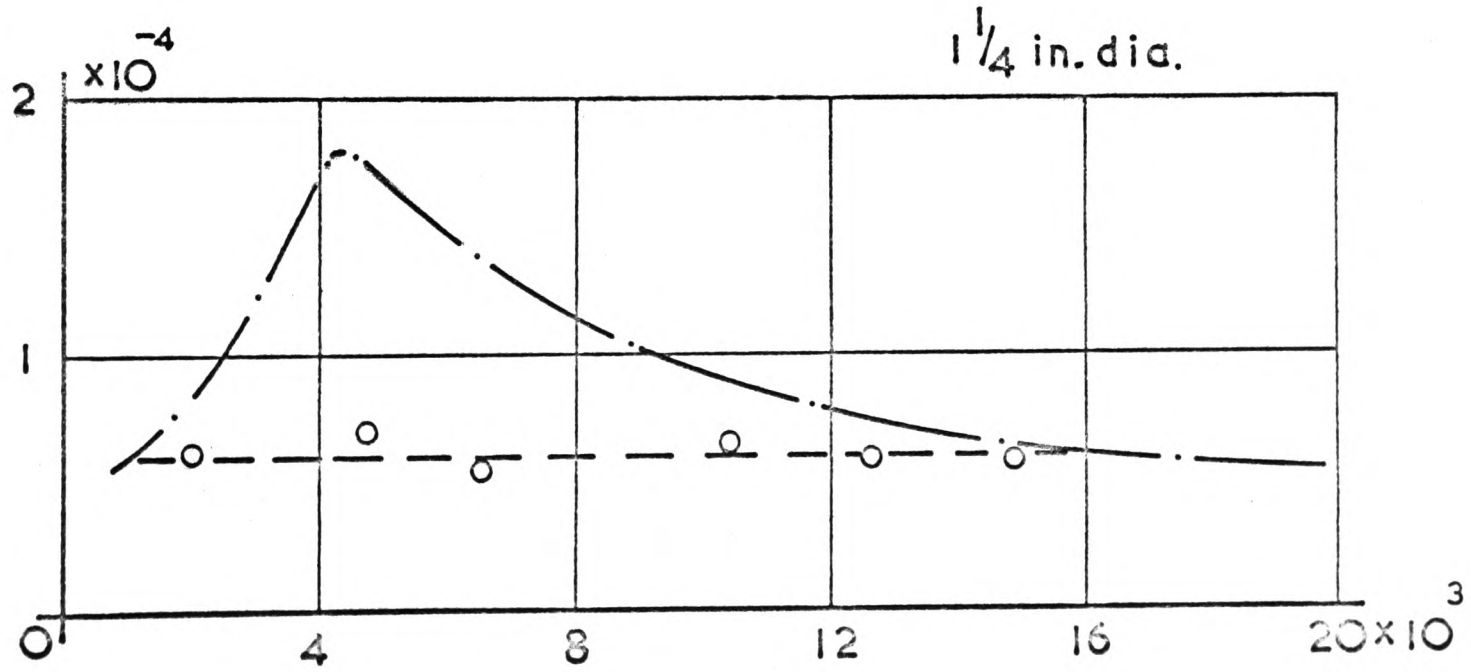

Frequency — c.p.s.

Transverse Vibration

FIG (14)

cover the full frequency range owing to the length of the specimens required. However, to gain some idea of the effect of the air an experiment was carried out using a 1 in. diameter 1 foot long specimen. This was vibrated in its first two longitudinal modes, first in air then in vacuum, and the damping factors measured. The results obtained are shown in Table (5).

MODE	FREQUENCY c.p.s.	DAMPING FACTOR - Q^{-1}	
		IN AIR	IN VACUUM
1	8420	0.54×10^{-4}	0.57×10^{-4}
2	16840	0.55×10^{-4}	0.50×10^{-4}

TABLE (5)

From the table it can be seen that the results in air and in vacuum are essentially the same and although by no means conclusive would appear to indicate that damping due to air (in longitudinal vibration) is negligeable over the frequency range considered.

- - - o O o - - -

8.0 ANCILLARY EXPERIMENT ON A HOMOGENEOUS MILD STEEL SPECIMEN

All the experimental work to date has concerned only cold rolled mild steel specimens. This type of steel is probably of much more general engineering interest than the more homogeneous "black bar" but it was considered that a little time spent in investigating the properties of a piece of "black bar" would not be wasted.

The object of this short section was to ascertain whether there were any great differences in the damping properties of cold rolled mild steel and a more homogeneous mild steel. It is obviously the internal damping properties which are of interest here as it seems unlikely that air damping would be affected by the type of steel employed.

A piece of 2 in. wide 1 in. deep "black" mild steel was machined to the dimensions $1\frac{3}{4}$ in. wide $\frac{7}{8}$ in. deep. The specimen was vibrated with its major axis horizontal in its transverse modes, first in air then in vacuum, at frequencies up to 20 Kc.p.s.; the damping factor corresponding to each mode was measured. The results obtained are shown in fig. (15). These can be seen to be of a similar nature to those obtained from the transverse vibration experiments of sections 6 and 7 and will be considered in the general discussion which follows.

- - - o O o - - -

-o- Results in Air

-●- Results in Vacuum

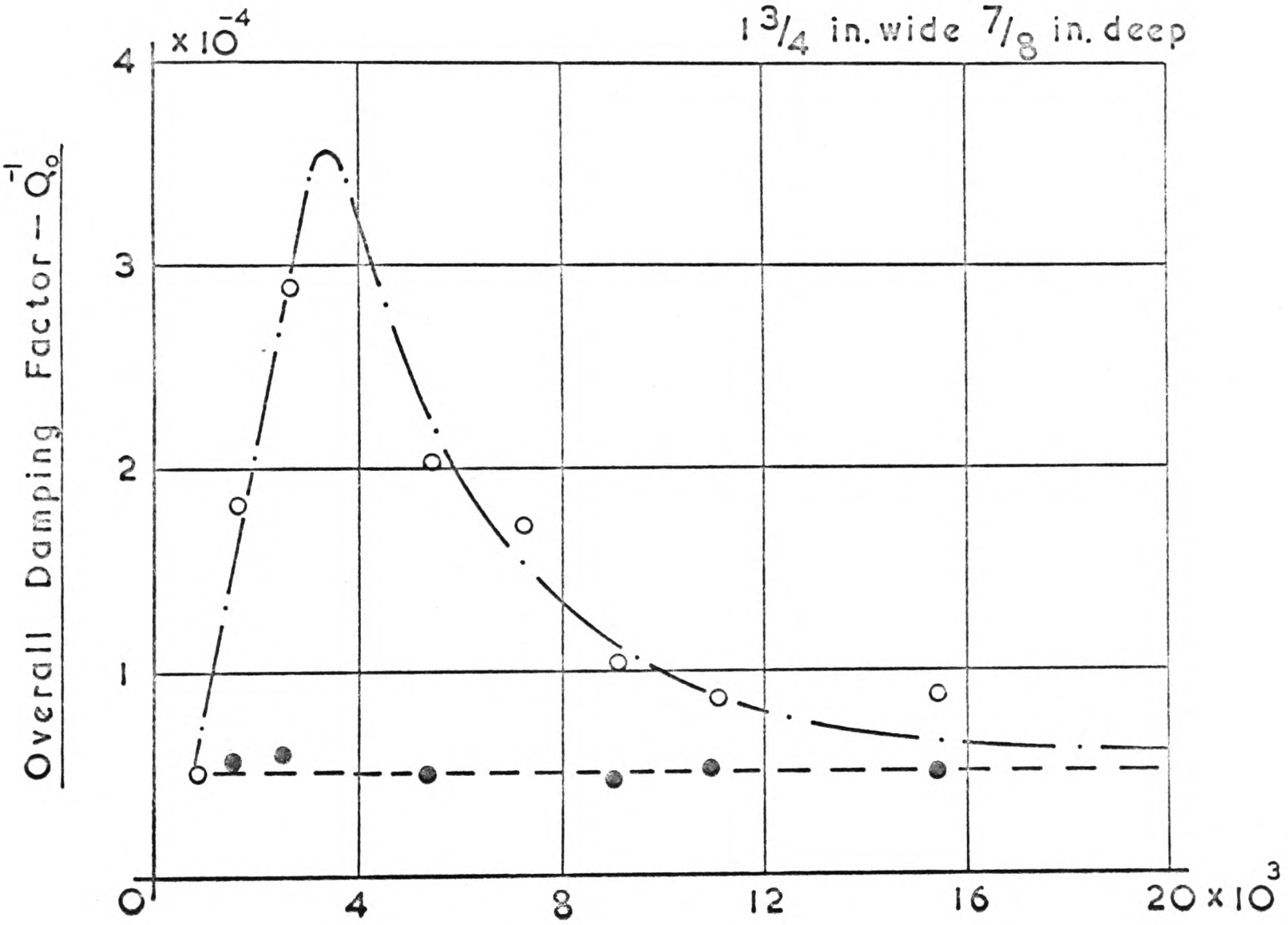

Transverse Vibration of Homogeneous Mild Steel Specimen

FIG (15)

9.0 GENERAL DISCUSSION OF EXPERIMENTAL RESULTS

Before discussing the implications of the experimental work a little space will be devoted to a consideration of some of the results obtained in the approximate frequency range 0 - 500 c.p.s. It was generally found that as the frequency of the modes of vibration of the specimens decreased from about 500 c.p.s. the value of the damping factor increased: it was also found that the smaller the specific mass of the specimen the greater the rate of increase became. The effect was not very apparent in the specimens with the largest masses. It is the authors opinion that the increases in the damping factor in this frequency range are due to motion at the suspension nodes. When, for example the $\frac{1}{4}$ in. wide $\frac{1}{4}$ in. deep specimen was vibrating in its lowest modes, even with extremely small forcing, the amplitudes of vibration were quite significant; consequently, for the reasons given in 5.4, the amplitudes at the nodes were significant and the subsequent losses to the suspension were increased. It was also found that the damping factors were somewhat dependant on amplitude of vibration which would indicate the presence of Coulomb damping. As mentioned previously the most obvious source of this kind of damping is the suspension. It was not possible with the existing experimental set up to eliminate these losses so it will simply be said here that in general the values of the damping factors obtained in the approximate frequency range 0 - 500 c.p.s. were not wholly reliable these being considered to be in excess of the actual values. For this reason such damping factors will generally be omitted from the graphs.

The experimental results in the remainder of the frequency range provide a qualitative picture of the damping phenomenon but in order that quantitative understanding be obtained it is necessary that the results be examined more closely.

Considering firstly the results obtained from the longitudinal vibration experiments: it can be seen that the damping factor displays no obvious dependence on any of the parameters, frequency, mode shape, cross sectional shape or cross sectional dimensions and that, allowing for some degree of scatter, it has the approximate constant value 0.6×10^{-4} for cold rolled mild steel. The results of the longitudinal vibration experiment in vacuum would also suggest that air damping in this type of vibration is negligible and therefore that the phenomenon observed in air are due wholly to internal damping. This leads to the conclusion that, at least within the limitations of this investigation, the internal damping of the longitudinal vibrations of cold rolled mild steel is due to some form of hysteresis which may be treated mathematically in terms of a hysteretic coefficient.

At this juncture it is expedient that the results obtained from the transverse vibration experiments in vacuum be examined. These show that the internal damping factor is again unaffected by frequency (the small peak in the 1 in. wide $\frac{1}{8}$ in. deep specimen curve will be explained later). Moreover if the results obtained in vacuum are characteristic of the behaviour of the remainder of the specimens, as it would seem reasonable to assume, then it may be said that the internal damping factor in transverse vibration behaves in an exactly similar manner to that in longitudinal vibration. Also, in the same way as in the longitudinal case, the internal damping

factor in transverse vibration is independent of mode shape or component shape and dimensions and indeed may again be given the approximate value 0.6×10^{-4}.

All the above leads to the conclusion that if a cold rolled mild steel body is performing a sinusoidal vibratory motion such that in any given plane the nature of stress is either uniform tension or compression or a combination of both then, provided the magnitudes of the stresses do not introduce non-linear effects, the internal damping factor may be considered to be a basic property of the material which has a constant value for frequencies up to 20 Kc.p.s.

Consider now the overall damping effects obtained from the transverse vibration experiments in air.

From what has preceded it would seem clear that the damping phenomenon observed may be considered to arise from two sources: (a) internal and (b) air. The internal damping has been shown to be constant throughout the frequency range covered thus it may be said that the peaks in the overall damping factor/frequency characteristics are due solely to the presence of the air. This being the case two new damping factors will be defined (i) the internal damping factor - Q_i^{-1} (ii) the air damping factor - Q_a^{-1} the sum of these being equal to the overall damping factor - Q_0^{-1}.

Examination of the results obtained from the cylindrical specimens shows that, irrespective of the diameters of the specimens, the maximum value of Q_a^{-1} is constant but that the frequencies at which the maxima occur appear to be governed in some way by the diameters of the specimens: there is no obvious relationship between these frequencies and the diameters. In the case of the

rectangular specimens it is seen that both the maximum values of Q_a^{-1} and the frequencies at which they occur are dependent on the cross sectional dimensions and configurations of the specimens. Fig. (16) shows the approximate experimental maxima of Q_a^{-1} plotted against the breadth to depth ratio of the specimens; this shows a near linear relationship. Again there is no obvious relationship between the frequencies at maxima and any of the parameters of the specimens.

It is apparent that the air damping factor is dependent on ratios of dimensions rather than on absolute dimensions. This is a very salient point for if it is considered that a circular section will show similarities in behaviour with a 1:1 breadth to depth ratio rectangular section then since all the 1:1 ratio rectangular sections gave the same maximum value of Q_a^{-1} it may be expected that all circular sections will behave in a similar manner. This observation is seen to be verified by the experiments. Indeed, if comparison is made of the experimental results for similar sections - such as the $\frac{1}{2}$ in. wide $\frac{1}{2}$ in deep specimen with the $\frac{1}{2}$ in. diameter specimen - it will be seen that the values of the maxima and the frequencies at which they occur are almost identical as are the general natures of the Q_a^{-1}/frequency characteristics. These observations alone suggest that the damping mechanism is the same for both the rectangular and the cylindrical specimens.

To determine the actual damping mechanism it is necessary to consider what kind of forces can be applied to the oscillating specimens by the air.

Aerodynamic forces on a body may arise in two ways: (a) from a distribution of normal pressures over the body and (b) from a

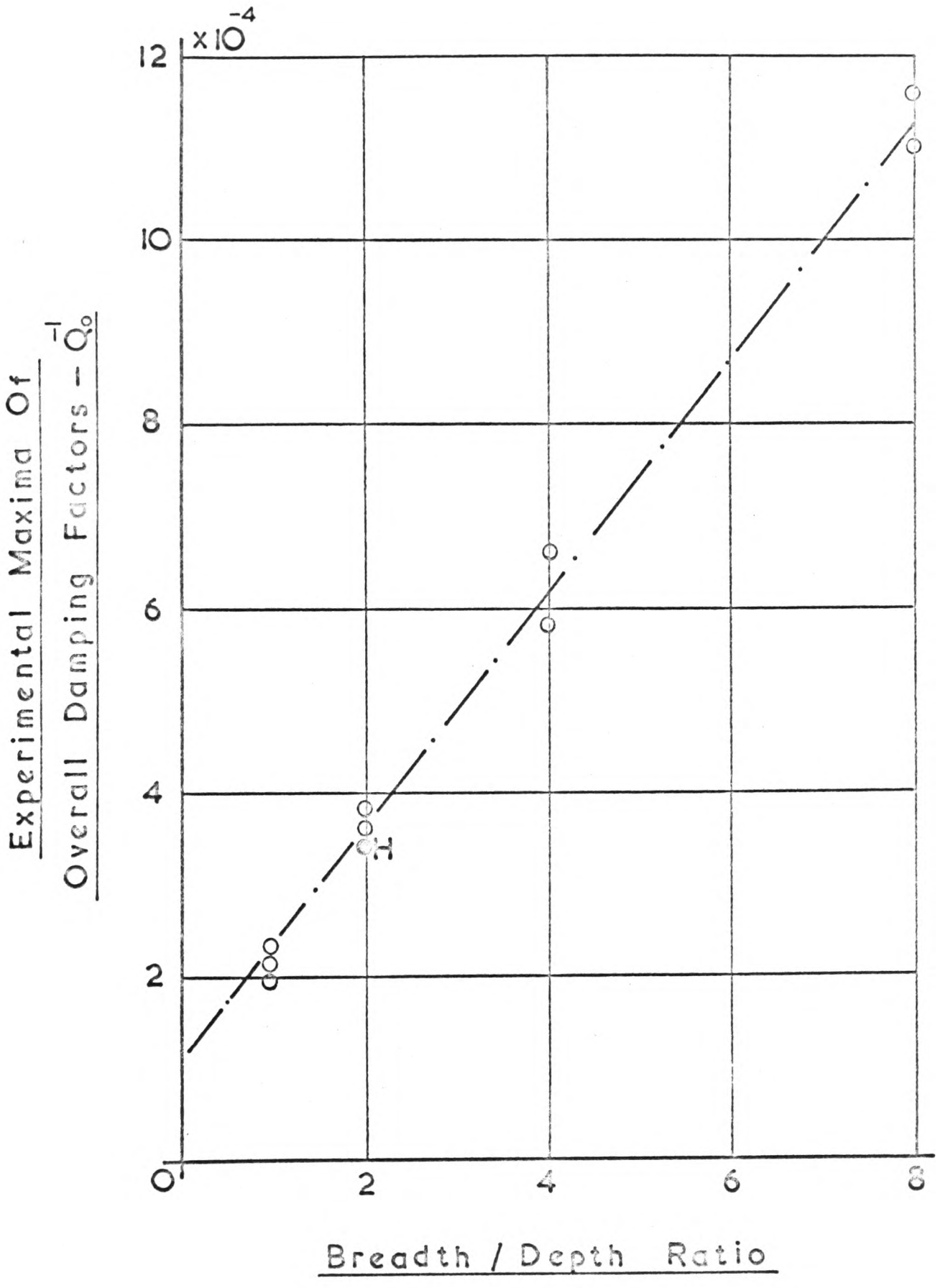

Rectangular Beams in Transverse Vibration

FIG (16)

distribution of skin friction over the body. The consideration of these aspects may be approached in a purely intuitive manner as follows.

Consider an infinitely long rectangular beam vibrating in a viscous fluid. Let the beam be of unit breadth and depth d and let its velocity be $v = v_0 e^{-i\omega t}$ normal to its breadth. Also, let the velocity be such that laminar flow can be assumed. Focusing attention on unit length of the beam it may be said that the total force resisting motion is comprised of two parts, one part acting on the upper and lower surfaces and one part acting on the sides. Now let the force on the upper and lower surfaces be a function of a number of parameters which will simply be denoted by α and let the total force due to both surfaces be represented in terms of an equivalent viscous coefficient by $F_1 = C(\alpha)v$. The force, F_2, on the sides will be purely viscous and will be proportional to vd; the constant of proportionality, K, is dependent only on the kinematic viscosity of the fluid. The total force resisting motion, $F_1 + F_2$, may also be represented in terms of an equivalent viscous coefficient and from (2.0.5) it is seen that this coefficient is $m\omega Q^{-1}$ where m is the mass per unit length of the beam. Therefore

$$m\omega Q^{-1} v = C(\alpha)v + Kdv \qquad (9.0.1)$$

and for unit breadth

$$\rho_s d\omega Q^{-1} = C(\alpha) + Kd$$

where ρ_s is the density of the beam.

Then $$Q^{-1} = \frac{C(\alpha)}{\rho_s d\omega} + \frac{K}{\rho_s \omega} \qquad (9.0.2)$$

The part of this expression which is of immediate interest is the quantity $K/\rho_s \omega$ which arises from the viscous forces on the sides of the beam. The experimental results do not indicate the presence of any such quantity and it may therefore be concluded that damping due to such viscous effects is negligible i.e. the air may be considered to be devoid of viscosity. In consequence of this a theoretical approach may be made on the assumption that irrotational (or potential) flow exists.

Further examination of the experimental results shows that in all cases the damping factors remain constant (i.e. at the value of Q_i^{-1}; $Q_a^{-1} = 0$) up to particular frequencies from which frequencies they rise to peaks. It is these frequencies at which Q_a^{-1} ceases to be zero that are of interest and for the moment these will be referred to as transition frequencies. If the ratios are taken of the wave lengths of sound in air to the wave lengths in the vibrating beams in the region of the transition frequencies it will be found that the values are in all cases approximately equal to unity. This is important as it suggests that the air damping phenomena obtained from the experimental work are due to acoustic radiation. The true transition frequency is that which makes the wave length ratio exactly equal to unity and in acoustic circles this frequency is referred to as the cut off frequency: this term will be adopted in the subsequent work of this thesis. Also, the air damping factor will be re-named the "acoustic damping factor" the same notation being retained - Q_a^{-1}.

The final point to be discussed concerns the results obtained from the experiments on the homogeneous mild steel specimen. This specimen had a 2:1 breadth to depth ratio and the maximum

value of Q_a^{-1} obtained is indicated by the letter H in fig. (16). It can be seen that this corresponds to the values obtained from the 2:1 cold rolled specimens. Also Q_i^{-1} is again constant over the frequency range and has approximately the same value as that of the cold rolled specimens. Although certainly not conclusive the above would suggest that with respect to internal damping there is little to choose between the two steels. The results of experiments performed, but not detailed in this thesis, on a $1\frac{3}{8}$ in. wide $\frac{3}{8}$ in. deep homogeneous mild steel specimen led to the same conclusion.

The results obtained from the transverse vibration experiments and the observations and deductions made in the discussion provide a sound basis for a theoretical approach to which the next section is devoted.

- - - o O o - - -

10.0 THEORY

It is clear that the oscillations of the beams will create some sort of wave motion in the air so the first task must be to obtain an equation of motion for these waves. Based on what was said in the discussion two fundamental assumptions will first be made:

(1) the air will be considered to be devoid of viscosity.

(2) irrotational, or potential, flow will be assumed.

Under these circumstances it is possible to write down the well known three dimensional wave equation for pressure,

$$\nabla^2 p + k_0^2 p = 0 \qquad (10.0.1)$$

where p is a function of x, y, z and t and k_0 is a wave number. (The principal notation is given in 10.1)

The real problem is one in three dimensions but the preliminary experimental work showed that length effects were negligeable, therefore by assuming the beams to be of infinite length the problem may be effectively reduced to one in two dimensions. That is, assuming

$$p = p(x,y)\ \cos kz\ \exp(-i\omega t) \qquad (10.0.2)$$

(10.0.1) becomes

$$\frac{\partial^2 p(x,y)}{\partial x^2} + \frac{\partial^2 p(x,y)}{\partial y^2} + k_d^2\, p(x,y) = 0 \qquad (10.0.3)$$

where $k_d^2 = k_0^2 - k^2$

This is the desired equation and in what follows solutions are developed for the cases of cylindrical and rectangular beams. The solutions for pressure enable the damping forces and hence the damping factors to be calculated.

10.1 PRINCIPAL NOTATION

The symbols used are listed in the approximate order in which they occur in the text.

Symbol	Meaning
∇^2	Laplacian: $\frac{\partial^2}{\partial x^2} + \frac{\partial^2}{\partial y^2} + \frac{\partial^2}{\partial z^2}$
p	Pressure
k_0	Acoustic wave number $= \frac{\omega}{c} = \frac{2\pi}{\lambda_0}$
λ_0	Acoustic wave length
ω	$2\pi f$
f	Frequency of vibration
c	Velocity of sound in air
x, y, z	Cartesian coordinates
k	Beam wave number $= \frac{2\pi}{\lambda}$
λ	Beam wave length
i	$\sqrt{-1}$
t	Time
k_d	$\sqrt{(k_0^2 - k^2)}$
r, θ	Cylindrical coordinates
ζ	$k_d r$
v	Radial surface velocity of cylindrical beams
	Surface velocity of rectangular beams
v_0	Maximum surface velocity of cylindrical beams in direction of motion.
	Maximum surface velocity of rectangular beams

a	Radius of cylindrical beams
ρ	Density of air
J_m	Bessel function of first kind of order m
Y_m	Bessel function of second kind of order m
F_O	Force per unit length in direction of motion of cylindrical beams
F_{OR}	Real part of F_O
F_{OI}	Imaginary part of F_O
Q_a^{-1}	Acoustic damping factor
C	Equivalent viscous coefficient
ρ_s	Density of mild steel
I_m	Modified Bessel function of the first kind of order m
K_m	Modified Bessel function of the second kind of order m
b	Breadth of rectangular beams
d	Depth of rectangular beams
ξ, η	Elliptic coordinates.
q	$(k_d \cdot \frac{b}{4})^2$
se_m	Periodic Mathieu function of order m:- sine-elliptic
ce_m	Periodic Mathieu function of order m:- cosine--elliptic
Ne_m	Combination non-periodic Mathieu function of order m

Me_m	Combination non-periodic Mathieu function of order m
$B_s^{(m)}$	Coefficients of se_m
$A_s^{(m)}$	Coefficients of ce_m
F_{TT}	Force per unit length in direction of motion on top surface of rectangular beam due to its own radiation
F_{TB}	Force per unit length in direction of motion on top surface of rectangular beam due to radiation from lower surface.
F_{total}	$2(F_{TT} + F_{TB})$ - Total force per unit length resisting motion of rectangular beams
J_r	Bessel function of first kind of order r
H_r	Hankel function of first kind of order r

- - - o O o - - -

10.2 THEORY FOR CYLINDRICAL BEAMS IN TRANSVERSE VIBRATION (SEE REF 11)

The coordinate system used is shown below.

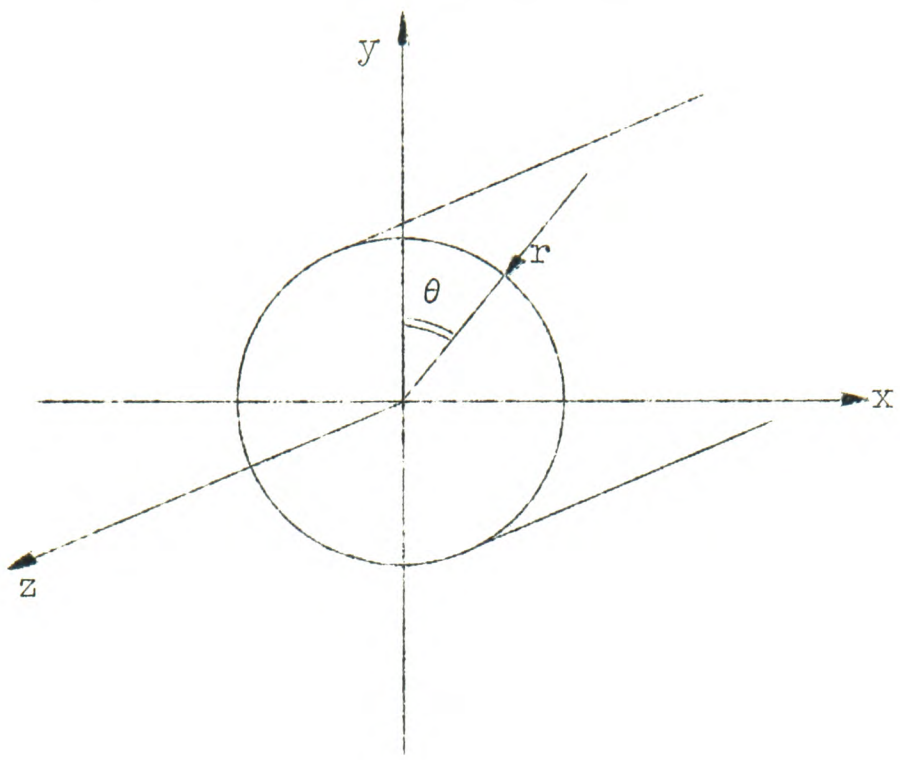

Since we are here concerned with cylindrical bodies it is convenient to transform equation (10.0.3) from its existing cartesian to a cylindrical coordinate system. This transformation is carried out in Appendix I with the final result,

$$\frac{1}{r^2}\frac{\partial^2 p(r,\theta)}{\partial\theta^2} + \frac{1}{r}\frac{\partial}{\partial r}\left[r\frac{\partial p(r,\theta)}{\partial r}\right] + k_d^2\, p(r,\theta) = 0 \qquad (10.2.1)$$

If we assume

$$p(r,\theta) = \Psi(r)\Phi(\theta) \qquad (10.2.2)$$

equation (10.2.1) becomes

$$\frac{1}{r^2}\Psi(r)\frac{d^2\Phi(\theta)}{d\theta^2} + \frac{1}{r}\Phi(\theta)\left[r\frac{d^2\Psi(r)}{dr^2} + \frac{d\Psi(r)}{dr}\right] + k_d^2\Psi(r)\Phi(\theta) = 0$$

which gives

$$\frac{1}{\Psi(r)}\left[r^2\frac{d^2\Psi(r)}{dr^2} + r\frac{d\Psi(r)}{dr}\right] + (rk_d)^2 = -\frac{1}{\Phi(\theta)}\frac{d^2\Phi(\theta)}{d\theta^2} \qquad (10.2.3)$$

The left hand side of (10.2.3) is a function of r only and the right hand side is a function of θ only. Now a function of r cannot equal a function of θ for all values of r and θ if both functions really vary with r and θ respectively thus the only way equation (10.2.3) can be true is if both sides are independent of both r and θ i.e. both sides must equal a constant. Letting this constant be m^2 we therefore obtain,

$$\frac{d^2\Phi}{d\theta^2} + m^2\Phi = 0 \qquad (10.2.4)$$

$$\frac{d^2\Psi}{dr^2} + \frac{1}{r}\frac{d\Psi}{dr} + (k_d^2 - \frac{m^2}{r^2})\Psi = 0 \qquad (10.2.5)$$

If in (10.2.5) we put $\zeta = k_d r$ we obtain

$$\frac{d^2\Psi}{d\zeta^2} + \frac{1}{\zeta}\frac{d\Psi}{d\zeta} + (1 - \frac{m^2}{\zeta^2})\Psi = 0 \qquad (10.2.6)$$

which is Bessel's Equation of order m.

Before solving equations (10.2.4) and (10.2.6) we will make recourse to the physical problem and fix the boundary conditions.

Let the radius of the cylinder be a and let the velocity distribution at r = a be given by

$$v = v_0 \cos\theta \cos kz \exp(-i\omega t) \qquad (10.2.7)$$

Since the cylinder is generating the waves these must be moving away from the origin so the solution for $p(r,\theta,z,t)$ must represent outgoing waves.

Also, Newton's equation of motion is

$$\text{grad. } (p(r,\theta,z,t)) = -\rho \frac{\partial v}{\partial t} \qquad (10.2.8)$$

therefore

$$\left(\frac{\partial p(r,\theta,z,t)}{\partial r}\right)_{r=a} = -\rho\frac{\partial v}{\partial t}$$

$$= i\rho\omega v_0 \cos\theta \cos kz \exp(-i\omega t) \qquad (10.2.9)$$

Now a general solution of (10.2.4) is

$$\Phi(\theta) = A\cos m\theta + B\sin m\theta \qquad (10.2.10)$$

where A and B are constants and to comply with the outgoing wave condition the solution of (10.2.6) must take the form

$$\psi(r) = A_m (J_m(\zeta) + i\, Y_m(\zeta)) \qquad (10.2.11)$$

where A_m is a complex constant.

Therefore the general solution for the pressure wave is

$$p = \left\{ \sum_{m=0}^{\infty} A_m(A\cos m\theta + B\sin m\theta) \cdot \right.$$

$$\left. \cdot (J_m(\zeta) + i\, Y_m(\zeta)) \right\} \cos kz \exp(-i\omega t) \qquad (10.2.12)$$

and therefore

$$\left(\frac{\partial p}{\partial r}\right)_{r=a} = \left\{ \sum_{m=0}^{\infty} k_d A_m (A\cos m\theta + B\sin m\theta) \cdot \right.$$

$$\left. \cdot (J'_m(k_d a) + iY'_m(k_d a)) \right\} \cos kz \exp(-i\omega t) \qquad (10.2.13)$$

where $J'_m(k_d a) = \left(\frac{dJ_m(k_d r)}{d(k_d r)}\right)_{r=a}$ etc.

Equating (10.2.9) and (10.2.13) we find

$$B = 0$$

$$m = 1$$

$$AA_m = \frac{i\rho\omega v_0}{k_d(J'_1(k_d a) + iY'_1(k_d a))}$$

therefore

$$p = \frac{i\rho\omega v_0 \cos\theta}{k_d} \left(\frac{J_1(k_d r) + iY_1(k_d r)}{J_1'(k_d a) + iY_1'(k_d a)} \right) \cos kz \exp(-i\omega t) \qquad (10.2.14)$$

The force per unit length on the cylinder in the direction of motion is given by

$$F_0 = a\int_0^{2\pi} p(a,\theta,z,t)\cos\theta \, d\theta$$

$$= \frac{i\pi a\rho\omega v_0}{k_d} \left(\frac{J_1(k_d a) + iY_1(k_d a)}{J_1'(k_d a) + iY_1'(k_d a)} \right) \cos kz \exp(-i\omega t) \qquad (10.2.15)$$

Separating into real and imaginary parts we obtain

$$F_{OR} = \left\{ \frac{\pi a\rho\omega}{k_d} \left(\frac{J_1 Y_1' - J_1' Y_1}{J_1'^2 + Y_1'^2} \right) \right\} v_0 \cos kz \exp(-i\omega t) \qquad (10.2.16)$$

$$F_{OI} = \left\{ i \frac{\pi a\rho\omega}{k_d} \left(\frac{J_1 J_1' + Y_1 Y_1'}{J_1'^2 + Y_1'^2} \right) \right\} v_0 \cos kz \exp(-i\omega t) \qquad (10.2.17)$$

where the argument of all the Bessel functions is $(k_d a)$

It can be seen that the imaginary part of the force is 90° out of phase with the velocity and therefore that its effect is equivalent to a mass reactance on the cylinder. The real part of the force is seen to be in phase with the velocity and we may therefore represent the part in $\{ \ldots \}$ by an equivalent viscous coefficient - C.

Now we have from 2.0 that in the case of a vibrating beam the damping factor is given by

$$Q^{-1} = \frac{C}{m\omega_0}$$

where m is the mass per unit length and ω_0 is a mode frequency.

Therefore substituting for C from (10.2.16) we find that the acoustic damping factor is given by

$$Q_a^{-1} = \frac{1}{k_d a} \cdot \frac{\rho}{\rho_s} \left(\frac{J_1(k_d a) Y_1'(k_d a) - J_1'(k_d a) Y_1(k_d a)}{J_1'^2(k_d a) + Y_1'^2(k_d a)} \right) \qquad (10.2.18)$$

Using the Wronskian relation

$$J_r(z) Y_r'(z) - J_r'(z) Y_r(z) = \frac{2}{\pi z} \qquad z \neq 0$$

equation (10.2.18) reduces to

$$Q_a^{-1} = \frac{2\rho}{\rho_s} \cdot \frac{1}{(k_d a)^2} \left(\frac{1}{J_1'^2(k_d a) + Y_1'^2(k_d a)} \right) \qquad (10.2.19)$$

This formula may be used in its present form to calculate the acoustic damping factor of cylindrical beams in transverse vibration when k_d is real i.e. when $k_0 > k$. However when $k_0 < k$, k_d is an imaginary quantity and therefore with ζ replaced by $i\zeta$, equation (10.2.6) becomes

$$\frac{d^2\Psi}{d\zeta^2} + \frac{1}{\zeta} \frac{d\Psi}{d\zeta} - \left(1 + \frac{m^2}{\zeta^2}\right) \Psi = 0 \qquad (10.2.20)$$

A complete solution of this equation is

$$\Psi(r) = A I_m(\zeta) + B K_m(\zeta) \qquad (10.2.21)$$

where A and B are constants.

The function $I_m(\zeta) \to \infty$ as $\zeta \to \infty$ and is not therefore a permissible solution. Hence the solution for $\Psi(r)$ takes the form

$$\Psi(r) = B K_m(\zeta) \qquad (10.2.22)$$

and proceeding as before we find

$$p = \frac{i\rho\omega v_0 \cos\theta}{k_d} \left(\frac{K_1(k_d r)}{K_1'(k_d a)} \right) \cos kz \exp(-i\omega t) \qquad (10.2.23)$$

Now all K functions decrease monotonically to zero through positive values as $\zeta \to \infty$ and are real for ζ real > 0. Also

$$K_m'(\zeta) = \frac{m}{\zeta} K_m(\zeta) - K_{m+1}(\zeta)$$

Evidently, then, the quantity $K_m(\zeta)/K_m'(\zeta)$ is always real for ζ real > 0; therefore the pressure and hence the force on the vibrating cylinder is purely reactive. That is to say that when $k_0 < k$ the acoustic radiation resistance is zero and in consequence the acoustic damping factor is also zero.

10.3 COMPARISON OF THEORY WITH EXPERIMENT - CYLINDRICAL BEAMS

Taking $\rho = 0.076$ LB/FT.^{3} and $\rho_s = 490$ LB/FT.^{3} equation (10.2.19) has been evaluated for values of $k_d a$ up to 10.0. The results are shown in graphical form in fig. (17). From this graph it can be seen that the acoustic damping factor rises from zero at $k_d a = 0$ (i.e. at $k_0 = k$) to a maximum at $k_d a \simeq 0.90$. To enable these theoretical results to be compared directly with the experimental results figs. (32) and (33) have been included in Appendix II: these figures show plots of k/frequency and k/k_d for the various diameters of beams.

Figs. (18) and (19) show the theoretical Q_a^{-1}/frequency characteristics together with the experimental results for the range of beam diameters used: the agreement between theory and experiment is seen to be very good. It can also be seen that the experimental results indicate that below the cut-off frequency, which occurs when $k_0 = k$, the acoustic damping factor is zero; this agrees with the theoretical prediction. In addition, if the frequencies at maxima corresponding to each diameter of beam are marked on the

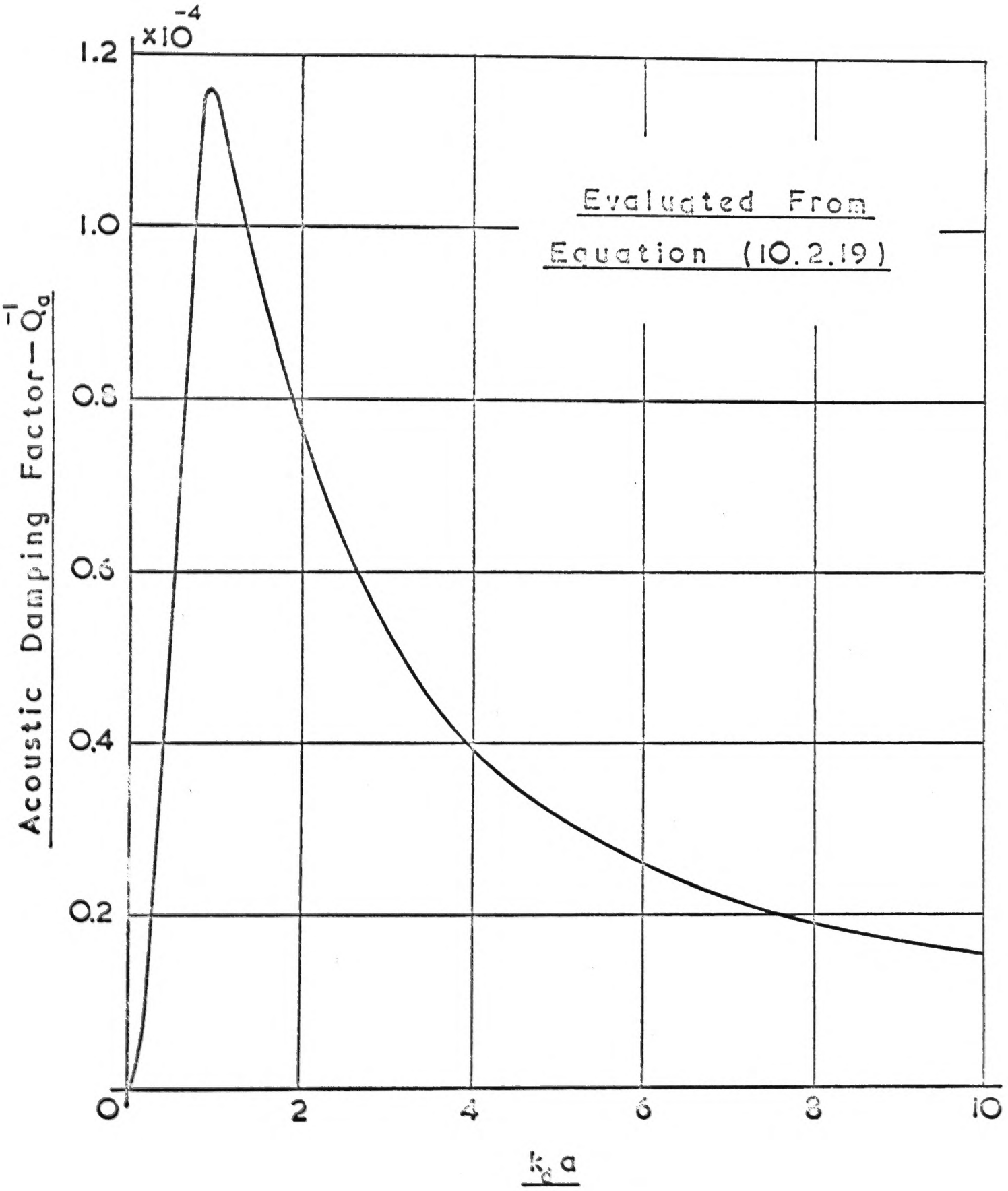

Cylindrical Beams in Transverse Vibration

FIG (17)

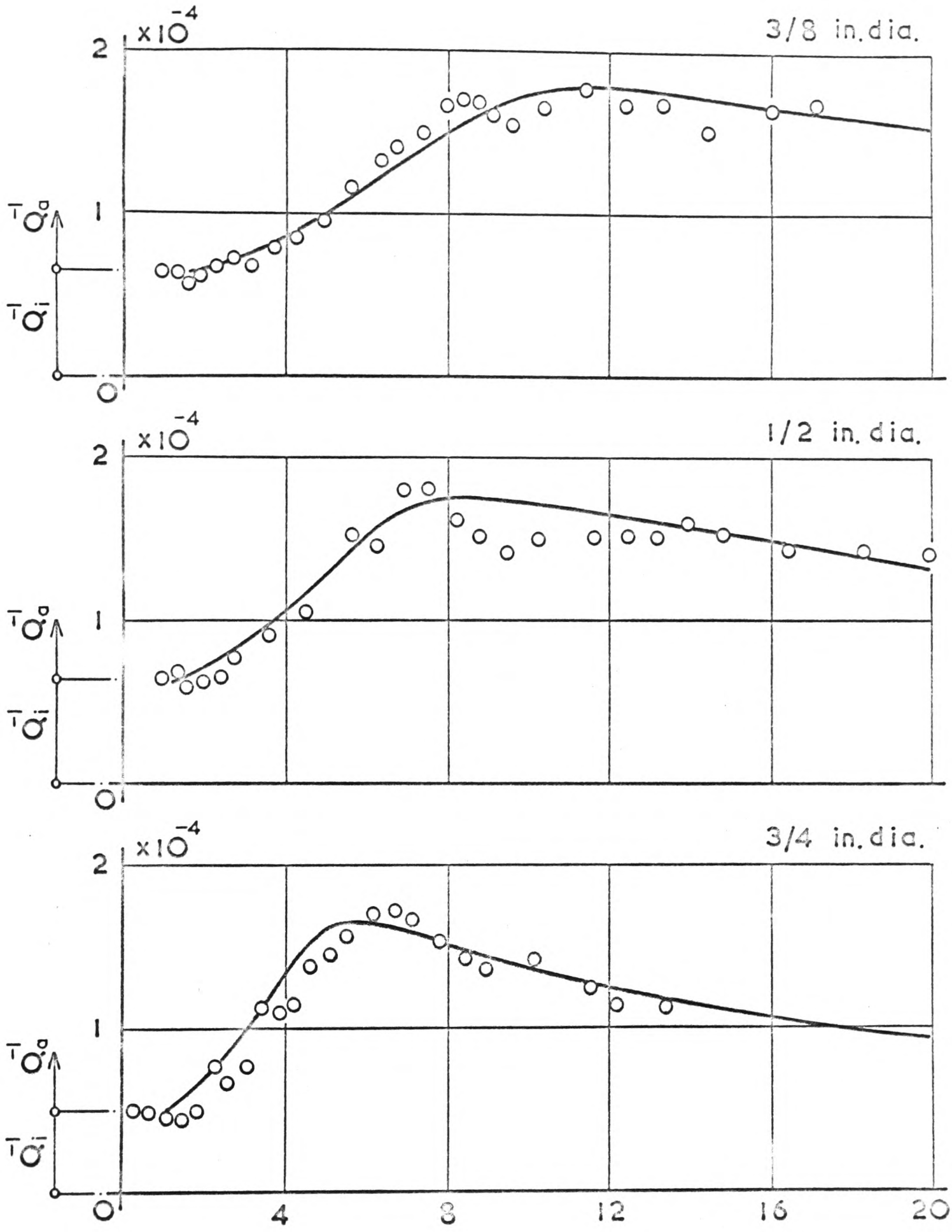

o Experimental Points — Theoretical Curves

Transverse Vibration

FIG (18)

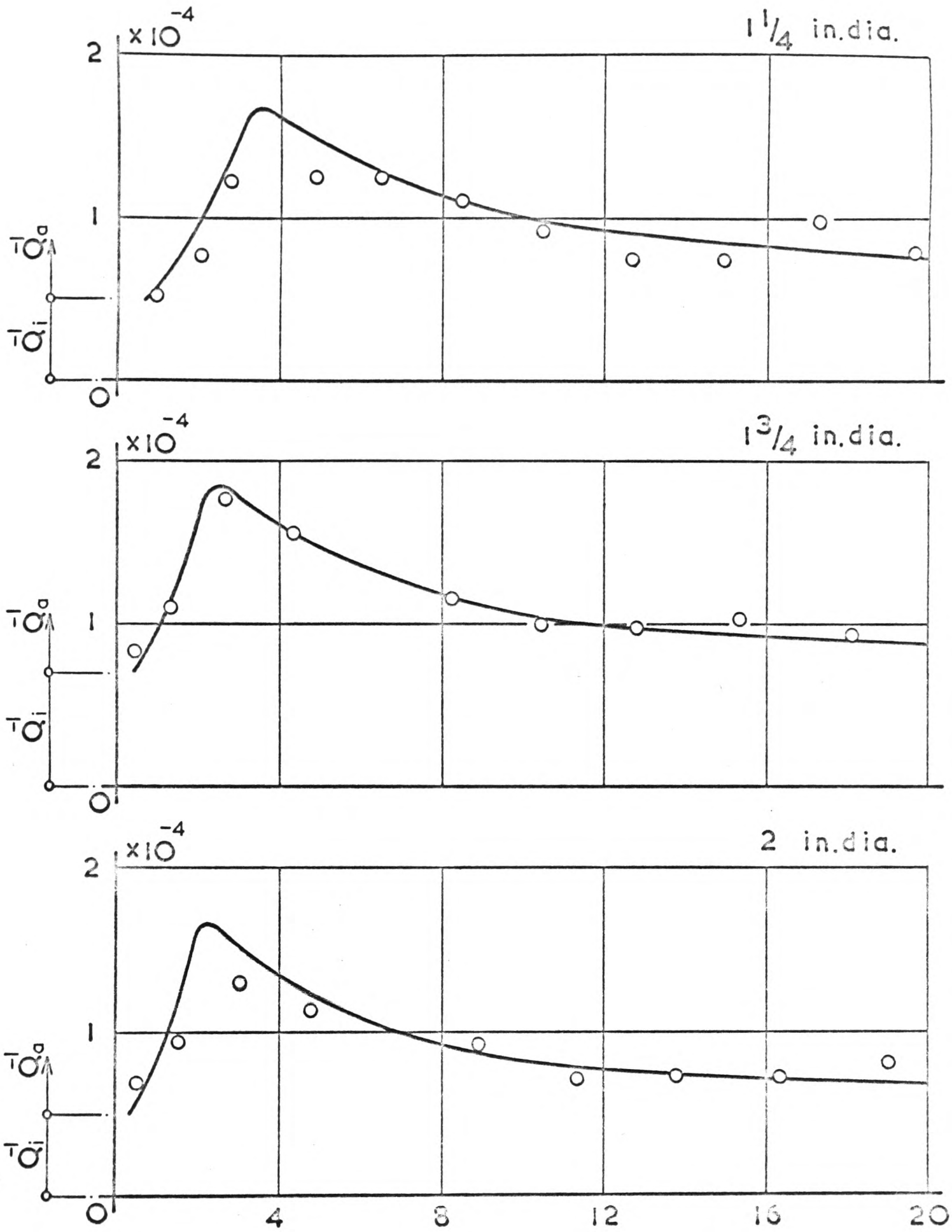

Frequency – c.p.s.

o Experimental Points — Theoretical Curves

Transverse Vibration

FIG (19)

curves of fig. (32) it is found that all the points lie on the line ka = constant = 0.375, therefore, since

$$(k_d a)^2 = (k_0 a)^2 - (ka)^2$$

then at the maxima

$$(k_0 a)^2 \simeq 0.95$$

and thence

$$\frac{2\pi a}{\lambda_0} \simeq 1$$

This means that maximum damping occurs when the wave length of the radiated sound is approximately equal to the circumference of the cylindrical beams.

- - - o 0 o - - -

10.4 THEORY FOR RECTANGULAR BEAMS IN TRANSVERSE VIBRATION

In the case of the cylindrical beams, satisfying the boundary conditions was made fairly simple by transforming equation (10.0.3) to cylindrical coordinates. Satisfying the boundary conditions on a rectangular beam is a much more complex matter; to take complete account of the conditions pertaining thereto would indeed be a formidable mathematical task.

To reduce the mathematical complexities to more readily manageable proportions a basic assumption regarding the pressure waves radiated from the beam will be made. It will be assumed that the pressure waves radiated from the upper and lower faces of the beam travel unrestricted to infinity in all directions and that the principle of superposition holds at all points.

To appreciate better the implications of this assumption consider the following.

In fig. (20a) let AB represent the upper face of the rectangular beam, CD the lower face and AC and BD the sides.

Now let the rectangle ABCD oscillate with a velocity $v = v_0 e^{-i\omega t}$ normal to AB and consider the instant when the displacement is in the positive y direction. At this instant a positive (i.e. compressive) pressure will be created in the surrounding medium at the point O on the upper face and a negative pressure will be created at the point O' on the lower face. Therefore, in terms of the surrounding medium, the conditions on the surface of the rectangle will be defined such that when the rectangle is moving in the positive y direction with velocity v then this velocity will be considered positive on the upper surface, leading to a local positive

pressure in the medium, and negative on the lower surface, leading to a local negative pressure in the medium. The oscillatory motion of all points such as O and O' will lead to the generation of pressure waves in the medium and these will be propogated at the speed of sound in the medium.

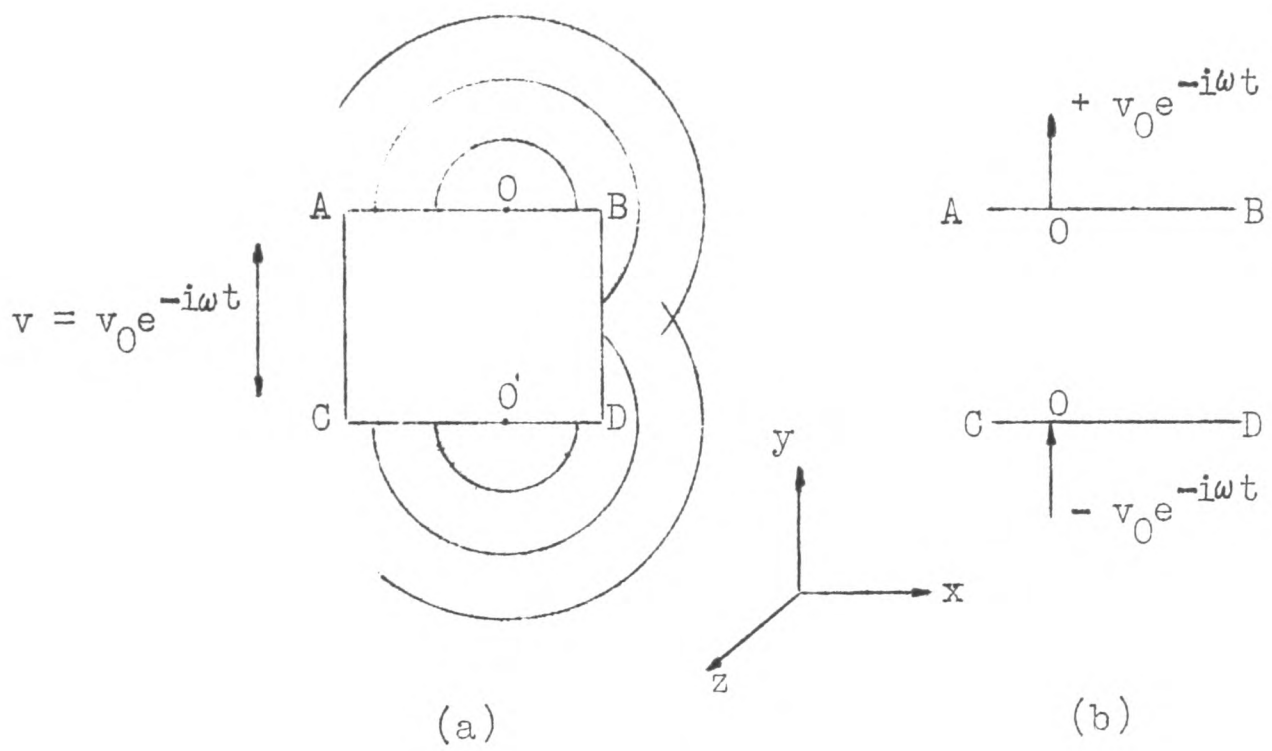

Fig.(20)

The cumulative effect of the radiations from all points such as O and O' is illustrated diagramatically in fig. (20a). Now consider the radiations from AB alone. It can be seen that the presence of the surfaces AC, CD and BD causes distortions of the radiated waves which would analytically be accounted for by fixing the appropriate boundary conditions. However, one of the underlying assumptions of all the theory is that the medium is devoid of viscosity and consequently no forces resisting the motion can be applied by the medium on the sides AC and BD. Therefore the sides have no effect other than to distort the pressure distribution on CD due to the radiations from AB. It will be assumed that the effect of this

distortion is negligeable and that the space between AB and CD is filled with the medium i.e. the boundaries AC and BD will be removed and the y^- side of AB and the y^+ side of CD will be considered to have zero velocity. Fig. (20b) shows the model which will be used to represent the beams in all subsequent work.

To reduce mathematical complications further, it will be assumed that the effect on the pressure distribution on the real surface CD due to the distortions of the radiations from AB by the real surface CD is negligeable. This is tantamount to saying that the pressures existing at an imaginary line CD due to radiations from AB are the same as those that exist on the real surface CD due to the radiations from AB.

To summarise: The rectangular cross section will be assumed to comprise two surfaces, AB and CD, of zero thickness and having the velocity distributions shown in fig. (20b). Furthermore, each surface will be assumed to be able to radiate pressure waves without distortion due to the presence of its neighbour. Finally, the principle of superposition will be assumed to hold at all points.

To calculate the total force resisting the motion of surface AB it is necessary to (a) calculate the force on AB due to its own radiation (b) calculate the force on AB due to the radiations from CD and (c) superpose (a) and (b). Since the force on CD is just of opposite sign to that on AB, the total force resisting the motion of the rectangle ABCD is simply twice (c).

The equation for the radiated pressure wave is again

$$\frac{\partial^2 p(x,y)}{\partial x^2} + \frac{\partial^2 p(x,y)}{\partial y^2} + k_d^2 p(x,y) = 0$$

It is convenient here to transform this equation to elliptic cylinder coordinates; this system is shown below.

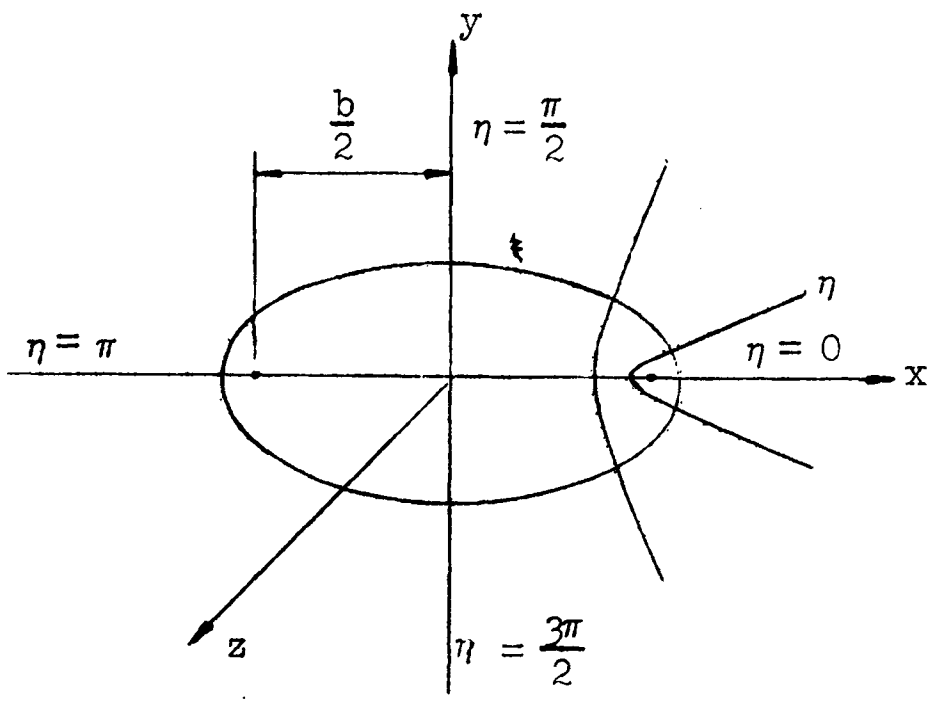

The transformation is effected in Appendix I with the final result.

$$\frac{\partial^2 P(\xi,\eta)}{\partial \xi^2} + \frac{\partial^2 P(\xi,\eta)}{\partial \eta^2} + 2q\,(\cosh 2\xi - \cos 2\eta)\,P(\xi,\eta) = 0 \qquad (10.4.1)$$

where $q = (k_d \frac{b}{4})^2$

Assuming a solution of the form

$$P(\xi,\eta) = \mu(\xi)\,\chi(\eta) \qquad (10.4.2)$$

we get

$$\frac{1}{\mu(\xi)} \frac{d^2\mu(\xi)}{d\xi^2} + 2q\cosh 2\xi = -\frac{1}{\chi(\eta)} \frac{d^2\chi(\eta)}{d\eta^2} + 2q\cos 2\eta$$

For the same reason as that given in 10.2, page 78, each side of this equation must equal a constant: letting this constant

be h we therefore obtain

$$\frac{d^2\chi(\eta)}{d\eta^2} + (h - 2q\cos 2\eta)\,\chi(\eta) = 0 \qquad (10.4.3)$$

$$\frac{d^2\mu(\xi)}{d\xi^2} - (h - 2q\cos h2\xi)\,\mu(\xi) = 0 \qquad (10.4.4)$$

These equations are Mathieu's equations. The first may be regarded as the canonical form of the equation and the second is generally known as the modified Mathieu equation :-(q > 0)

To solve equations (10.4.3) and (10.4.4) it is first necessary to fix the boundary conditions. We shall first concern ourselves solely with the surface AB shown in fig. (21).

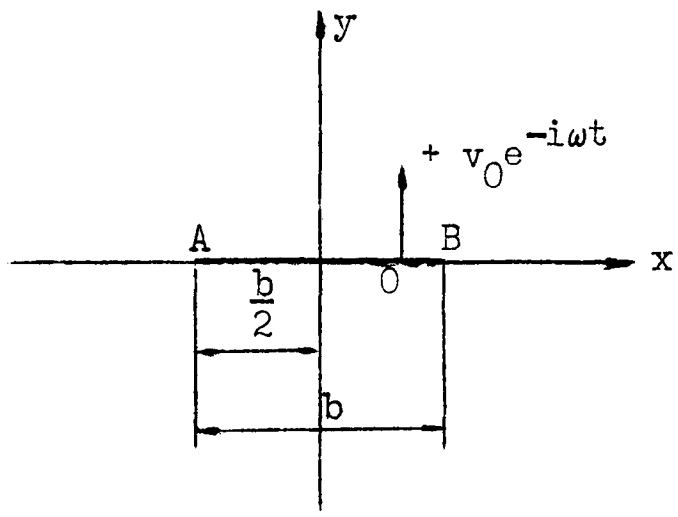

Fig. (21)

The strip AB, of zero thickness, is obtained by letting the elliptic coordinate $\xi = 0$ in which case the breadth b is the inter-focal distance. The velocity distribution is $v = v_0e^{-i\omega t}$ on the y^+ side and zero on the y^- side of the strip and this distribution may be represented in terms of the elliptic coordinate η by the step function shown below.

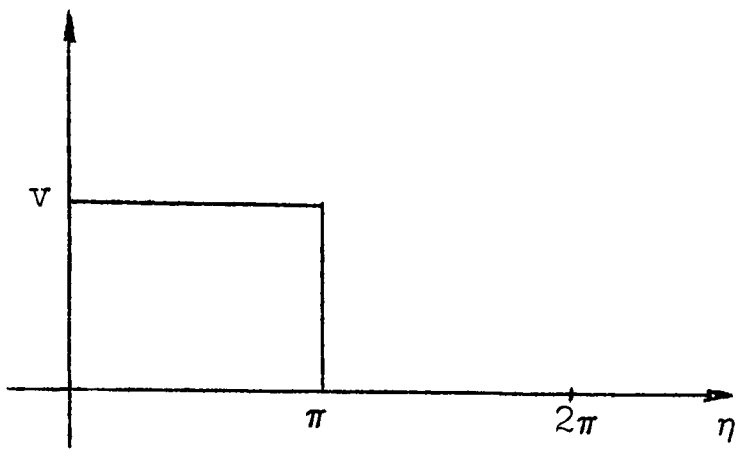

If unit step function be denoted $F(\eta)$ then the velocity distribution is given by $v = v_0 F(\eta) e^{-i\omega t}$.

In the physical problem AB represents the upper surface of a vibrating rectangular beam therefore if the beam is considered to be of infinite length the velocity at any point on the upper surface may be represented by

$$v = v_0 \, F(\eta) \cos kz \exp(-i\omega t) \qquad (10.4.5)$$

Newton's equation of motion is

$$\text{grad } (p(\xi,\eta,z,t)) = -\rho \frac{\partial v}{\partial t} \qquad (10.4.6)$$

and what is required here is $\left(\frac{\partial p}{\partial y}\right)_{y=0}$

Now $$\frac{\partial p}{\partial y} = \left| \frac{2}{b \cosh \xi \sin \eta} \right| \cdot \frac{\partial p}{\partial \xi}$$

therefore $$\left(\frac{\partial p}{\partial y}\right)_{y=0} = \frac{2}{b|\sin \eta|} \left(\frac{\partial p}{\partial \xi}\right)_{\xi=0}$$

thus $$\left(\frac{\partial p}{\partial \xi}\right)_{\xi=0} = -\tfrac{1}{2}\rho\, b\left|\sin\eta\right| \frac{\partial v}{\partial t}$$

$$= i\omega\rho \frac{b}{2} v_0 \left|\sin\eta\right| F(\eta)\cos kz \exp(-i\omega t) \qquad (10.4.7)$$

but $$p(\xi,\eta,z,t) = P(\xi,\eta)\cos kz \exp(-i\omega t)$$

therefore

$$\left(\frac{\partial P(\xi,\eta)}{\partial \xi}\right)_{\xi=0} = i\omega\rho \frac{b}{2} v_0 F(\eta)\left|\sin\eta\right| \qquad (10.4.8)$$

The function $F(\eta)\sin\eta$ is neither even or odd in η therefore $P(\xi,\eta)$ must likewise be neither even or odd in η. To satisfy this requirement the solution of (10.4.3) must be a combination of the functions se_m and ce_m. Also, the direction of the wave propogation is away from the origin and to satisfy this requirement the solution of (10.4.4) must be a combination of the functions $Ne_m^{(1)}$ and $Me_m^{(1)}$. In accordance with these conditions the following general form of solution for $P(\xi,\eta)$ will be assumed.

$$P(\xi,\eta) = \sum_m \left(\alpha_m se_m(\eta,q) Ne_m^{(1)}(\xi,q) + \beta_m ce_m(\eta,q) Me_m^{(1)}(\xi,q)\right) \qquad (10.4.9)$$

where α_m, β_m are arbitrary constants to be determined from the boundary conditions.

We therefore have

$$\left(\frac{\partial P}{\partial \xi}\right)_{\xi=0} = \sum_m \left(\alpha_m se_m(\eta,q) Ne_m^{(1)'}(0,q) + \beta_m ce_m(\eta,q) Me_m^{(1)'}(0,q)\right) \qquad (10.4.10)$$

where $$Ne_m^{(1)'}(0,q) = \left(\frac{\partial}{\partial \xi} Ne_m^{(1)}(\xi,q)\right)_{\xi=0} \quad \text{etc.}$$

Before we can equate (10.4.10) and (10.4.8) it is necessary to expand the function $F(\eta)\sin\eta$ in a series of the eigenfunctions $se_m(\eta,q)$ and $ce_m(\eta,q)$. Thus let

$$F(\eta)\left|\sin\eta\right| = \sum_m (C_m se_m(\eta,q) + D_m ce_m(\eta,q)) \qquad (10.4.11)$$

Now $F(\eta)\left|\sin\eta\right| = \sin\eta \qquad 0 < \eta < \pi$

$= 0 \qquad \pi < \eta < 2\pi$

Taking normalised forms for se_m and ce_m so that

$$\frac{1}{\pi}\int_0^{2\pi} se_m^2\, d\eta = \frac{1}{\pi}\int_0^{2\pi} ce_m^2\, d\eta = 1$$

and using the orthogonality of se_m and ce_m we get

$$C_m = \frac{1}{\pi}\int_0^{\pi} \sin\eta\ se_m(\eta,q)\, d\eta$$

$$D_m = \frac{1}{\pi}\int_0^{\pi} \sin\eta\ ce_m(\eta,q)\, d\eta$$

but $$se_m(\eta,q) = \sum_s B_s^{(m)} \sin s\eta$$

$$ce_m(\eta,q) = \sum_s A_s^{(m)} \cos s\eta$$

therefore $$C_m = \frac{1}{\pi}\int_0^{\pi} \sum_s B_s^{(m)} \sin s\eta \sin\eta\, d\eta$$

$$D_m = \frac{1}{\pi}\int_0^{\pi} \sum_s A_s^{(m)} \cos s\eta \sin\eta\, d\eta$$

The convergence of these series allows term by term integration and on performing the integrations we find

$$C_m = 0 \quad \text{for} \quad s \neq 1$$

$$= \tfrac{1}{2} B_1^{(m)} \quad \text{for} \quad s = 1$$

$$D_m = 0 \quad \text{for} \quad s \quad \text{odd}$$

$$= -\frac{2}{\pi} \sum_{s} \frac{1}{(s^2 - 1)} A_s^{(m)} \quad \text{for} \quad s \quad \text{even}$$

In the expansion for $se(\eta,q)$ the integers m and s are even or odd together and may take either of the two forms $m = 2n + 2$ or $2n + 1$ and $s = 2r + 2$ or $2r + 1$. Since for C_m, $s = 1$ then we must have $m = 2n + 1$. In the case of the ce functions again m and s are even or odd together and may take either of the two forms $m = 2n$ or $2n + 1$ and $s = 2r$ or $2r + 1$. Since for D_m, s is even we must have $s = 2r$ and $m = 2n$.

Substituting for C_m and D_m in (10.4.11) we get

$$F(\eta)\left|\sin\eta\right| = \sum_{n=0}^{\infty}\left(\tfrac{1}{2}B_1^{(2n+1)} se_{2n+1}(\eta,q) - \frac{2}{\pi}\left[\sum_{r=0} \frac{1}{(4r^2-1)} A_{2r}^{(2n)}\right] ce_{2n}(\eta,q)\right) \tag{10.4.12}$$

Therefore from (10.4.8) we obtain

$$\left(\frac{\partial P}{\partial \xi}\right)_{\xi=0} = i\omega\rho \frac{b}{2} v_0 \sum_{n=0}^{\infty}\left(\tfrac{1}{2}B_1^{(2n+1)} se_{2n+1}(\eta,q) - \frac{2}{\pi}\left[\sum_{r=0}^{\infty} \frac{1}{(4r^2-1)} A_{2r}^{(2n)}\right] ce_{2n}(\eta,q)\right) \tag{10.4.13}$$

Equation (10.4.10) may be written

$$\left(\frac{\partial P}{\partial \xi}\right)_{\xi=0} = \sum_{n=0}^{\infty}\Big(\alpha_{2n+1}\, se_{2n+1}(\eta,q)\, Ne_{2n+1}^{(1)'}(0,q) + \alpha_{2n+2}\, se_{2n+2}(\eta,q)\, Ne_{2n+2}^{(1)'}(0,q) + \beta_{2n}\, ce_{2n}(\eta,q)\, Me_{2n}^{(1)'}(0,q) + \beta_{2n+1}\, ce_{2n+1}(\eta,q)\, Me_{2n+1}^{(1)'}(0,q)\Big) \tag{10.4.14}$$

and equating coefficients of like functions in (10.4.13) and (10.4.14) we find

$$\alpha_{2n+2} = \beta_{2n+1} = 0$$

$$\alpha_{2n+1} = \frac{i\omega\rho\frac{b}{2}\, v_0 \cdot \frac{1}{2}B_1^{(2n+1)}}{Ne_{2n+1}^{(1)'}(0,q)}$$

$$\beta_{2n} = \frac{-i\omega\rho\frac{b}{2}\, v_0 \cdot \frac{2}{\pi}\left[\sum_{r=0}^{\infty} \frac{1}{(4r^2-1)} A_{2r}^{(2n)}\right]}{Me_{2n}^{(1)'}(0,q)}$$

therefore from (10.4.9) we obtain

$$P(\xi,\eta) = i\omega\rho\frac{b}{2} v_0 \sum_{n=0}^{\infty} \left\{ \tfrac{1}{2}B_1^{(2n+1)} se_{2n+1}(\eta,q) \frac{Ne_{2n+1}^{(1)}(\xi,q)}{Ne_{2n+1}^{(1)'}(0,q)} \right.$$

$$\left. - \frac{2}{\pi}\left[\sum_{r=0} \frac{1}{(4r^2-1)} A_{2r}^{(2n)}\right] ce_{2n}(\eta,q) \frac{Me_{2n}^{(1)}(\xi,q)}{Me_{2n}^{(1)'}(0,q)} \right\} \qquad (10.4.15)$$

This is the equation for the pressure wave radiated from AB.

To calculate force consider an elemental length ds of any elliptic surface ξ = constant. The force on such an element is $p(\xi,\eta,z,t)$ ds and the component in the y direction is $p(\xi,\eta,z,t)$ ds $\cdot \frac{dx}{ds}$ and since $x = \frac{b}{2}\cosh\xi\cos\eta$ then

$$\text{Force in y direction} = -\frac{b}{2}\cosh\xi\, p(\xi,\eta,z,t)\sin\eta\, d\eta \qquad (10.4.16)$$

In the case of the strip AB $\xi = 0$ therefore the normal component of force per unit length on the y^+ side of AB is given by

$$F_{TT} = \int_0^{\pi} \frac{b}{2} P(0,\eta)\cos kz \exp(-i\omega t)\sin\eta\, d\eta \qquad (10.4.17)$$

(the term $\cos kz \exp(\mp i\omega t)$ will be omitted for brevity in what follows)

Putting $\xi = 0$ in (10.4.15) and substituting in (10.4.17) we get

$$F_{TT} = i\omega\rho\left(\frac{b}{2}\right)^2 v_0 \sum_{n=0}^{\infty}\Bigg\{ \tfrac{1}{2}B_1^{(2n+1)} \frac{Ne_{2n+1}^{(1)}(0,q)}{Ne_{2n+1}^{(1)'}(0,q)} \left(\sum_{r=0}^{\infty} B_{2r+1}^{(2n+1)} \int_0^{\pi} \sin(2r+1)\eta \sin\eta \, d\eta \right)$$

$$- \frac{2}{\pi}\left[\sum_{r=0}^{\infty} \frac{1}{(4r^2-1)} A_{2r}^{(2n)} \right] \frac{Me_{2n}^{(1)}(0,q)}{Me_{2n}^{(1)'}(0,q)} \left(\sum_{r=0}^{\infty} A_{2r}^{(2n)} \int_0^{\pi} \cos 2r\eta \sin\eta \, d\eta \right) \Bigg\}$$

and performing the integrations we obtain the final result

$$F_{TT} = i\omega\rho\left(\frac{b}{2}\right)^2 v_0 \sum_{n=0}^{\infty}\Bigg\{ \frac{\pi}{4} \left(B_1^{(2n+1)}\right)^2 \frac{Ne_{2n+1}^{(1)}(0,q)}{Ne_{2n+1}^{(1)'}(0,q)}$$

$$+ \frac{4}{\pi}\left[\sum_{r=0}^{\infty} \frac{1}{(4r^2-1)} A_{2r}^{(2n)} \right]^2 \frac{Me_{2n}^{(1)}(0,q)}{Me_{2n}^{(1)'}(0,q)} \Bigg\} \qquad (10.4.18)$$

This is the total normal force per unit length on the top surface of the vibrating beam due solely to acoustic radiation from that surface.

It is now necessary to calculate the force on the surface AB due to acoustic radiation from the surface CD.

We must first obtain an expression for the pressure wave radiated from the surface CD which has the velocity distribution shown in fig. (22). This velocity distribution may, in the same way as for the surface AB, be represented in terms of the coordinate η by a stop function $F(\eta)$. In this case we have

$$F(\eta)\,|\sin\eta| = 0 \qquad 0 < \eta < \pi$$

$$= -\,|\sin\eta| \qquad \pi < \eta < 2\pi$$

and on performing analysis similar to that of the foregoing we obtain for the pressure wave

$$P(\xi,\eta) = i\omega\rho \frac{b}{2} v_0 \sum_{n=0}^{\infty} \left\{ \tfrac{1}{2} B_1^{(2n+1)} se_{2n+1}(\eta,q) \frac{Ne_{2n+1}^{(1)}(\xi,q)}{Ne_{2n+1}^{(1)\prime}(0,q)} \right.$$

$$\left. + \frac{2}{\pi} \left[\sum_{r=0}^{\infty} \frac{1}{(4r^2-1)} A_{2r}^{(2n)} \right] ce_{2n}(\eta,q) \frac{Me_{2n}^{(1)}(\xi,q)}{Me_{2n}^{(1)\prime}(0,q)} \right\} \qquad (10.4.19)$$

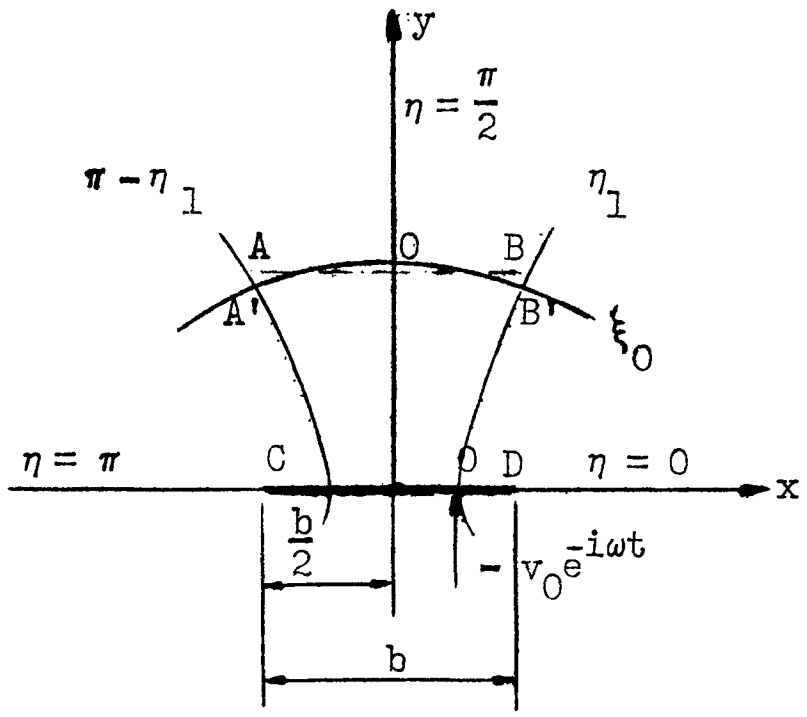

Fig. (22)

What is actually required is the integral of this pressure along the line AB. To do this it would be necessary to keep the product $\sinh\xi \sin\eta$ constant: adherence to such a requirement would lead to considerable difficulties in the evaluation of the integrals of the products se.Ne and ce.Me. However since approximations relating to the radiated pressure wave have already been made it does not seem reasonable to add this complication. If instead it is assumed that the force on the part of the elliptic surface, ξ_0, A'OB' fig. (22), is essentially the same as the force on the surface AB then there will only be one variable, η, and it will

be a simple matter to integrate the pressure between the limits η_1 and $\pi - \eta_1$. Under these circumstances the normal force per unit length on AB due to the radiations from CD is from (10.4.16)

$$F_{TB} = \int_{\eta_1}^{\pi-\eta_1} \frac{b}{2} \cosh \xi_0 \, P(\xi_0, \eta) \cos kz \exp(-i\omega t) \sin\eta \, d\eta \qquad (10.4.20)$$

(again the term $\cos kz \exp(-i\omega t)$ will be omitted for brevity in what follows)

For a rectangular beam the quantity ξ_0 is determined from the depth of the beam and for a given ξ_0 the quantity η_1 is determined from the breadth of the beam.

Putting $\xi = \xi_0$ in (10.4.19) and substituting in (10.4.20) gives

$$F_{TB} = i\omega\rho\left(\frac{b}{2}\right)^2 v_0 \cosh \xi_0 \sum_{n=0}^{\infty} \left\{ \left(\tfrac{1}{2} B_1^{(2n+1)} \frac{Ne_{2n+1}^{(1)}(\xi_0, q)}{Ne_{2n+1}^{(1)'}(0, q)} \cdot \right.\right.$$

$$\left. \cdot \int_{\eta_1}^{\pi-\eta_1} se_{2n+1}(\eta, q) \sin\eta \, d\eta \right) + \left(\frac{2}{\pi} \left[\sum_{r=0}^{\infty} \frac{1}{(4r^2-1)} A_{2r}^{(2n)} \right] \frac{Me_{2n}^{(1)}(\xi_0, q)}{Me_{2n}^{(1)'}(0, q)} \cdot \right.$$

$$\left.\left. \cdot \int_{\eta_1}^{\pi-\eta_1} ce_{2n}(\eta, q) \sin\eta \, d\eta \right) \right\} \qquad (10.4.21)$$

Thus the total force per unit length resisting the motion of AB is given by $(F_{TT} + F_{TB})$ and therefore the total force per unit length resisting the motion of the rectangle ABCD is

$$F_{total} = 2 (F_{TT} + F_{TB}) \qquad (10.4.22)$$

Within the assumptions used in its development F_{total} is the force, due to acoustic radiation, resisting the motion of unit length of a rectangular beam performing sinusoidal transverse oscillations.

This force may, in the same way as for the cylindrical beams, be separated into real and imaginary parts. The imaginary part

is 90° out of phase with the velocity and again represents a mass reactance on the beam. The real part is in phase with the velocity and therefore the coefficient of the velocity may as before be represented by an equivalent viscous coefficient. Having evaluated this coefficient for any particular beam the acoustic damping factor is then obtained from equation (2.0.5).

All the above applies when q is positive i.e. when $k_0 > k$. When $k_0 < k$ it can be shown using, the formulae given by McLachlan[25] that the quantities $^{Ne}/_{Ne'}$ and $^{Me}/_{Me'}$ in equations (10.4.18) and (10.4.21) are always real and therefore that F_{total} is always imaginary. That is, the force is purely reactive and thus the acoustic damping factor is zero. This result corresponds to that obtained in the case of the cylindrical beams.

10.5 EVALUATION OF ACOUSTIC DAMPING FACTOR - RECTANGULAR BEAMS

The evaluation of equation (10.4.22) would be fairly straightforward if tabulated values of Mathieu Functions and coefficients were available over a sufficiently wide range of the parameters involved. Unfortunately this is not the case and consequently, to obtain numerical results, it is necessary to calculate the values of the Me and Ne type functions and to use interpolation to find the coefficients $A_{2r}^{(2n)}$ and $B_{2r+1}^{(2n+1)}$.

To illustrate the method used a typical calculation will be given here.

The values of the ratios of the Me and Ne type functions were calculated using the following formulae (see McLachlan[25])

$$\frac{Me^{(1)}_{2n}(\xi,q)}{Me^{(1)'}_{2n}(0,q)} = \frac{\sum_{r=0}^{\infty}(-1)^r A^{(2n)}_{2r} J_r(v_1) H^{(1)}_r(v_2)}{\sum_{r=0}^{\infty}(q)^{\frac{1}{2}}(-1)^r\left(A^{(2n)}_{2r}(J_r H^{(1)'}_r - H^{(1)}_r J'_r)\right)} \qquad (10.5.1)$$

$$\frac{Ne^{(1)}_{2n+1}(\xi,q)}{Ne^{(1)'}_{2n+1}(0,q)} = \frac{\sum_{r=0}^{\infty}(-1)^r B^{(2n+1)}_{2r+1}\left(J_r(v_1)H^{(1)}_{r+1}(v_2) - J_{r+1}(v_1)H^{(1)}_r(v_2)\right)}{\sum_{r=0}^{\infty}(q)^{\frac{1}{2}}(-1)^r B^{(2n+1)}_{2r+1}\left(J_r H^{(1)'}_{r+1} - H^{(1)}_{r+1}J'_r - J_{r+1}H^{(1)'}_r + H^{(1)}_r J'_{r+1}\right)} \qquad (10.5.2)$$

where the argument of the Bessel functions in the denominators is $(q)^{\frac{1}{2}}$ and $v_1 = (q)^{\frac{1}{2}}e^{-\xi}$, $v_2 = (q)^{\frac{1}{2}}e^{\xi}$.

Tabulated values of the Bessel functions were obtained from Watson's, Theory of Bessel Functions and the differentials of the functions were evaluated using the appropriate formulae given in this treatise.

Graphical interpolation was used to obtain the coefficients $A^{(2n)}_{2r}$ and $B^{(2n+1)}_{2r+1}$: fig. (23) shows plots of these coefficients as continuous functions of q. The values of the coefficients tabulated by Ince[8] were used to construct the graphs.

As an example of the type of calculation involved consider the case of a 4:1 breadth to depth ratio beam, say 1 in. wide $\frac{1}{4}$ in. deep.

Considering first the evaluation of F_{TT} with q = 0.49 and n = 0. Fig. (23) then gives

$$B^1_1 = 0.999; \quad B^1_3 = -0.057; \quad B^1_5 = 0$$

$$A^0_0 = 0.693; \quad A^0_2 = -0.177; \quad A^0_4 = 0.007; \quad A^0_6 = 0$$

therefore $$\frac{\pi}{4}(B^1_1)^2 = \underline{0.786}$$

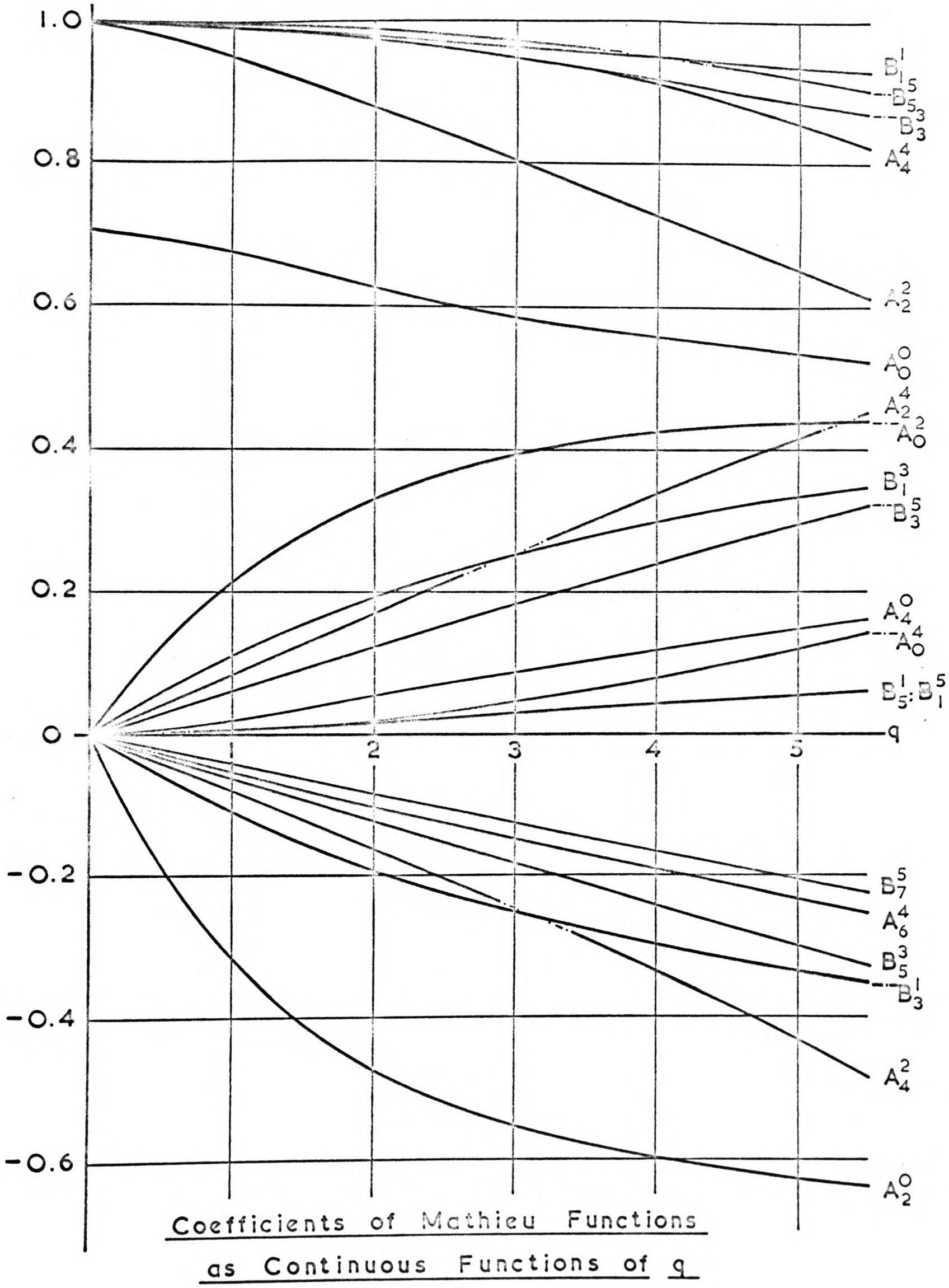

Coefficients of Mathieu Functions

as Continuous Functions of q

FIG (23)

$$\frac{4}{\pi}\left[\sum_{r=0}^{\infty}\frac{1}{(4r^2-1)}\ A_{2r}^{0}\right]^2 = \underline{0.721}$$

On substituting the values of the Bessel functions and their derivatives together with the above coefficients in equations (10.5.1) and (10.5.2) and extending the summations to three terms (which was generally found to be adequate) we obtain

$$\frac{Me_0^{(1)}(0,0.49)}{Me_0^{(1)'}(0,0.49)} = \frac{0.557 - i\ 0.181}{i\ 0.558}$$

$$\frac{Ne_1^{(1)}(0,0.49)}{Ne_1^{(1)'}(0,0.49)} = \frac{-\ i\ 0.961}{0.660 + i\ 0.427}$$

Therefore the first term in the summation of (10.4.18) is

$$\left[0.786\left(\frac{-\ i\ 0.961}{0.660 + i\ 0.427}\right) + 0.721\left(\frac{0.557 - i\ 0.181}{i\ 0.558}\right)\right]$$

$$= (-\ 0.754 - i\ 1.527)$$

Carrying out the above procedure for n = 1 and n = 2 the value of the summation of (10.4.18), (this summation always converged in two or three terms), becomes (- 0.786 - i 1.528).

Thus $F_{TT} = \omega\rho\left(\frac{b}{2}\right)^2 v_0(1.528 - i\ 0.786)$ (10.5.3)

To evaluate F_{TB} it is first necessary to fix the values of ξ_0 and η_1.

Now $x = \frac{b}{2}\cosh\xi\cos\eta$

$y = \frac{b}{2}\sinh\xi\sin\eta$

and in this case b = 1.0 inch.

The actual y ordinate is 0.25 inches but taking account of the assumption made in developing F_{TB} it will be assumed that at x = 0

the y coordinate of the elliptic surface, ξ_0, is 0.313 inches (the surfaces chosen were always such that the differences between the actual y ordinate and the ordinates of the surface at $x = \pm \frac{b}{2}$ and $x = 0$ were of the same order. This was a purely arbitrary choice it being considered that such a surface would be subject to forces of the same order as those on AB). This gives $\xi_0 = 0.590$ rads. η_1 is calculated at $x = \frac{b}{2}$ and with b = 1.0 inch, $\eta_1 = 0.560$ rads.

Thus the arguments of the Bessel functions in the numerators of (10.5.1) and (10.5.2) are

$$v_1 = (q)^{\frac{1}{2}} e^{-\xi_0} = 0.38$$

$$v_2 = (q)^{\frac{1}{2}} e^{-\xi_0} = 1.26$$

Using term by term integration to evaluate the integrals of (10.4.21) and calculating the values of the other terms in the same way as for F_{TT} gives

$$F_{TB} = \omega\rho \left(\frac{b}{2}\right)^2 v_0 (0.197 - i\ 0.210) \qquad (10.5.4)$$

Therefore from (10.4.22)

$$F_{total} = 2 (F_{TT} + F_{TB})$$

$$= \omega\rho \left(\frac{b}{2}\right)^2 v_0 (3.450 - i\ 1.992) \qquad (10.5.5)$$

Thus using equation (2.0.5)

$$Q_a^{-1} = \frac{\omega\rho \left(\frac{b}{2}\right)^2 \cdot 3.450}{\omega b d\, \rho_s}$$

$$= \frac{3.450}{4} \cdot \frac{b}{d} \cdot \frac{\rho}{\rho_s} \qquad (10.5.6)$$

where d is the depth of the beam.

With $\rho = 0.076$ lb/ft.^{3} and $\rho_s = 490$ lb/ft.^{3} (10.5.6) gives

$$\underline{Q_a^{-1} = 5.35 \times 10^{-4}}$$

Selecting further values of q and performing the calculations as above the Q_a^{-1}/q characteristic for the beam is obtained.

10.6 COMPARISON OF THEORY WITH EXPERIMENT - RECTANGULAR BEAMS.

The procedure outlined in the previous sub-section was carried out for beams with 8:1, 4:1, 2:1 and 1:1 breadth to depth ratios and the results are shown in fig. (24). The curves show that the acoustic damping factor is zero when q = 0 (i.e. when $k_0 = k$) and that the values of the damping factors for q > 0 depend on the breadth to depth ratios of the beams. It can be seen that the maximum values of Q_a^{-1} and the values of q at which they occur are also dependent on the breadth to depth ratios of the beams.

To enable direct comparison with the experimental results figs. (34) and (35) have been included in Appendix II: these figures show plots of k/frequency and $k/q/b^2$ for the various beam depths.

Figs. (25) - (30) show the theoretical Q_a^{-1}/frequency characteristics together with the experimental results for the range of beams used. Considering the assumptions made in developing the theory, the agreement between theory and experiment is seen to be remarkably good. As predicted by the theory the experimental results clearly show the existence of cut off frequencies. (No theoretical curves are shown for the very low breadth to depth ratio beams as the peaks are so small that, in general, experiment

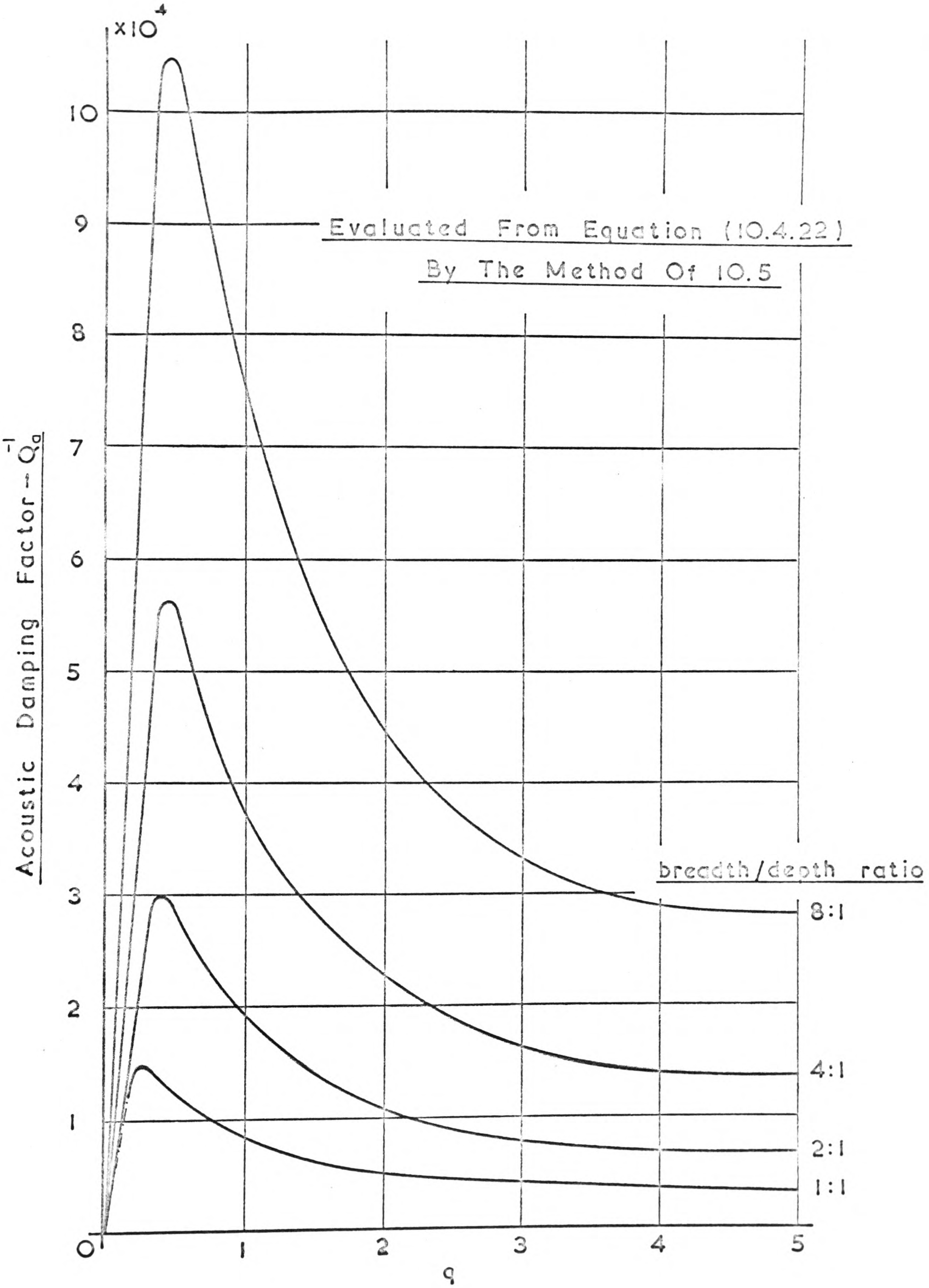

Rectangular Beams in Transverse Vibration

FIG (24)

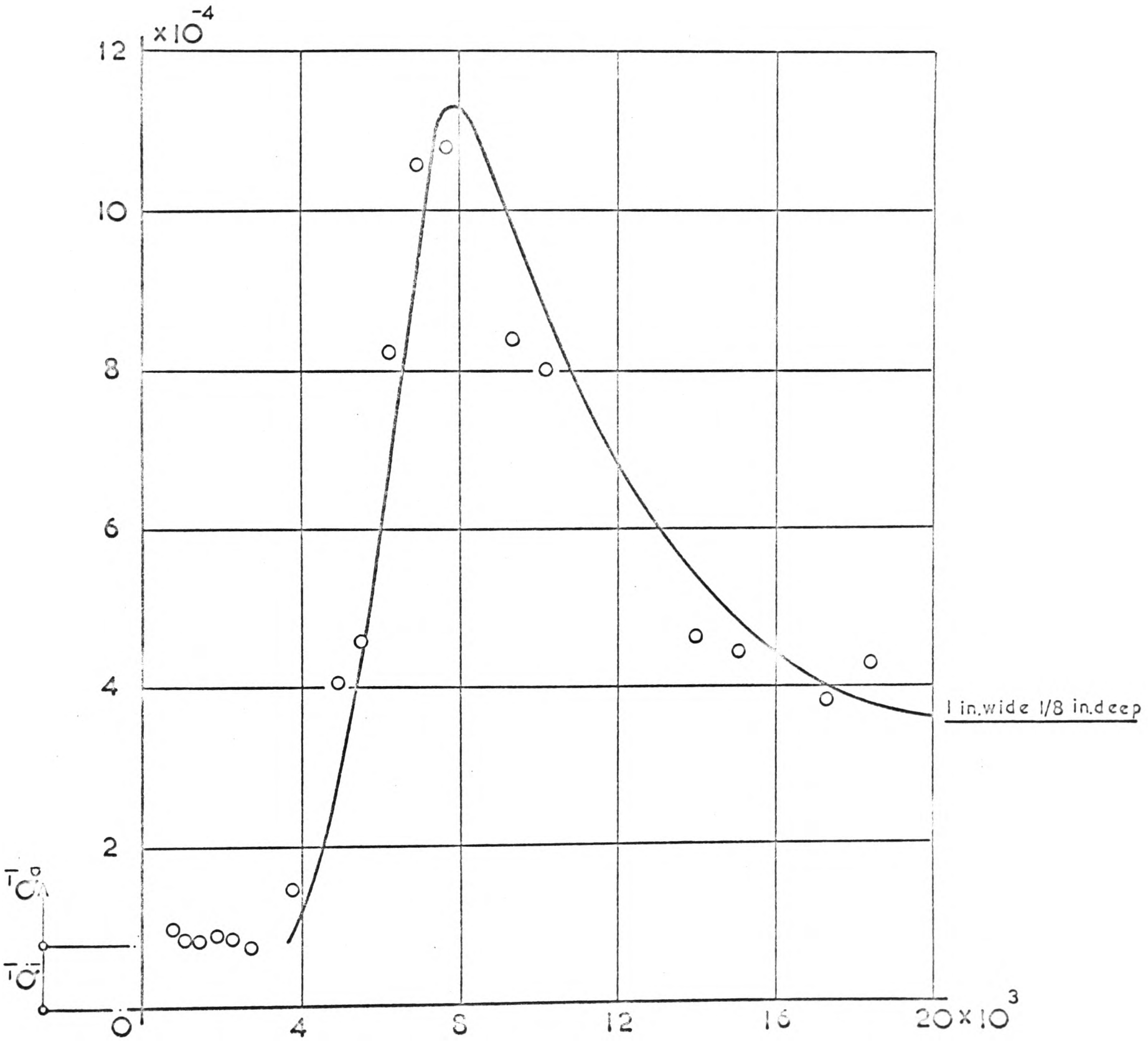

Frequency — c.p.s.

o Experimental Points — Theoretical Curve

Transverse Vibration

FIG (25)

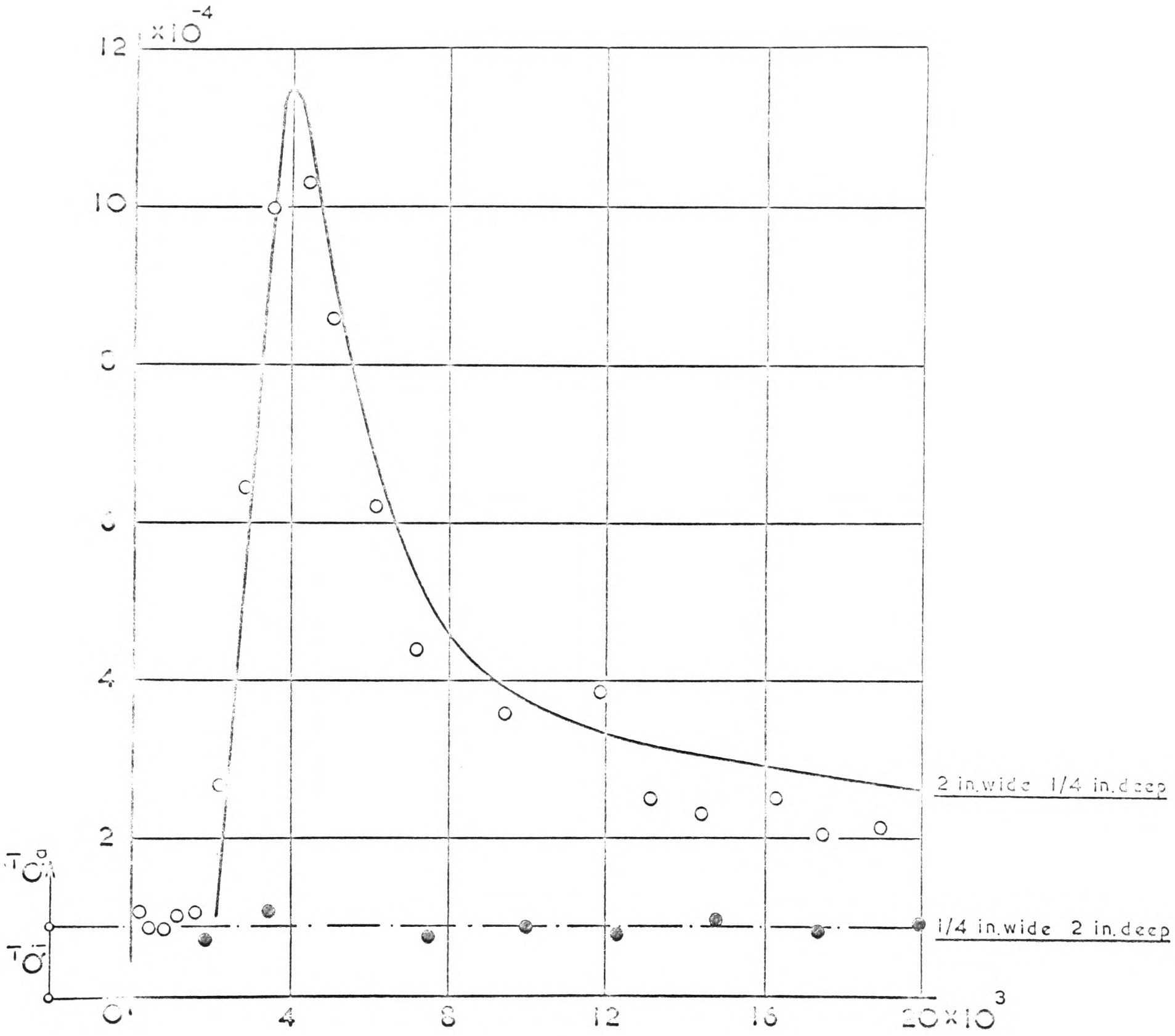

Frequency – c.p.s.

Experimental Points — Theoretical Curve

Transverse Vibration

FIG (26)

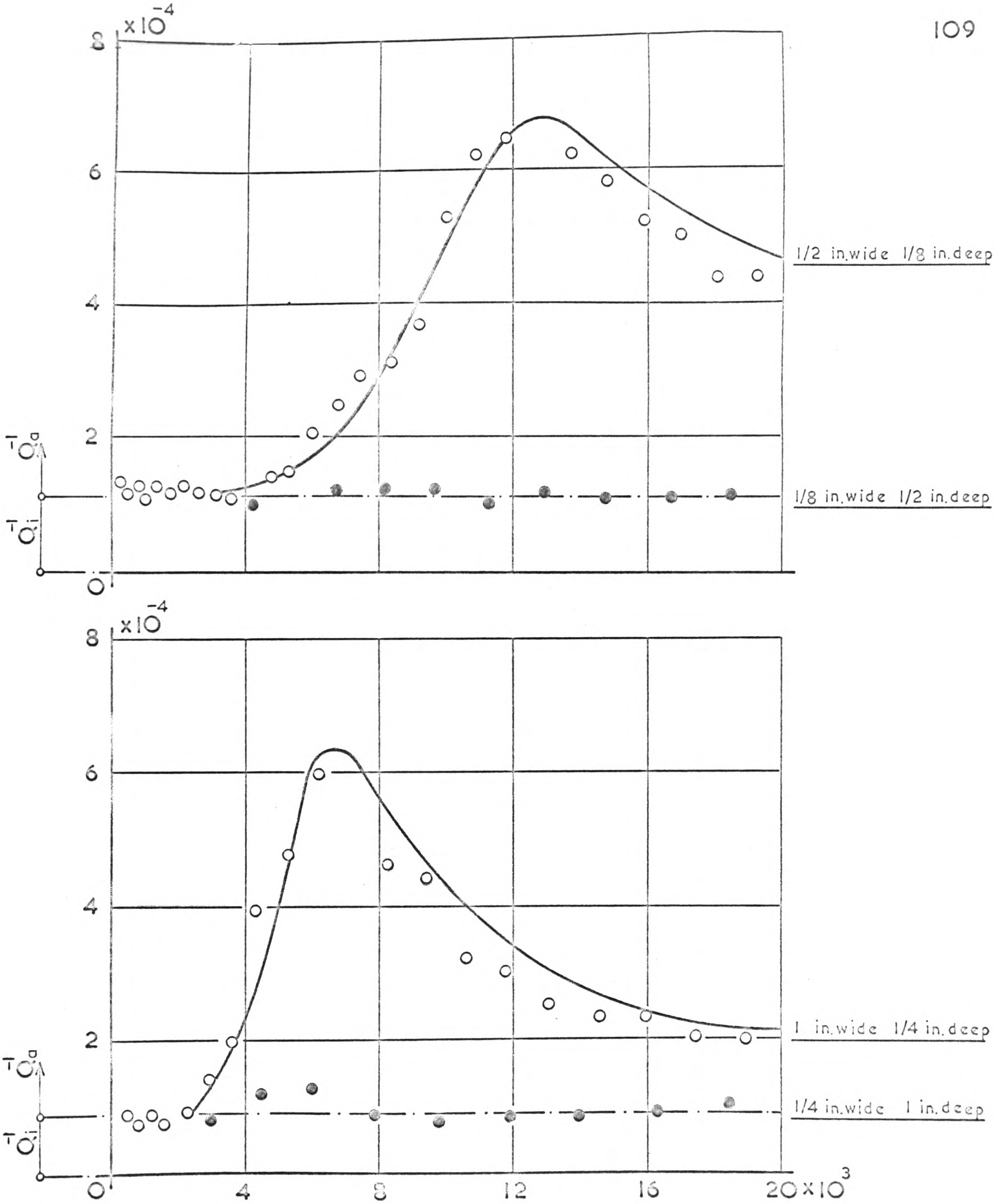

Frequency — c.p.s.

○● Experimental Points — Theoretical Curves

Transverse Vibration

FIG (27)

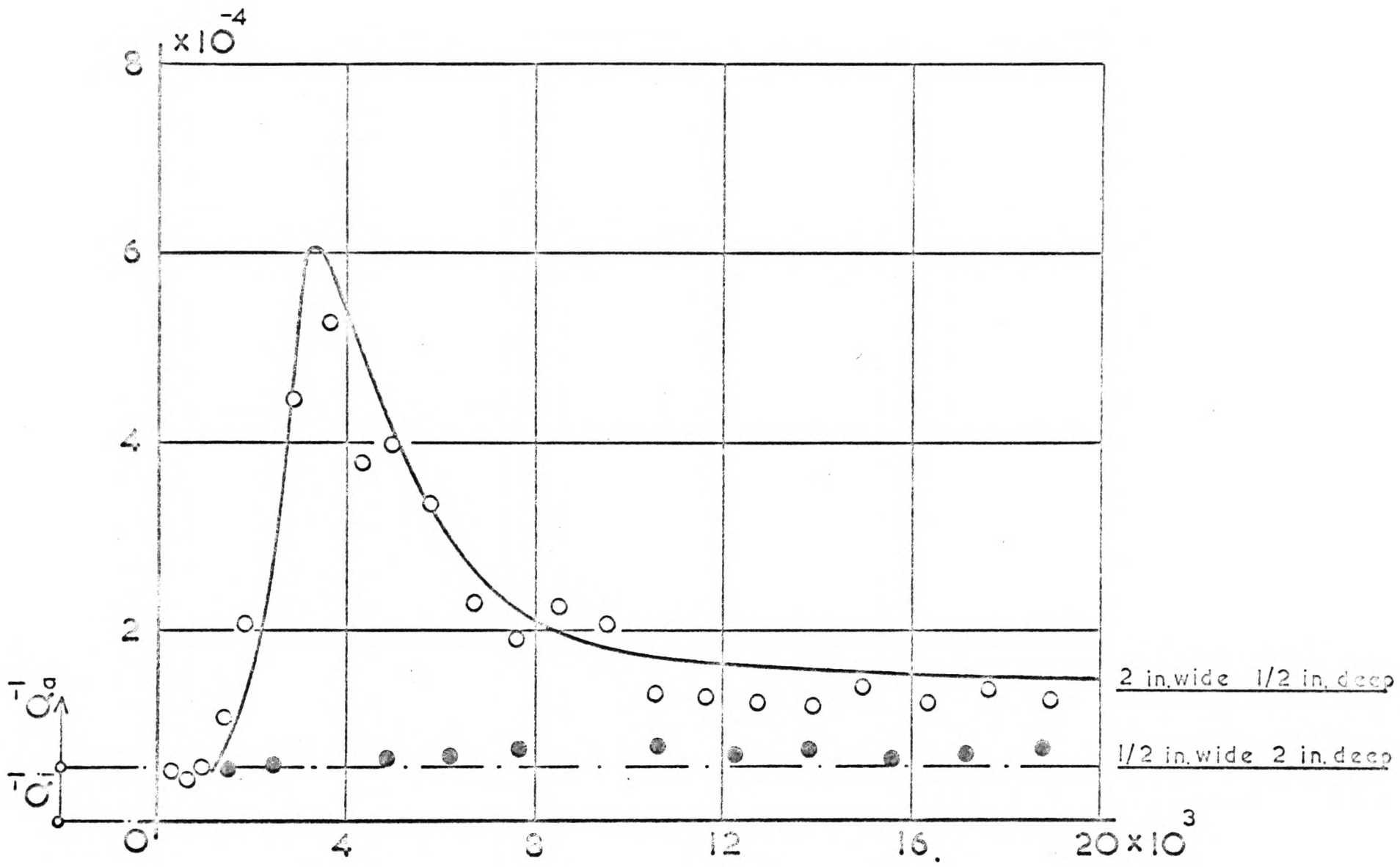

Frequency – c.p.s.

Experimental Points — Theoretical Curve

Transverse Vibration

FIG (28)

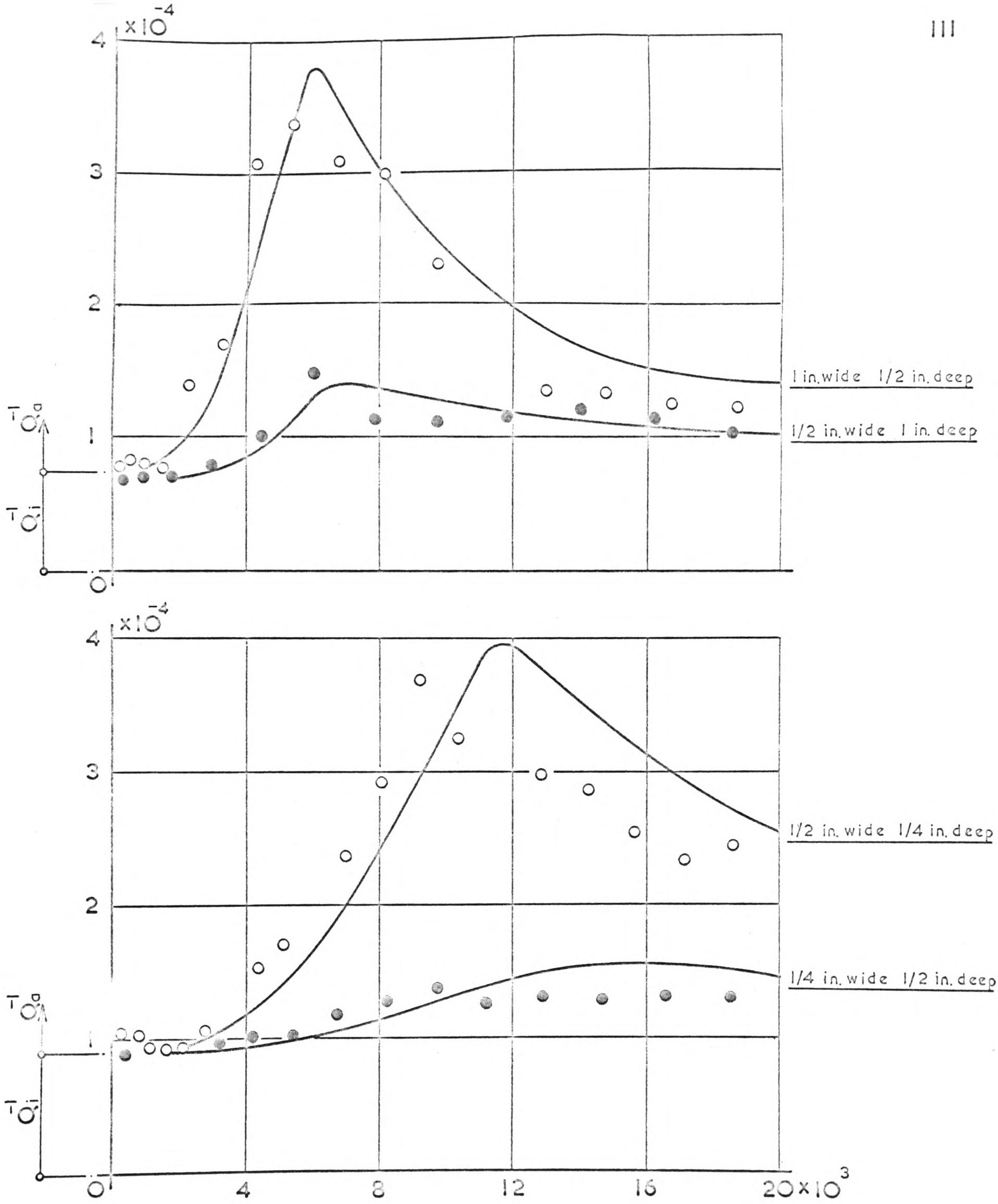

Frequency — c. p. s.

Experimental Points —Theoretical Curves

Transverse Vibration

FIG (29)

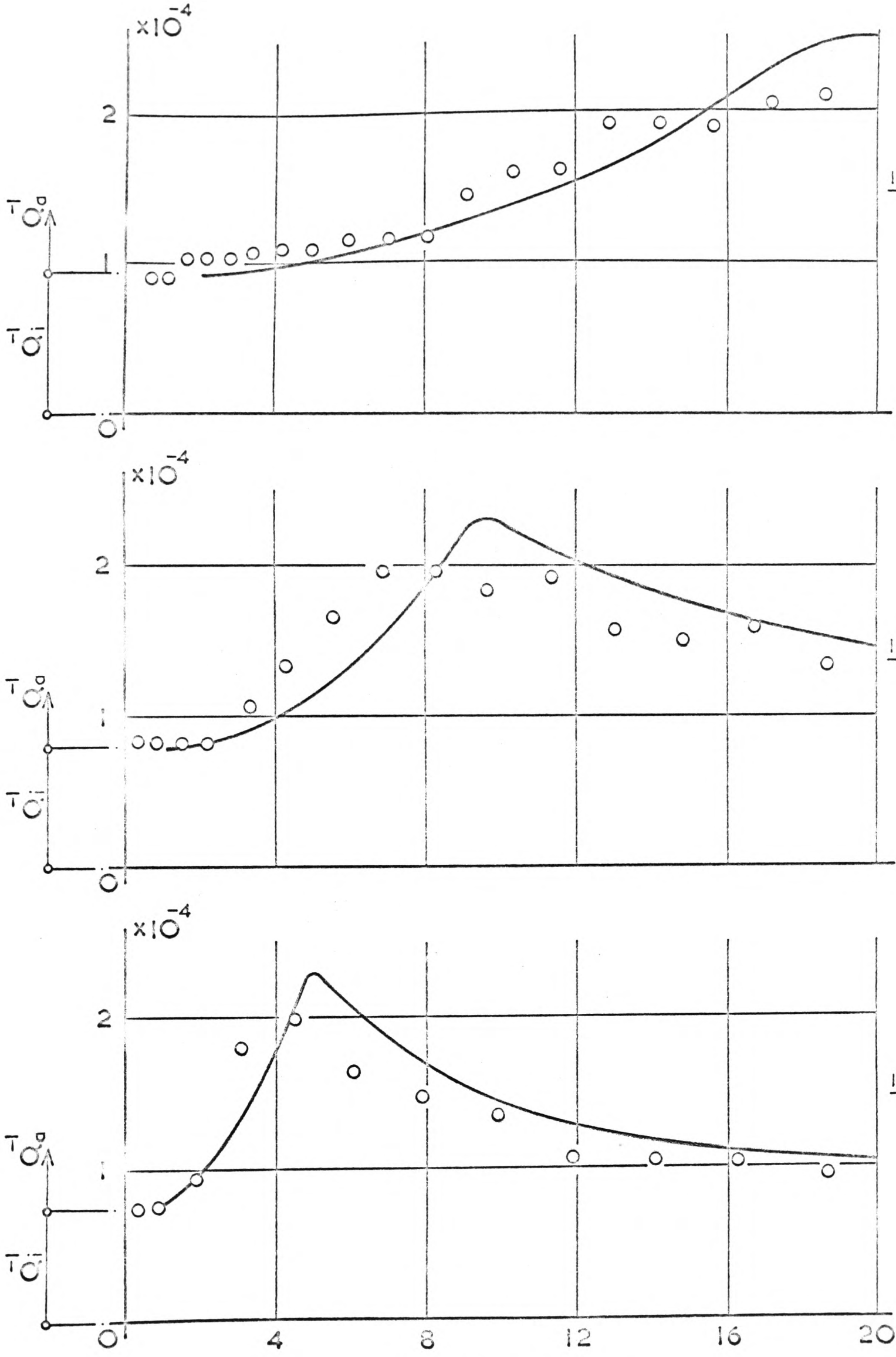

o Experimental Points — Theoretical Curves

Transverse Vibration

FIG (30)

failed to indicate their existence).

If the values of k at the maxima of Q_a^{-1} are marked on the curves of fig. (34), it is found that the points lie on lines of k × depth = constant, the values of the constants depending on the breadth to depth ratios of the beams. Also, if the values of λ_0 at the maxima are evaluated for each beam it is found that λ_0 bears a constant relationship to the perimiters of the beams i.e. at the maxima of Q_a^{-1}.

$$\lambda_0 \simeq 1.5\ (b + d)$$

Thus maximum damping occurs when the wave length of the radiated sound is approximately equal to three quarters of the perimiter of the beam cross section.

- - - o 0 o - - -

11.0 DISCUSSION

It has been shown that the damping phenomena observed in this investigation are due to a combination of internal damping and acoustic damping.

The experimental work has indicated that internal damping is hysteretic in nature which agrees with the findings of a number of researchers (although they in general worked at higher stresses) but would appear at first sight to be at variance with the results obtained by Zener and other physicists. The discrepancy may however be connected with the physical dimensions of the specimens used.

The work of physicists has generally been aimed at explaining how internal damping arises and ascertaining what the primary causes are. Zener, for example, has devoted a considerable amount of attention to the study of thermoelastic coupling, this being thought to be a major source of the damping of transverse vibrations. In transverse vibration thermal currents will flow between the compressed and extended parts of the body and if the period of vibration is comparable to the time it takes for thermal equilibrium to be attained there will be an irreversible conversion of mechanical energy to thermal energy; this loss of mechanical energy appears as a damping of the motion of the body. It does however seem that this effect is only of importance when the body is very thin or, for larger bodies, when the frequency is very low.

Zener gives a formula for predicting the frequency at which the damping effects of this thermoelastic coupling are at a maximum. Using this formula for the case of the thinnest specimen used in this work, viz. $\frac{1}{8}$ in., it is found that the frequency at maximum is

less than 100 c.p.s. For the remainder of the specimens the frequencies are even lower. It has already been mentioned that the experimental results obtained at frequencies of this order were unreliable.

It is not therefore possible to draw any definite conclusions regarding damping by thermal currents but it may be said that such damping does not manifest itself in bodies with significant dimensions, at least in the frequency range 500 c.p.s. to 20 Kc.p.s. The damping does instead seem to be the result of a form of hysteresis, the loss per cycle depending solely on the area of the hysteresis loop which in turn is a constant proportion of the maximum kinetic energy of the body.

The fact that no great difference was found in the damping properties of cold rolled mild steel and a more homogeneous mild steel is another anomaly which is probably explained by again considering the dimensions of the specimens. Clearly the larger the body the smaller will be the percentage of "hard case", resulting from cold rolling, to virgin material. It could then reasonably be expected that the effects of cold rolling on damping properties would be small in large bodies but that such effects may be pronounced in small bodies. Further investigation is necessary before any definite statement can be made on the effects of cold rolling. The experiment performed here has nevertheless served a useful purpose in that it has shown that generalisations regarding cold rolling are of little value.

It has been shown that the theories developed in section 10 describe very accurately the observed air damping effects these having thus been demonstrated to be the result of acoustic radiation. Also, the comparison between the theoretical and the

experimental results substantiates the basic assumptions made in the theory, namely, that the air was inviscid and that end effects were negligeable i.e. the beams were of infinite length. The latter assumption may however prove erroneous when the lengths of the beams are comparable to the diameters, whence end effects may become important, but from a practical viewpoint the acoustic damping of such beams would probably be of little interest.

Junger has developed theory which runs on parallel lines to that given in 10.2 for cylindrical beams. It was however considered that the theory should be presented in the form given here firstly to preserve continuity of the thesis and secondly to show the derivation of the acoustic damping factor, which was the quantity measured in the experimental work.

The acoustic damping of the cylindrical beams has been shown to reach a maximum when the wave length of the radiated sound is approximately equal to the circumference of the beams. This particular phenomenon is typical of the behaviour of sound waves in that they are generally insensitive to objects smaller than their own wave length but when the dimensions of the objects are such that they are comparable with the sound wave length then interference effects can occur. Here, interference effects are seen to result in a damping of the motion of the beams.

It was also shown that when the damping is a maximum, ka = constant = 0.375; this is a direct consequence of the fact that λ_0 is approximately equal to the circumference of the beams. The relationship is simply demonstrated by considering the case of a pin ended beam. For such a beam Bernoulli-Euler theory gives for the mode frequencies $\omega_i = \frac{i^2\pi^2}{L^2}\sqrt{\frac{EI}{A\rho_s}}$: the wave lengths are

given by $\lambda = {}^{2L}/_{i}$. Taking $\lambda_0 = \frac{2\pi c}{\omega_i} = 2\pi a$ at maximum damping and inserting the appropriate values of E, ρ_s and c, ka is found to equal a constant as above.

To introduce depth effects in the theory relating to rectangular beams a considerable amount of simplification was made. Nevertheless the assumptions on which the simplifications were based seem to have been justified since the predicted and observed phenomena are in good agreement.

Evaluation of equation (10.4.22) shows that, for a given breadth of beam, the most important effect of introducing depth is to alter the value of q at which the acoustic damping factor reaches its maximum. For small breadth/depth ratios q at maximum damping approaches zero while for large breadth/depth ratios q at maximum approaches the limiting value of approximately 0.5 which occurs in the case of a strip with zero thickness.

The experimental work indicated that the relationship between the maxima of Q_a^{-1} and the breadth/depth ratios may be linear - (fig. (16)). Examination of fig. (24) shows that the relationship is, strictly speaking, not linear but that very little error would be introduced if linearity were assumed. The larger the breadth/depth ratio the more nearly true would such an assumption become. Beyond $q \simeq 1.5$ the values of the acoustic damping factors are in fact directly proportional to the breadth/depth ratios.

Whereas in the case of the cylindrical beams the acoustic damping was found to reach its maximum when λ_0 was approximately equal to the circumference of the beams, it was found that maximum damping of the rectangular beams occured when λ_0 was approximately

equal to three quarters of the circumference. This shows that the radiated sound waves "see" a body which is slightly smaller than the actual body and suggests that the waves are insensitive to the sharp corners of the rectangular beams. In the same way as for the cylindrical beams there exists atmaximum damping of the rectangular beams the relationship kd = constants, the values of the constants depending on the breadth/depth ratios of the beams. Again this is the result of the relationship that exists between the sound wave length and the circumference, namely $\lambda_0 \simeq 1.5\ (b + d)$. By substituting this value of λ_0 in the frequency equation for a pin ended beam the values of the constants are obtained.

It is thus clear that the effects of the radiations from cylindrical and rectangular beams have certain features in common and that the ultimate damping effects of the radiations are determined by the relationship between the radiated sound wave length, the wave length in the vibrating body and the physical dimensions of the vibrating body.

Before closing this discussion a word will be said about the results obtained from the "in vacuo" experiment on the 1 in. wide $\frac{1}{8}$ in. deep specimen, fig. (13). The small peak in the curve is the result of acoustic radiation; this is readily explained as follows. The vacuum chamber pressure was 50 m.m. Hg. (which has for convenience been referred to as vacuum); this is approximately 1/15 th atmospheric and since, at constant temperature, pressure is proportional to density, the density ratio is 1:15. It can be seen from equation (10.4.22) that, with all other parameters held constant, the acoustic damping factor is proportional to

the air density. Hence, the ratio of the peak values in "vacuo" and in air should be 1:15 which is seen to be the case, from fig. (13).

In making a final appraisal of the project as a whole a point worthy of mention is the considerable time spent on preliminary investigations. Such a series of investigations were considered essential as some initial work had shown that the damping was of a very low order and that to approach the actual research programme with any degree of confidence it would be necessary to have a full awareness of any extraneous damping which may exist. The consistency obtained in the experimental work seems to be sufficient justification for the time spent on the preliminaries.

It is considered that in general the initial objectives of the research have been realised and that although it was not possible to give a theoretical explanation of the observed internal damping phenomena a good measure of success was achieved in explaning the air damping phenomena.

- - - o O o - - -

12.0 CONCLUSIONS

The principal conclusions drawn from the foregoing are as follows.

(i) If a mild steel body is performing harmonic oscillations and the induced stresses are either uniform tension or compression or a combination of both then, provided the stresses are such that non-linear effects are absent, the internal damping will be the result of a form of hysteresis, the damping factor being independent of frequency in the range 500 c.p.s. to 20 Kc.p.s.

(ii) Within the limitations of (i) and provided the amount of "hard case" to virgin material is small the internal damping factor of cold rolled mild steel may be ascribed the approximate value 0.6×10^{-4}.

(iii) If a body is performing small amplitude harmonic oscillations in air then the primary cause of damping by the air is acoustic radiation. Such damping is dependent on the type of oscillation, the shape of the body, the density of the air and the frequency of the oscillations.

(iv) The acoustic damping of the longitudinal vibrations of rods, at least up to 2 in. diameter, is negligeable for frequencies up to 20 Kc.p.s.

(v) The acoustic damping of the transverse vibrations of beams is dependent on the wave length of the radiated sound the wave length in the beams and the circumference of the beams. When the wave length of the radiated sound is greater than the wave length in the beams there is no acoustic damping the principal effect of the radiations

being to produce a mass reactance on the beams. The effect of the mass reactance on the beams used here was negligeable but it may have a considerable effect on, for example, thin cylinders. For cylindrical beams maximum acoustic damping occurs when the wave length of the radiated sound is ≃ the circumference of the beams and the value of the maximum is the same for all diameters. For rectangular beams maximum acoustic damping occurs when the wave length of the radiated sound is ≃ three quarters of the circumference of the beams and the values of the maxim are nearly directly proportional to the breadth/depth ratios of the beams.

It is appreciated that the damping measured in this investigation is small and that in practical applications other forms of damping may predominate. It is nevertheless considered that by broadening the field of knowledge of damping mechanisms and in particular by showing the relative importance of each, a greater understanding of the problem as a whole will be obtained.

- - - o O o - - -

13.0 SUGGESTED FURTHER FIELDS OF STUDY

The work described in this thesis has been subjected to specific limitations in order that the complexity of the subject be reduced to manageable proportions. The results do however provide a good basis for further work in which some of the restrictions may be removed and they also suggest further interesting fields of study.

It was stated that the experimental results obtained at frequencies up to 500 c.p.s. were not wholly reliable for reasons given in the text. It would seem desireable that this range be investigated further. To do so an effectively loss free suspension system would be necessary or a completely new experimental set up would have to be designed.

Only non-amplitude dependent internal damping has been studied. It is however generally recognised that internal damping is a function of stress amplitude when the stresses are significant, particularly when they are in the region of the fatigue limit. The relationship between internal damping and stress is open to question: early researchers Hopkinson and Williams found fourth order dependence, Rowett found third order dependence and Kimballand Lovell found second order dependence (which is equivalent to saying the logarithmic decrement is constant). Lazan has studied internal damping at high stress and has found stress exponents as high as 30 these depending on stress magnitude, temperature and stress history. Clearly, a systematic approach to the problem is required to eliminate these anomalies.

There is also evidence, Robertson and Yorgiadis[34], that internal damping under shear stress differs from that under direct stress. An experiment was carried out in this work in which the

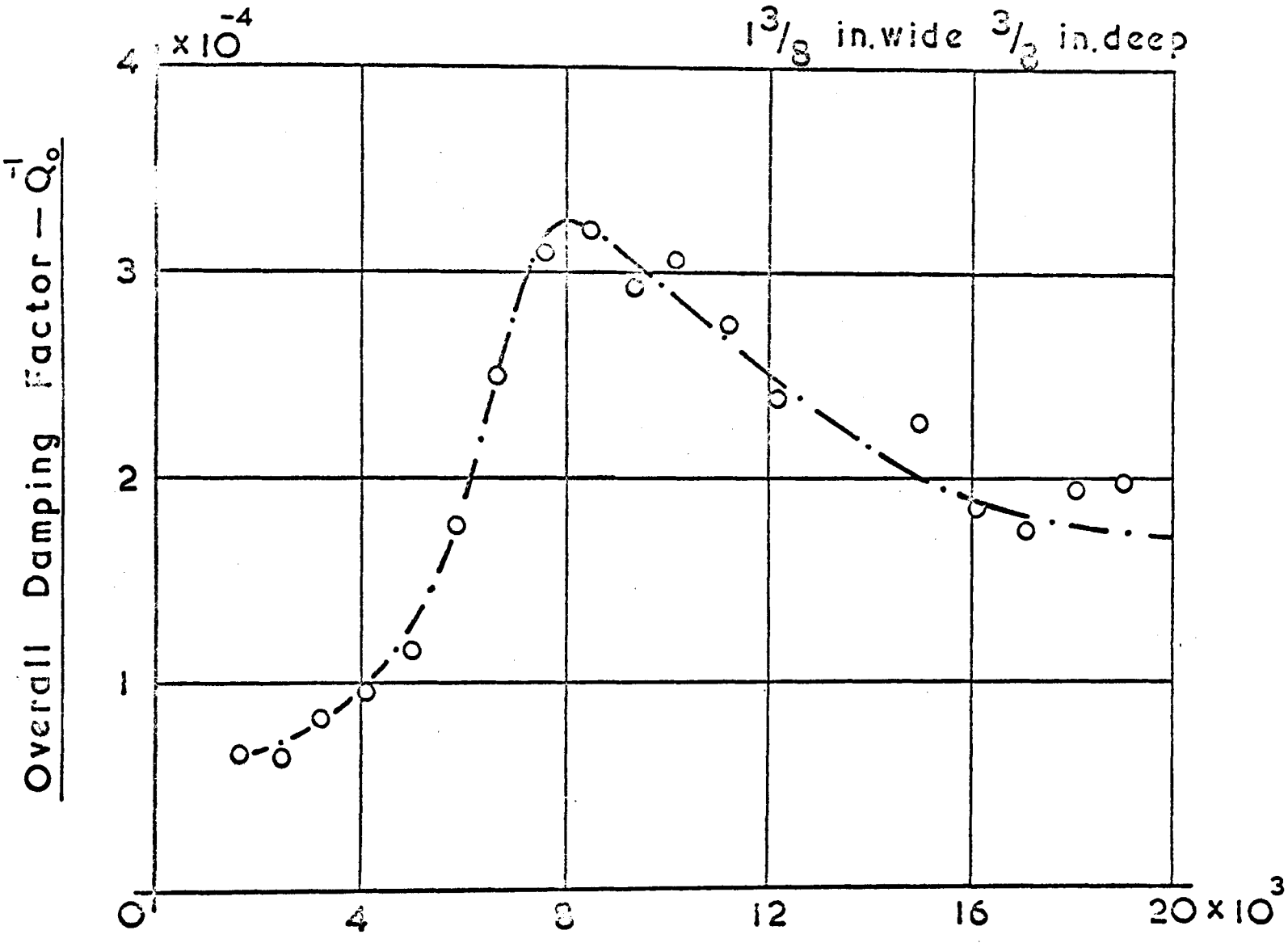

Torsional Vibration of Rectangular Beam

FIG (31)

Q_0^{-1}/frequency characteristic for a $1\frac{3}{8}$ in. wide $\frac{3}{8}$ in. deep cold rolled mild steel specimen in torsional vibration was obtained; this is shown in fig. (31). There was insufficient time to pursue the investigation further but the results are noteworthy in that they display similarities with those obtained from the transverse vibration experiments. It would be an interesting exercise to obtain the damping characteristic in vacuum which would show the extent of the acoustic losses. A theoretical approach could then possibly be made on similar lines to that given in the text for transverse vibration.

In the field of acoustics there are inumerable possibilities. The results of this investigation have shown the importance of the relationships between the radiated sound wave length, the structural wave length and the physical dimensions of the bodies. It would be interesting to see what relationships exist in vibrating plates (see Green[6]) or thin rectangular or cylindrical bodies. The paper by Foxwell and Franklin would seem to indicate that failure to account for internal radiative effects may lead to error in predicting the dynamic response of such bodies as thin cylinders.

The above and many more fields require fuller investigation.

In conclusion it may be said that the need for basic research to be related to the engineers requirements is becoming increasingly important and it is indeed true to say that the rapid technological advancements being made at this time can be largely attributed to the close collaboration between present day scientists and engineers.

- - - o 0 o - - -

BIBLIOGRAPHY

1. BISHOP, R.E.D. — The treatment of damping forces in vibration theory, J. Roy. Aero. Soc., V 59, p. 738, 1955.

2. BISHOP, R.E.D., and JOHNSON, D.C. — The Mechanics of Vibration, Cambridge Univ. Press., 1960.

3. COMRIE, L.J. — Mathematical Tables, W. & R. Chambers Ltd., 1949.

4. DEN HARTOG, J.P. — Mechanical Vibrations, McGraw-Hill Book Co. Inc., 1940.

5. FOXWELL, J.H. and FRANKLIN, R.E. — The vibration of thin walled stiffened cylinders in an acoustic field, Aero. Quarterly, V 10, p. 47, 1959.

6. GREEN, D.C. — Vibration and sound radiation of damped and undamped flat plates, J. Acoustic Soc. Amer., V 33, No. 10, p. 1315, 1961.

7. HOPKINSON, B. and WILLIAMS, G. T. — The elastic hysteresis of steel, Proc. Roy. Soc., V 87, p. 502, 1912.

8. INCE, E.L. — Tables of elliptic cylinder functions, Proc. Roy. Soc. Edin., V 52, p. 355, 1931/32.

9. JACOBSEN, L.S. — Steady forced vibration as influenced by damping, A.S.M.E. Trans., V 52, No. 1, p. 169, 1930.

10. JUNGER, M.C. — Sound scattering by thin elastic shells, J. Acoustic Soc. Amer., V 24, No. 4, p. 366, 1952.

11. JUNGER, M.C. — The physical interpretation of the expression for an outgoing wave in cylindrical coordinates, J. Acoustic Soc. Amer., V 25, No. 1, p. 40, 1953.

12. KIMBALL, A.L. — Friction and damping in vibrations, A.S.M.E. Trans., V 63, p. A37: p. A135, 1941.

13. KIMBALL, A.L. and LOVELL, D.E. — Internal friction in solids, Phys. Rev., V 30, p. 948, 1927.

14. KIRKPATRICK, E.T. — Tables of Modified Mathieu Functions, Math. Aids, V 13-14, p. 118, 1959/60.

15. KOLSKY, H. — Stress Waves in Solids, Clarendon Press, 1953.

16. LANCASTER, P. — Free vibration and hysteretic damping, J. Roy. Aero. Soc., V 64, p. 229, 1960.

17. LAZAN, B.J. — Effect of damping constants and stress distribution on the resonance response of members, J. Appl. Mech., V 20, p. 201, 1953.

18. LEADERMAN, H. — Creep, elastic hysteresis and damping in bakelite under torsion, A.S.M.E. Trans, V 61, p. A79, 1939.

19. LINDSAY, R.B. — Mechanical Radiation, McGraw-Hill Book Co. Inc., 1960.

20. LOWENTHAL, S. and TOURNOIS, P. — Radiation impedance of membranes and flat plates; their acoustic coupling with the propogating medium, J. Acoustic Soc. Amer., V 35, p. 1423, 1963.

21. MAIDANIK, G. — Radiation from fluid loaded plates, J. Sound and Vib., V 3, No. 3, p. 288, 1966.

22. MANGIAROTTY, R.A. — The acoustic radiation damping of vibrating panels, M.Sc. Thesis, Southampton Univ., 1960.

23. MARTINEK, J. and YEH, G.C. — Forced vibration of a clamped rectangular plate in fluid media, J. Appl. Mech., V 22, No. 4, p. 568, 1955.

24. MAZELSKY, B. — Theoretical aerodynamic properties of vanishing aspect ratio harmonically oscillating rigid airfoils in a compressible medium, J. Aero. Sci., V 23, p. 639, 1956.

25. McLACHLAN, N.W. — Theory and Application of Mathieu Functions, Clarendon Press, 1947.

26. McLACHLAN, N.W. — Bessel Functions for Engineers, Clarendon Press, 1955.

27. MEAD, J.D. — The internal damping due to structural joints and techniques for general damping measurements, A.R.C. report C.P. No. 452, 19,870, 1959.

28. MORSE, P.M. and FESHBACH, H. — Methods of Theoretical Physics, Parts I and II, McGraw-Hill Book Co. Inc., 1953.

29. MORSE, P.M. — Vibration and Sound, McGraw-Hill Book Inc., 1948.

30. MYKLESTAD, N.O. — The concept of complex damping, J. Appl. Mech., V 19, p. 284, 1952.

31. OCKLESTON, A.J. — The damping of the lateral vibrations of a mild steel bar, Phil. Mag., V 26, p. 705, 1938.

32. PLUNKETT, R. — Survey of vibration damping, Appl. Mech. Rev., V 6, No. 7, p. 313, 1953.

33. RAYLEIGH, J.W.S. — The Theory of Sound, Dover Publications, 1945.

34. ROBERTSON, J.M. and YORGIADIS, A.J. — Internal friction in engineering materials, J. Appl. Mech., V 68, p. A173, 1946.

35. ROWETT, F.E. — Elastic hysteresis in steel, Proc. Roy. Soc., V 89, p. 528, 1914.

36. WATCHMAN, J.B. and TEFFT, W.E. — Effect of suspension position on apparent values of internal friction, Rev. Sci. Instr., V 29, No. 6, p. 517, 1958.

37. WATSON, G.N. — A Treatise on the Theory of Bessel Functions, Cambridge Univ. Press, 1952.

38. ZENER, C. — Internal friction in solids, Proc. Phys. Soc. London, V 52, p. 152, 1940.

39. ZENER, C. — Elasticity and Anelasticity of Metals, Chicago Univ. Press, 1956.

40. National Bureau of Standards, Tables Relating to Mathieu Functions, Columbia Univ. Press, 1951.

ACKNOWLEDGEMENTS

The author is grateful to the Science Research Council for the financial support which allowed this research to be undertaken.

The work was carried out in the University of Edinburgh, Department of Mechanical Engineering and the author is indebted to the late Professor R. N. Arnold and to Professor L. G. Jaeger for providing the necessary facilities.

Thanks are due to Professor J. D. Robson, Glasgow University (formerly Dr. J. D. Robson, Edinburgh University) and to Dr. A. D. S. Barr for their supervision of the research and for their ready council.

A special word of thanks to Mr. George Smith for his assistance during the experimental work and to Miss Marjorie Easson for her patient typing of the thesis.

- - - o 0 o - - -

APPENDICES

APPENDIX I

COORDINATE TRANSFORMATIONS

a) CARTESIAN TO CYLINDRICAL

The coordinate systems are shown on page 77.

$$x = r \sin\theta$$

$$y = r \cos\theta$$

$$r^2 = x^2 + y^2$$

Now
$$\frac{\partial r}{\partial x} = \frac{x}{r} = \sin\theta$$

$$\frac{\partial r}{\partial y} = \frac{y}{r} = \cos\theta$$

$$\frac{\partial \theta}{\partial x} = \frac{y}{r^2} = \frac{\cos\theta}{r}$$

$$\frac{\partial \theta}{\partial y} = -\frac{x}{r^2} = -\frac{\sin\theta}{r}$$

Therefore

$$\frac{\partial}{\partial x} = \frac{\partial}{\partial r} \cdot \frac{\partial r}{\partial x} + \frac{\partial}{\partial \theta} \cdot \frac{\partial \theta}{\partial x}$$

$$= \sin\theta \frac{\partial}{\partial r} + \frac{1}{r} \cos\theta \frac{\partial}{\partial \theta}$$

and
$$\frac{\partial}{\partial y} = \frac{\partial}{\partial r} \cdot \frac{\partial r}{\partial y} + \frac{\partial}{\partial \theta} \cdot \frac{\partial \theta}{\partial y}$$

$$= \cos\theta \frac{\partial}{\partial r} - \frac{1}{r} \sin\theta \frac{\partial}{\partial \theta}$$

Using the above operators it is found that

$$\nabla^2 = \frac{\partial^2}{\partial x^2} + \frac{\partial^2}{\partial y^2}$$

$$= \frac{\partial^2}{\partial r^2} + \frac{1}{r} \frac{\partial}{\partial r} + \frac{1}{r^2} \frac{\partial^2}{\partial \theta^2}$$

b) CARTESIAN TO ELLIPTIC CYLINDER

The coordinate systems are shown on page 90.

$$x = \frac{b}{2}\cosh\xi\cos\eta$$

$$y = \frac{b}{2}\sinh\xi\sin\eta$$

where b is the interfocal distance.

Writing

$$Z = x + iy = \frac{b}{2}\cosh(\xi + i\eta) = \frac{b}{2}\cosh\nu$$

$$\bar{Z} = x - iy = \frac{b}{2}\cosh(\xi - i\eta) = \frac{b}{2}\cosh\bar{\nu}$$

then $Z\bar{Z} = x^2 + y^2$, $\quad \nu\bar{\nu} = \xi^2 + \eta^2$

and $$\frac{4\partial^2 Z\bar{Z}}{\partial Z\partial\bar{Z}} = \left(\frac{\partial^2}{\partial x^2} + \frac{\partial^2}{\partial y^2}\right) Z\bar{Z}$$

$$\frac{4\partial^2 \nu\bar{\nu}}{\partial\nu\partial\bar{\nu}} = \left(\frac{\partial^2}{\partial\xi^2} + \frac{\partial^2}{\partial\eta^2}\right) \nu\bar{\nu}$$

Also $$\frac{\partial\nu}{\partial Z} = \frac{2}{b\sinh\nu}, \quad \frac{\partial\bar{\nu}}{\partial\bar{Z}} = \frac{2}{b\sinh\bar{\nu}}$$

therefore $$\frac{\partial}{\partial Z} = \frac{2}{b\sinh\nu}\cdot\frac{\partial}{\partial\nu}, \quad \frac{\partial}{\partial\bar{Z}} = \frac{2}{b\sinh\bar{\nu}}\cdot\frac{\partial}{\partial\bar{\nu}}$$

and thus $$\frac{4\partial^2}{\partial Z\partial\bar{Z}} = \frac{16}{b^2\sinh\nu\sinh\bar{\nu}}\cdot\frac{\partial^2}{\partial\nu\partial\bar{\nu}}$$

which gives

$$\nabla^2 = \frac{\partial^2}{\partial x^2} + \frac{\partial^2}{\partial y^2}$$

$$= \frac{8}{b^2(\cosh 2\xi - \cos 2\eta)}\left(\frac{\partial^2}{\partial\xi^2} + \frac{\partial^2}{\partial\eta^2}\right)$$

- - - o 0 o - - -

APPENDIX II

This appendix contains graphs giving the relationships between the various parameters used in the theory.

For the lowest modes of vibration the values of the beam wave numbers, k, were calculated using beam wave lengths obtained from ref. 2. For the higher modes it was assumed that the beam wave lengths were equal to $^{2L}/_{i}$ where L is the beam length and i the mode number.

In the k/frequency graphs the calculated values of k are plotted against the mode frequencies obtained experimentally.

- - - o 0 o - - -

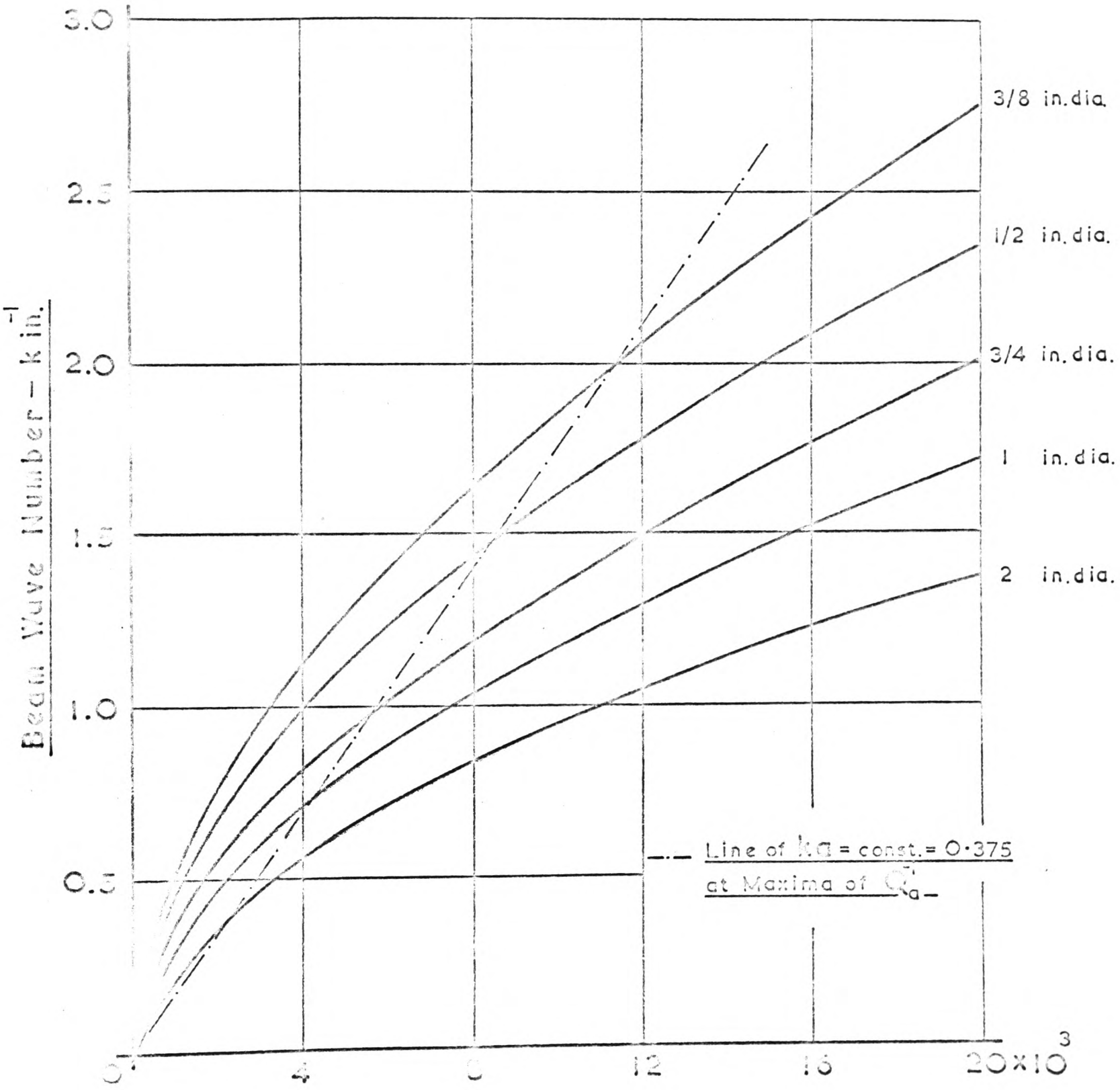

Cylindrical Beams in Transverse Vibration

FIG (32)

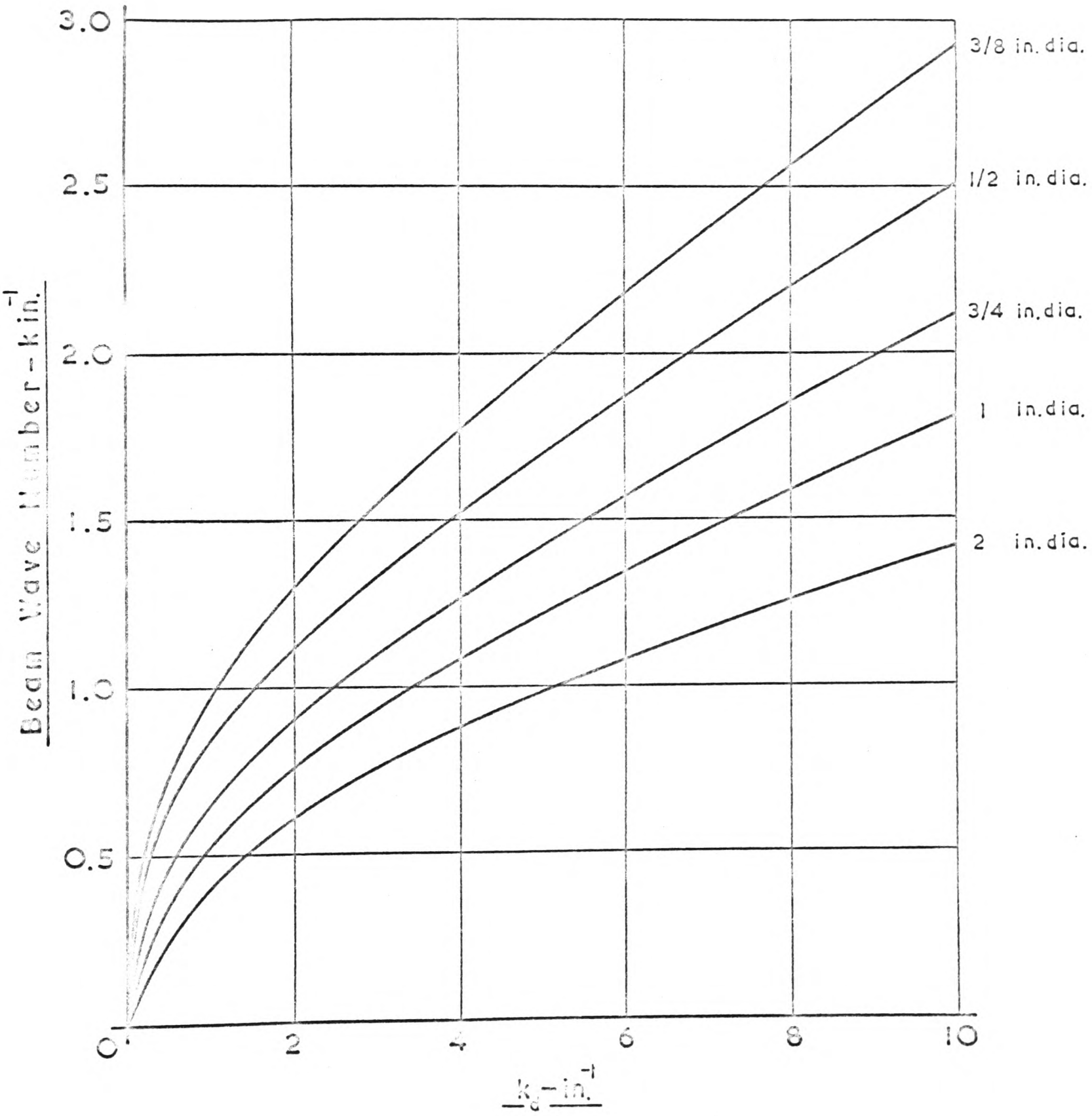

Cylindrical Beams in Transverse Vibration

FIG (33)

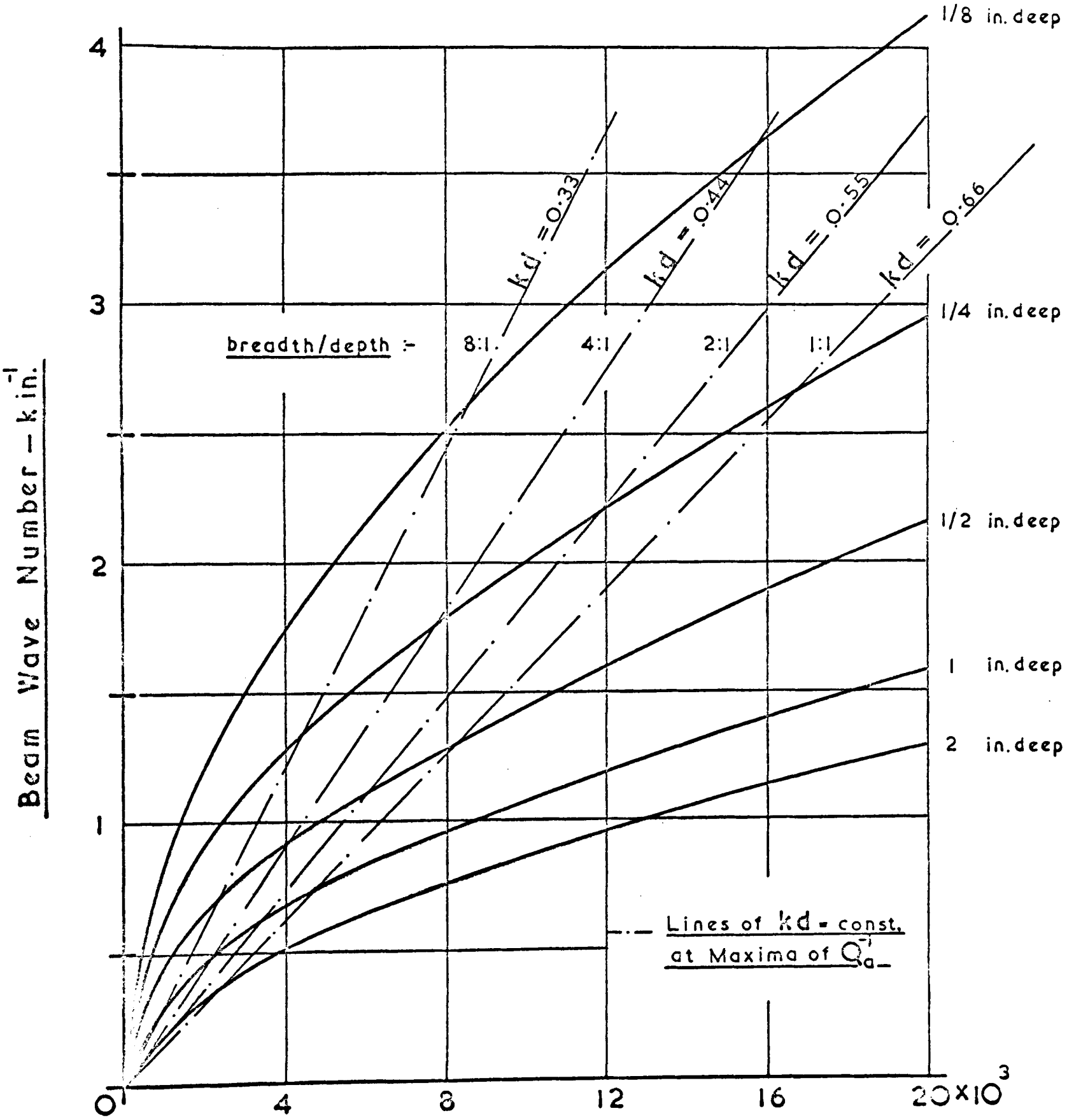

Rectangular Beams in Transverse Vibration

FIG (34)

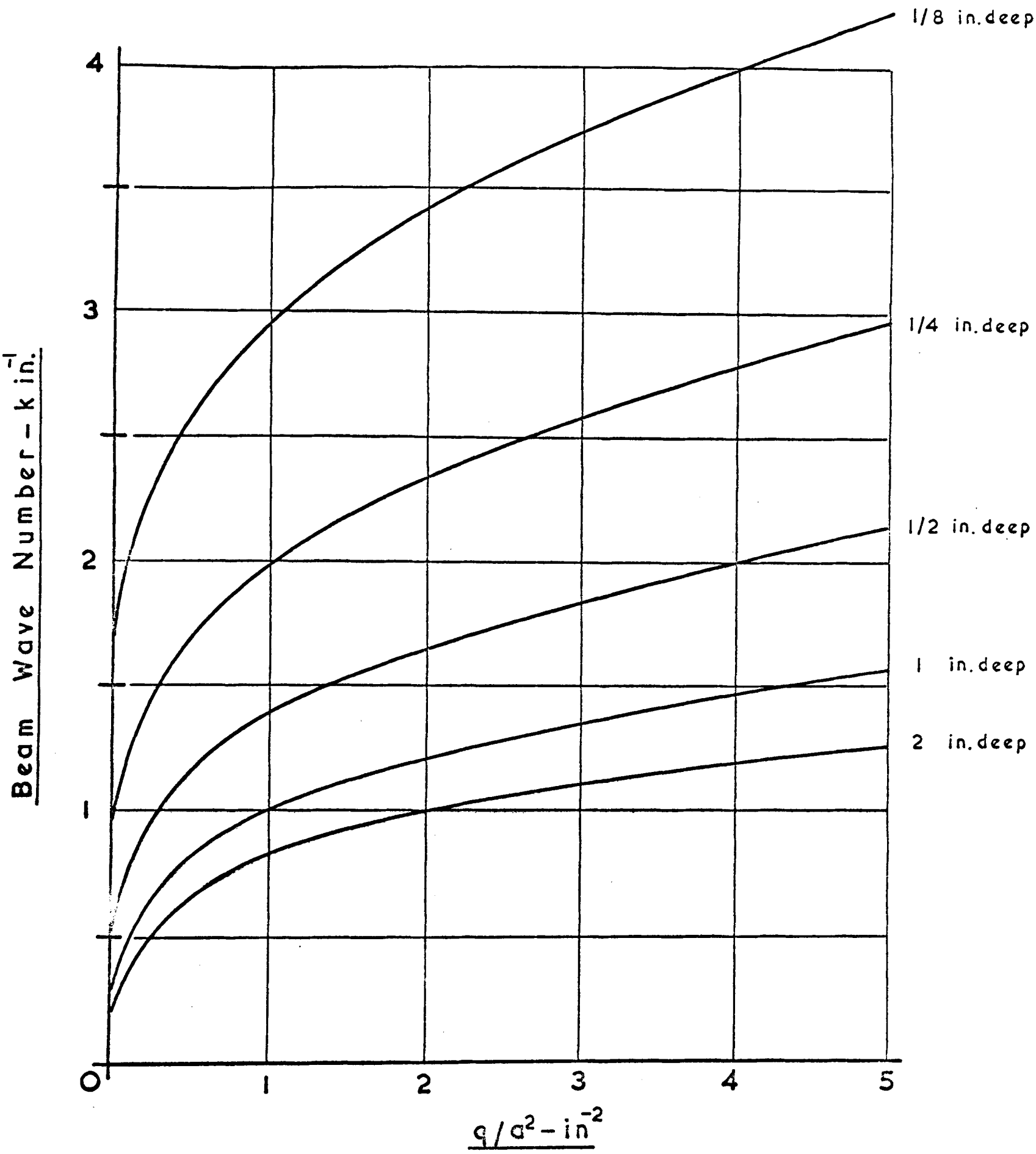

Rectangular Beams in Transverse Vibration

FIG (35)